

NUREG/CR-5653  
PNL-7476

---

# Recriticality in a BWR Following a Core Damage Event

---

Prepared by  
W. B. Scott, D. G. Harrison, R. A. Libby, R. D. Tokarz/PNL  
R. D. Wooton, R. S. Denning, R. W. Tayloe, Jr./BMI

Pacific Northwest Laboratory

Battelle Memorial Institute

Prepared for  
U.S. Nuclear Regulatory Commission

9012280221 901130  
PDR NUREG  
CR-5653 R PDR

## AVAILABILITY NOTICE

### Availability of Reference Materials Cited in NRC Publications

Most documents cited in NRC publications will be available from one of the following sources:

1. The NRC Public Document Room, 2120 L Street, NW, Lower Level, Washington, DC 20555
2. The Superintendent of Documents, U.S. Government Printing Office, P.O. Box 37082, Washington, DC 20013-7082
3. The National Technical Information Service, Springfield, VA 22161

Although the listing that follows represents the majority of documents cited in NRC publications, it is not intended to be exhaustive.

Referenced documents available for inspection and copying for a fee from the NRC Public Document Room include NRC correspondence and internal NRC memoranda; NRC Office of Inspection and Enforcement bulletins, circulars, information notices, inspection and investigation notices; Licensee Event Reports; vendor reports and correspondence; Commission papers; and applicant and licensee documents and correspondence.

The following documents in the NUREG series are available for purchase from the GPO Sales Program: formal NRC staff and contractor reports, NRC-sponsored conference proceedings, and NRC booklets and brochures. Also available are Regulatory Guides, NRC regulations in the *Code of Federal Regulations*, and *Nuclear Regulatory Commission Issuances*.

Documents available from the National Technical Information Service include NUREG series reports and technical reports prepared by other federal agencies and reports prepared by the Atomic Energy Commission, the runner agency to the Nuclear Regulatory Commission.

Documents available from public and special technical libraries include all open literature items, such as books, journal and periodical articles, and transactions. *Federal Register* notices, federal and state legislation, and congressional reports can usually be obtained from these libraries.

Documents such as theses, dissertations, foreign reports and translations, and non-NRC conference proceedings are available for purchase from the organization sponsoring the publication cited.

Single copies of NRC draft reports are available free, to the extent of supply, upon written request to the Office of Information Resources Management, Distribution Section, U.S. Nuclear Regulatory Commission, Washington, DC 20555.

Copies of industry codes and standards used in a substantive manner in the NRC regulatory process are maintained at the NRC Library, 7920 Norfolk Avenue, Bethesda, Maryland, and are available there for reference use by the public. Codes and standards are usually copyrighted and may be purchased from the originating organization or, if they are American National Standards, from the American National Standards Institute, 1430 Broadway, New York, NY 10018.

## DISCLAIMER NOTICE

This report was prepared as an account of work sponsored by an agency of the United States Government. Neither the United States Government nor any agency thereof, or any of their employees, makes any warranty, expressed or implied, or assumes any legal liability of responsibility for any third party's use, or the results of such use, of any information, apparatus, product or process disclosed in this report, or represents that its use by such third party would not infringe privately owned rights.



NUREG/CR-5653  
PNL-7476  
RC, R1, R3

---

---

# Recriticality in a BWR Following a Core Damage Event

---

---

Manuscript Completed: November 1990  
Date Published: December 1990

Prepared by  
W. B. Scott, D. G. Harrison, R. A. Libby, R. D. Tokarz, Pacific Northwest Laboratory  
R. D. Wooton, R. S. Denning, R. W. Tayloe, Jr., Battelle Memorial Institute

Pacific Northwest Laboratory  
Richland, WA 99352

Subcontractor:  
Battelle Memorial Institute  
Columbus, OH 43201

Prepared for  
Division of Systems Research  
Office of Nuclear Regulatory Research  
U.S. Nuclear Regulatory Commission  
Washington, DC 20555  
NRC FIN B2930

## ABSTRACT

This report describes the results of a study conducted by Pacific Northwest Laboratory to assist the U.S. Nuclear Regulatory Commission in evaluating the potential for recriticality in boiling water reactors (BWRs) during certain low probability severe accidents.

Based on a conservative bounding analysis, this report concludes that there is a potential for recriticality in BWRs if core reflood occurs after control blade melting has begun but prior to significant fuel rod melting. However, a recriticality event will most likely not generate a pressure pulse significant enough to fail the vessel. Instead, a quasi-steady power level would result and the containment pressure and temperature would increase until the containment failure pressure is reached, unless actions are taken to terminate the event.

Two strategies are identified that would aid in regaining control of the reactor and terminate the recriticality event before containment failure pressures are reached. The first strategy involves initiating boration injection at or before the time of core reflood if the potential for control blade melting exists. The second strategy involves initiating residual heat removal suppression pool cooling to remove the heat load generated by the recriticality event and thus extend the time available for boration.

## SUMMARY

The U. S. Nuclear Regulatory Commission (NRC) initiated a program to investigate the potential for recriticality in boiling water reactors (BWRs)<sup>1</sup> as a part of its Accident Management Program. This report describes the results of a study conducted by Pacific Northwest Laboratory<sup>2</sup> (PNL) to assist the NRC in evaluating:

- The potential for recriticality in BWRs during low probability severe accidents.
- The severe accidents that create a potential for recriticality.
- The possible consequences of the recriticality.
- The strategies for regaining control of the reactor when recriticality is a potential concern.

Due to modelling and phenomenological uncertainties related to void fraction, debris bed size, particle size, etc. and the lack of an analytical tool capable of performing the complex analyses required to address the complex interactions of these parameters, a conservative bounding analysis was conducted. If the conservative bounding analysis indicates acceptable consequences (e.g., no recriticality or a recriticality event resulting in a benign pressure pulse that is non-threatening to the integrity of the containment and accident management strategies can be implemented to successfully prepare for and terminate the event), further, more sophisticated model development and analyses may not be necessary to resolve the modelling and phenomenological uncertainties. However, if the bounding analysis indicates unacceptable consequences (e.g., a significant recriticality event that creates a large pressure pulse and potentially fails the containment), further research should be identified to resolve the uncertainties and phenomenological issues.

The report concludes that there is a potential for recriticality in BWRs during certain low probability severe accidents, but the recriticality event will most likely not generate a pressure pulse significant enough to fail the vessel. Instead, a quasi-steady power level would result and the containment pressure and temperature would increase until the containment failure pressure

---

<sup>1</sup>For a pressurized water reactor, core reflood is normally accomplished using borated water supplies and recriticality is generally perceived not to be very credible. However, for a BWR, reflood is normally accomplished using unborated water; and recriticality is believed to be credible. Therefore, this report addresses the potential for recriticality events only in BWRs.

<sup>2</sup>PNL is operated for the Department of Energy by Battelle Memorial Institute.

is reached, unless actions are taken to terminate the event. Two accident management strategies are identified that would aid in terminating the recriticality event before containment failure pressures are reached. The first accident management strategy is to initiate boration injection at or before the time of core reflood. The second accident management strategy is to initiate residual heat removal (RHR) suppression pool cooling as quickly as possible so as to remove some of the heat load and thus extend the time available for boration.

The following sections summarize each of the recriticality evaluation areas identified above.

#### Potential for Recriticality

Analyses of severe accident phenomenology in BWRs indicate that, while the core is in the process of heating and melting, one of the earliest components to melt and relocate are the steel blades that contain the B<sub>4</sub>C control material. Because the control material is encased in stainless steel blades that have a much lower melting point than the zirconium fuel cladding and the fuel itself, as the core heats up, the control material may melt and leave the core. If the core were to be reflooded following the relocation of the control blades and prior to the relocation of the core into a rubble bed, the possibility exists for the core to become critical again without an adequate means of control.

Without adequate training and proper procedures, the operations staff may be very surprised and confused to find that their actions to recover core cooling may have entered them into anticipated transient without scram (ATWS) conditions. This type of confusion or lack of training can cause the operations staff to disbelieve instrumentation and alarms and to take inappropriate actions. Recognition that this type of event can occur and development of accident management strategies to handle these events can aid in the prevention, mitigation, and termination of such events.

#### Accident Scenarios for Recriticality

Primarily using the NUREG-1150 risk study for the Peach Bottom plant as the technical basis, severe accident sequences with the highest predicted frequencies were selected to characterize the conditions that would likely contribute to core melt scenarios where recriticality may be possible. The accident sequences consisted of station blackout and ATWS events.

Station blackout is defined as the loss of all ac power, except that which is powered through an inverter from the station batteries. In this context, the station blackout involves the loss of both the normal ac power source from the offsite electrical grid and the emergency ac power source from the onsite diesel generators. From this point, station blackout events are



divided into two groups for the timing to core damage. The first group, called short-term station blackouts (SSBOs), includes those accident sequences where core damage begins within 1 hour of the initiating transient or event. In the short-term station blackout sequences, either the station batteries fail or the high pressure coolant injection (HPCI) and reactor core isolation coolant (RCIC) pumps independently fail early in the sequence. If the station batteries are failed at the time of the station blackout, the loss of dc power will also fail the ability to depressurize the reactor and causes a loss of vital instrumentation. If the batteries are available but the HPCI and RCIC pumps fail, depressurization and vital instrumentation may be available.

The second group of station blackout sequences are the long-term station blackout (LSBO) events, where core damage occurs after 1 hour, typically 9 to 12 hours after the initiating transient or event. Core damage occurs after the station batteries are depleted. These two groups of station blackout are essentially similar in consequences with the exception that core power is lower in the long-term sequences due to decay. Once all electrical power is lost, the ability to cool the core is lost. Water level decreases, core temperature increases, and core damage results.

For both station blackout groups, in which core damage has begun, if ac power is restored and unborated coolant injection is initiated within the time window between the beginning of control blade melting to the beginning of fuel rod melting, the potential for a recriticality event to occur may exist. Since core damage will proceed from the central region of the core radially outward, the potential for recriticality in the outer regions may occur at a much later time than that for the central region and in fact may occur after fuel rod collapse and debris bed formation within the central region. Therefore, the recriticality time window was conservatively estimated to be the time from the start of control blade melting to the time of vessel failure. For short-term station blackout sequences, the time window is from 91 to 161 minutes long, starting 109 to 127 minutes after the initiating event, respectively. For the long-term station blackout sequences, the time window is approximately 118 minutes long, starting over 600 minutes after the initiating event. It is estimated that between 12% and 1% of the time, depending on the specific sequence, ac power will be restored and coolant injection will be initiated within the recriticality time window.

An ATWS event occurs when, upon receipt of a scram signal following an unspecified transient, the control rods fail to insert into the core due to a mechanical failure of the rod control system. In these sequences, manual insertion of the control rods is unsuccessful. In some ATWS sequences, various systems used to recover from an ATWS (e.g., standby liquid control system and the high pressure coolant injection system) fail and allow the water level to drop until core overheating and damage begin. If coolant injection is subsequently initiated, recriticality becomes possible. However, for ATWS scenarios without boration (or inadequate boration), the containment will eventually fail and core melt will occur regardless of the occurrence of a recriticality event. If adequate boration does occur, the potential for

recriticality is possible only if the boron concentration is diluted by extended injection. Therefore, recriticality during an ATWS does not appear to be the major concern, prompt termination of the ATWS is.

### Consequences of Recriticality

Analysis showed that without the control blades, relatively high reactivities are possible with standing fuel rods or over a broad range of fuel particle sizes and fuel volume fractions for both unborated and fairly heavily borated reflood conditions. The consequences of the potential recriticality are important to estimate quantitatively for selecting the most appropriate and effective accident management strategies. If the potential consequences are very severe, it might be preferable not to reflood the core if the only available water supply is insufficiently borated. If the consequences are minor, the current procedures to reflood immediately upon recovery with the maximum flow rate of water (borated or unborated) is a necessary approach.

The primary concern is, of course, a super prompt-critical excursion which would result in rapid disintegration of fuel, rapid molten fuel coolant interaction, and the production of a large pressure pulse capable of directly failing the reactor vessel. The analyses conducted in this study indicate that the rapid disintegration of fuel is not likely under the conditions of reflooding a hot core, which may or may not be degraded. Analysis also indicates that a maximum power excursion produces a fuel enthalpy of 73 cal/g, corresponding to a temperature rise of 1300°F in the fuel. Doppler feedback is the principle mechanism for terminating rapid transients in low enriched uranium-water systems and is adequate to limit the energetics of reflood recriticality to a level below which the reactor vessel would be threatened by a pressure pulse.

If the reactor remains critical following an initial excursion at the time of reflooding (i.e., reflood is conducted without boration), it will either enter an oscillatory mode in which water periodically enters and is expelled from the core or it will approach a quasi-steady power level. In either case, the average power level achieved will be determined by the balance between the reactivity added and the feedback mechanisms. Based on the analyses conducted in this study, a recriticality event is likely to produce core power levels less than about 20% of normal power (and probably not much more than 10% of normal power), but may be significantly above the decay heat level ( $\approx 2\%$  after 15 minutes).

The main concern of remaining critical during and after reflood becomes the increasing temperature of the suppression pool and the potential for containment over-pressurization. Without the RHR system providing suppression pool cooling and assuming that the power level is at 10% of full power, analysis indicates that the containment will be over-pressurized in slightly more than a half hour. With full RHR suppression pool cooling capacity

utilized, the excess steam (i.e., that above the RHR capacity) to the suppression pool would represent only 3% of full power. Under these conditions, over two hours are available to shutdown the reactor before the containment would be over-pressurized. In either case, if the reactor is not shutdown, the containment will become over-pressurized and the suppression pool will reach saturation conditions, which will cause the core cooling systems to fail. This could subsequently lead to further core damage and a direct release path to the environment. (This situation is true for the Peach Bottom plant, which was used as the reference BWR. It is recognized that newer plants may have low pressure systems that can operate under saturation conditions).

To shutdown the reactor, without the availability of control blades (which may have relocated from the core), boration is required. Analyses indicate that approximately 700 ppm  $^{10}\text{B}$  are required to ensure subcriticality for all conditions, including standing fuel rods. The standby liquid control (SLC) system, which is the primary method of emergency boration, is designed to provide boration in one-half to two hours, depending on the flow rate of the boration pumps. Therefore, the boration rate appears to be marginally adequate to avoid containment over-pressurization, if it is initiated at the same time as the core reflood and if the boration concentration is adequate to terminate the reaction. The time allowed for boration is increased if RHR suppression pool cooling is utilized at full capacity at the time of core reflood. However, the use of RHR at full capacity in the suppression pool cooling mode would require that reactor vessel coolant injection be performed by another system (e.g., HPCI, RCIC, or low pressure core spray).

It should be noted that emergency boration, under the conditions described above, does not prevent the occurrence of a recriticality event, but rather, terminates the event and prevents any severe consequences from the event. To prevent the potential for recriticality, the boration must occur prior to core reflood. However, as stated previously, recriticality is not expected to fail the vessel and the main concern becomes the continuance of the event to the point of containment failure.

### Recovery Strategies

Recovery of control in a postulated station blackout or ATWS event is a primary concern. Two accident management strategies for terminating a recriticality event are identified in this study and are described below.

The first recommended strategy is to borate at the time of reflood for core damage events where control blade material may have relocated from the core or not inserted. The first boration alternative in BWRs is to use the SLC system, which is normally borated for response to ATWS events.

If the SLC system is unavailable or fails, numerous alternate methods of boration could be considered.<sup>1</sup> These alternative methods include connecting the SLC tank to the HPCI turbine-driven pump suction using temporary connections (such as firehoses and appropriate fittings) for injection into the core, or boration of the injection water supply (i.e., the condensate storage tank). In the latter strategy, a large quantity of sodium pentaborate would be stored in a location convenient to the tank and equipment and procedures would be in place to quickly borate the water supply to the appropriate concentration of  $10^8$ . Since the condensate storage tank is the normal suction source for the HPCI and RCIC system, temporary connections would not be necessary to use these systems for boration injection.

Other options include depressurizing and using low pressure systems. However, all low pressure systems are presently dependent on ac power, which may not be available in some scenarios (e.g., continued station blackout). A low pressure system pump that is not completely dependent on the normal ac power supplies (e.g., turbine-driven low pressure pump, dc-powered pony motor for pumps, dedicated diesel generator, etc.) could alleviate this concern.

The second accident management strategy involves suppression pool cooling. For heat removal in ATWS events, full RHR suppression pool cooling is established as quickly as possible. RHR is capable of removing more than 7% of full core power. This strategy, while usually applied to ATWS events, is equally effective for severe accidents where control material may have relocated from the core. The use of RHR would greatly extend the amount of time available to terminate the recriticality event and in so doing prevent the containment from failing. Such a strategy presumes the operability of the RHR system and the availability of ac power supplies. In addition, using the RHR system in the suppression pool cooling mode requires that another system be used for injection into the reactor vessel.

### Impact of Implementing Strategies

The effect of the above accident management strategies on the probability of containment failure due to over-pressurization was investigated to determine the benefit of implementing these strategies. As stated earlier, the dominant accident sequences for Peach Bottom are short-term and long-term station blackout events, with core damage frequencies of  $4.5E-6$  per reactor year and  $1.7E-6$  per reactor year, respectively. The potential for recriticality following station blackout exists if ac power is restored and unborated coolant injection is initiated within a time window of potential recriticality. It was estimated that between 12% and 1% of the time, depending on the specific sequence, ac power would be restored and coolant

---

<sup>1</sup>In private communications with a BWR plant, the authors verified the existence of alternate emergency boration procedures and boron supplies to borate to the levels necessary to limit recriticality.



injection would be initiated within the recriticality time window. For short-term station blackout, the probability of recriticality was estimated to be  $5.6E-7$  per reactor year. For long-term station blackout, the probability of recriticality was estimated to be  $6.9E-7$  per reactor year.

Based on present operating philosophies and guidance it was assumed that the operators would not immediately borate and initiate RHR suppression pool cooling at the time of core reflood. Thus, the probability of suppression pool saturation and containment over-pressurization in about one half hour is the same as the probability of a recriticality event occurring. Again, this probability is  $5.6E-7$  per reactor year for short-term station blackout and  $6.9E-7$  per reactor year for long-term station blackout.

If the above accident management strategies were implemented at a plant, a recriticality event could be terminated prior to reaching saturation conditions in the suppression pool and in so doing avert containment failure. The probability that the above accident management strategies fail to avert containment failure is estimated in this report. Since the primary means of boration (i.e., from the SLC system) may only be marginally adequate if the excess steam to the suppression pool is greater than that generated when the reactor is generating about 10% power, which may occur if RHR suppression pool cooling fails, failure of either accident management strategy was assumed to eventually result in containment failure. The probability of boration failure was estimated to be  $5.0E-2$ , based on the NUREG/CR-4550 ATWS analysis value for operator failure to initiate boration within a very short time frame (approximately 4 minutes). It is assumed that the boration concentration when successfully injected is adequate to terminate the reaction. The value for RHR suppression pool cooling failure was also estimated to be  $5.0E-2$ , assuming ac power was restored and the dominant failure is operator failure to immediately establish adequate RHR suppression pool cooling.

If the accident management strategies were implemented, the probability of a short-term station blackout event, followed by a recriticality event, and the event not being terminated prior to containment failure was estimated to be  $5.6E-8$  per reactor year. For long-term station blackout, the probability of the accident management strategies failing to avert eventual containment failure was estimated to be  $6.9E-8$  per reactor year.

The results of the analysis are provided in Table 1. These results indicate that implementation of the accident management strategies suggested in this report should provide approximately a factor of 10 reduction in the potential for a recriticality event to cause containment failure (and subsequently further core damage).

TABLE 1. Recriticality Analysis Results for Station Blackout Sequences

<u>Sequence</u>	<u>Probability of Core Damage (per reactor year)</u>	<u>Probability of Containment Failure Without Strategies (per reactor year)<sup>1</sup></u>	<u>Probability of Containment Failure Using Strategies (per reactor year)</u>
SSBO	4.5E-6	5.6E-7	5.6E-8
LSBO	1.7E-6	6.9E-7	6.9E-8
TOTAL	6.2E-6	1.25E-6	1.25E-7

<sup>1</sup>This is also the probability per reactor year of a recriticality event.

## CONTENTS

ABSTRACT . . . . .	iii
SUMMARY . . . . .	v
1.0 INTRODUCTION . . . . .	1.1
2.0 POTENTIAL FOR RECRITICALITY . . . . .	2.1
2.1 BWR CORE MELTDOWN PHENOMENOLOGY . . . . .	2.1
2.1.1 Control Blade Melting . . . . .	2.2
2.1.2 Core Geometry Changes . . . . .	2.4
2.2 CORE MELT CALCULATIONS . . . . .	2.11
2.2.1 MARCH Code Calculations . . . . .	2.11
2.2.2 Results of Calculations . . . . .	2.15
2.3 DOMAIN AND POTENTIAL CONSEQUENCES OF RECRITICALITY . . . . .	2.37
2.3.1 Domain of Critical Configurations . . . . .	2.38
2.3.2 Excursion Analysis . . . . .	2.50
2.3.3 Debris Bed Dryout Power Limits . . . . .	2.53
2.3.4 Containment System Effects . . . . .	2.63
2.4 REFERENCES . . . . .	2.66
3.0 ACCIDENT SEQUENCES . . . . .	3.1
3.1 STATION BLACKOUT (SBO) . . . . .	3.1
3.1.1 Loss of Offsite Power Event Tree Headings . . . . .	3.11
3.1.2 Short-term Station Blackout (SSBO) . . . . .	3.14
3.1.3 Long-term Station Blackout (LSBO) . . . . .	3.16
3.1.4 Recriticality Potential Following Station Blackout . . . . .	3.19
3.2 ANTICIPATED TRANSIENT WITHOUT SCRAM . . . . .	3.28
3.2.1 ATWS Event Tree Headings . . . . .	3.28
3.2.2 Dominant ATWS Sequences . . . . .	3.34
3.2.3 Recriticality Potential Following ATWS . . . . .	3.37
3.3 REFERENCES . . . . .	3.39

CONTENTS (contd)

4.0	STRATEGY DESCRIPTIONS . . . . .	4.1
4.1	REFLOOD BORATION STRATEGY FOR CORE MELT EVENTS . . . . .	4.1
4.1.1	Strategy . . . . .	4.1
4.1.2	Justification . . . . .	4.2
4.2	HEAT REMOVAL STRATEGY FOR CORE MELT EVENTS . . . . .	4.3
4.2.1	Strategy . . . . .	4.3
4.2.2	Justification . . . . .	4.3
5.0	CONCLUSIONS . . . . .	5.1
5.1	RELATIVE TIMING OF CONTROL BLADE AND FUEL ROD MELTING . . . . .	5.1
5.2	CORE GEOMETRY CHANGES OCCURRING DURING MELTING AND CORE REFLOOD . . . . .	5.2
5.3	NATURE OF THE REACTIVITY TRANSIENT . . . . .	5.2
APPENDIX A:	$K_{\infty}$ CALCULATIONS . . . . .	A.1
APPENDIX B:	SPREADSHEET INPUT . . . . .	B.1
APPENDIX C:	NITAWL INPUT . . . . .	C.1
APPENDIX D:	XSDRNPM INPUT . . . . .	D.1
APPENDIX E:	MCDAN INPUT . . . . .	E.1
APPENDIX F:	DANCOFF CORRECTION FACTORS . . . . .	F.1
APPENDIX G:	INSTRUMENTATION CONSIDERATIONS . . . . .	G.1



TABLES

<u>Table</u>	<u>Page</u>
1. Recriticality Analysis Results for Station Blackout Sequences . . . . .	xii
2.1. Summary of Key Accident Events . . . . .	2.12
2.2. Early Mlt Station Blackout Events (Case PBEM2) . . . . .	2.30
2.3. Calculated Maximum $k_{\infty}$ for Spherical Particles in Water . . . . .	2.40
2.4. Maximum Calculated $k_{\infty}$ for Pellet Equivalent Particles in Water . . . . .	2.46
2.5. Calculated $k_{\infty}$ Values for Fuel Rods at Assembly Pitch in Water . . . . .	2.48
2.6. Calculated Critical Masses for Spherical Particles and Pellets in Water . . . . .	2.49
2.7. Capacity of BWR Makeup Pumps . . . . .	2.62
3.1. Short-term Station Blackout Dominant Cutsets . . . . .	3.17
3.2. Long-term Station Blackout Dominant Cutsets . . . . .	3.20
3.3. Recriticality Time Windows for Station Blackout Sequences . . . . .	3.21
3.4. Recriticality Potential for SSBO Dominant Cutsets . . . . .	3.23
3.5. Accident Management Strategies Implemented for SSBO Dominant Cutsets . . . . .	3.25
3.6. Recriticality Potential for LSBO Dominant Cutsets . . . . .	3.26
3.7. Accident Management Strategies Implemented for LSBO Dominant Cutsets . . . . .	3.27
3.8. Recriticality Analysis Results for Station Blackout Sequences . . . . .	3.29
3.9. ATWS Dominant Cutsets . . . . .	3.38

TABLES (contd)

<u>Table</u>	<u>Page</u>
A.1. Calculated $k_{\infty}$ for Spherical Particles in Water (0 PPM $^{10}\text{B}$ ) . . .	A.1
A.2. Calculated $k_{\infty}$ for Spherical Particles in Water (200 PPM $^{10}\text{B}$ ) . .	A.2
A.3. Calculated $k_{\infty}$ for Spherical Particles in Water (500 PPM $^{10}\text{B}$ ) . .	A.3
A.4. Calculated $k_{\infty}$ for Spherical Particles in Water (1000 PPM $^{10}\text{B}$ ) . .	A.4
F.1. Dancoff Factors for Spherical Particles in Water . . . . .	F.1

## FIGURES

<u>Figure</u>	<u>Page</u>
2.1. DF-4 Cross Section . . . . .	2.3
2.2. BWR Flow Areas with Loss of Structures (ORNL) . . . . .	2.5
2.3. Sketch of Reactor Vessel and Core at Start of Melting . . . . .	2.6
2.4. Volume of Lower Plenum Debris (ORNL) . . . . .	2.7
2.5. TMI-2 End-State Accident Configuration . . . . .	2.9
2.6. Logarithmic Plot of the Cumulative Weight Distribution for TMI-2 Core Debris Grab Samples . . . . .	2.10
2.7. Mixture Level as a Function of Dimensionless Time $(t - t_u)/\tau$ for Cases PBTBO and PBTBS . . . . .	2.14
2.8. Grand Gulf Accident Event Timing . . . . .	2.16
2.9. Peach Bottom Accident Event Timing . . . . .	2.17
2.10. Average Core Temperature Change, $(T - T_0)$ , as a Function of Dimensionless Time After Core Uncovery, $(t - t_u)/\tau$ , for Group 1 . . . . .	2.18
2.11. Average Core Temperature Change, $(T - T_0)$ , as a Function of Dimensionless Time After Core Uncovery, $(t - t_u)/\tau$ , for Group 2 . . . . .	2.19
2.12. Average Core Temperature Change, $(T - T_0)$ , as a Function of Dimensionless Time After Core Uncovery, $(t - t_u)/\tau$ , for Cases PBTBS, PBTBO . . . . .	2.20
2.13. Fraction Fuel Rods Melted as a Function of Dimensionless Time After Core Uncovery, $(t - t_u)/\tau$ , for Group 1 . . . . .	2.21
2.14. Fraction Fuel Rods Melted as a Function of Dimensionless Time After Core Uncovery, $(t - t_u)/\tau$ , for Group 2 . . . . .	2.22
2.15. Fraction Control Blades Melted as a Function of the Average Core Temperature for All Cases . . . . .	2.24
2.16. Fraction Control Blades, Channel Boxes, and Fuel Rods Melted as a Function of Dimensionless Time After Core Uncovery, $(t - t_u)/\tau$ , for Case PBTBO . . . . .	2.25

FIGURES (contd)

<u>Figure</u>	<u>Page</u>
2.17. Fraction Control Blades, Channel Boxes, and Fuel Rods Melted as a Function of Dimensionless Time After Core Uncovery, $(t - t_u)/\tau$ , for Case PBTBS . . . . .	2.26
2.18. Fraction Control Blades, Melted by Radial Region as a Function of Dimensionless Time After Core Uncovery, $(t - t_u)/\tau$ for Case PBTBO . . . . .	2.27
2.19. Highest Elevation of Unmelted Control Blade as a Function of Core Radius and Time After Core Uncovery, $(t - t_u)$ , for Case PBTBO . . . . .	2.28
2.20. Vessel Pressure versus Time for Peach Bottom Early Melt Station Blackout (PBEM2) . . . . .	2.31
2.21. Reactor Vessel Water Level versus Time for Peach Bottom Early Melt Station Blackout (PBEM2) . . . . .	2.32
2.22. Core Temperature versus Time for Peach Bottom Early Melt Station Blackout (PBEM2) . . . . .	2.33
2.23. Melt Fraction versus Time for Peach Bottom Early Melt Station Blackout (PBEM2) . . . . .	2.34
2.24. Fraction of Core in Lower Head versus Time for Peach Bottom Early Melt Station Blackout (PBEM2) . . . . .	2.35
2.25. Lower Head Debris Temperature versus Time for Peach Bottom Early Melt Station Blackout (PBEM2) . . . . .	2.36
2.26. Calculated $K_{\infty}$ for $UO_2$ Fuel Particles in Water with 0 PPM $^{10}B$ . . . . .	2.41
2.27. Calculated $K_{\infty}$ for $UO_2$ Fuel Particles in Water with 200 PPM $^{10}B$ . . . . .	2.42
2.28. Calculated $K_{\infty}$ for $UO_2$ Fuel Particles in Water with 500 PPM $^{10}B$ . . . . .	2.43
2.29. Calculated $K_{\infty}$ for $UO_2$ Fuel Particles in Water with 1000 PPM $^{10}B$ . . . . .	2.44
2.30. Envelope of Calculated $K_{\infty}$ s for $UO_2$ Fuel Particles in Water with $^{10}B$ Concentrations of 0, 200, 500, and 1000 PPM . . . . .	2.45



FIGURES (contd)

<u>Figure</u>	<u>Page</u>
2.31. Steady-State Dryout Heat Flux and Bed Quench Heat Flux Data Compared With Steady-State Lipinski Model (P=0.1 MPa, e=0.4) (From References 2.17 and 2.18) . . . . .	2.55
2.32. Lipinski Correlation of Debris Bed Dryout Heat Flux (Ref. 2.18) . . . . .	2.56
2.33. Fraction of Core Enclosed in Debris Bed as a Function of Bed Diameter . . . . .	2.57
2.34. Debris Bed Dryout Power Density Limit at 15 and 200 psia for 0.1 and 0.5 inch Particle, $F_A = 2.0$ . . . . .	2.58
2.35. Ratio of Debris Bed Power to Core Operating Power . . . . .	2.60
2.36. Coolant Boiloff Rate From a Critical Debris Bed . . . . .	2.61
2.37. Containment Over-pressure Time as a Function of Energy to Pool . . . . .	2.65
3.1. Peach Bottom Loss of Offsite Power Event Tree . . . . .	3.3
3.2. Station Blackout Event Tree . . . . .	3.15
3.3. Peach Bottom Case B ATWS Event Tree . . . . .	3.30
3.4. Simplified ATWS Event Tree . . . . .	3.35

## 1.0 INTRODUCTION

This report addresses the potential for a recriticality, following a low probability severe accident and subsequent reflooding of the fuel in a Boiling Water Reactor (BWR). It provides scenario sequence definition and accident management strategies that could be used to mitigate or terminate the postulated recriticality events.

Analyses of severe BWR accidents indicate that, while the core is in the process of heating and melting, one of the earliest components to melt and relocate are the steel blades that contain the  $B_4C$  control material. If the core were then to be reflooded following relocation of the control blades, the possibility exists for the core to become critical again without an adequate means of control. This study's objective is to explore the likelihood of recriticality and the consequences thereof. If a significant likelihood of recriticality exists, accident management procedures would be warranted which could prevent recriticality or mitigate the consequences of recriticality, in order to return the plant to a safe stable state.

Due to modelling and phenomenological uncertainties related to void fraction, debris bed size, particle size, etc. and the lack of an analytical tool capable of performing the complex analyses required to address the complex interactions of these parameters, a conservative bounding analysis was conducted. If the conservative bounding analysis indicates acceptable consequences (e.g., no recriticality or a recriticality event resulting in a benign pressure pulse that is non-threatening to the integrity of the containment and accident management strategies can be implemented to successfully prepare for and terminate the event), further, more sophisticated model development and analyses may not be necessary to resolve the modelling and phenomenological uncertainties. However, if the bounding analysis indicates unacceptable consequences (e.g., a significant recriticality event that creates a large pressure pulse and potentially fails the containment), further research should be identified to resolve the uncertainties and phenomenological issues.

In order to establish whether the development of accident management strategies to control recriticality is necessary, some important questions must be addressed.

- Is recriticality credible following the initial stages of severe core damage?
- How likely is recriticality? Is it a factor in risk dominant sequences? How long is the time window for recriticality? Are recovery actions likely to occur in the time window?

- Would existing equipment and procedures result in the appropriate control actions without the need for additional accident management procedures?

The determination of the most appropriate accident management strategies requires resolution of an additional issue.

- What are the potential consequences of recriticality? Is an excursion possible which has the potential to disrupt fuel and fail the vessel and/or containment? Would a quasi-steady power level be developed? If so, at what level?

Primarily using the NUREG-1150 risk study for the Peach Bottom plant as a technical basis, the sequences with the highest predicted frequencies are used to characterize accident sequences which would be likely to result in core damage. The most likely recovery mechanisms that could arrest these sequences are then identified. It is assumed that if the cooling water systems can be recovered, the operators would use the systems to restore core cooling as quickly as possible. The reflooding of the core with the attendant potential for initiating recriticality would then be a concern.

The accident management strategies discussed in this report focus on the control of recriticality by means of soluble poison addition and containment heat removal. The offered strategies are not developed in the degree of detail that would be required for operating procedures for a specific plant. It is recognized that the development of specific, effective procedures are most appropriately accomplished by the plant staff.

To provide the needed analysis of existing information, Section 2.0 of this report addresses recriticality; 3.0 sequence definition; 4.0 strategy description; and 5.0 conclusions and recommendations.

## 2.0 POTENTIAL FOR RECRITICALITY

This chapter addresses the potential for recriticality. It begins with core melt phenomenology, continues with core melt calculations, provides potential recriticality considerations, and concludes with potential consequences of recriticality.

### 2.1 BWR CORE MELTDOWN PHENOMENOLOGY

During a severe accident, the neutron absorbing control rods and control blades are expected to melt before the fuel rods. This occurs because the control materials are contained in metallic structures which have lower melting points than the oxide ( $UO_2$ ) fuel rod material. Thus, the control rods and fuel rods will become separated during the core melt; and reflooding of the core has the potential to result in recriticality. For a pressurized water reactor (PWR), reflooding is normally accomplished using borated water supplies; and recriticality is generally perceived not to be very credible. However, for a boiling water reactor (BWR), reflood is normally accomplished using unborated water; and recriticality is believed to be credible. Therefore, this report addresses the potential for recriticality events only in BWRs.

Core heatup commences when the core becomes uncovered. The timing of core uncovering, heatup, and melting may occur over tens of minutes or a few hours, and depends on the nature of the accident sequence. There are a number of phenomenological issues or areas of uncertainty in this core melt process. These include:

- The melting and relocation of the control blades, the fuel rod cladding, and the fuel rods.
- The effects of the core melt and relocation on steam generation, flow blockages, steam-zirconium reactions, and hydrogen generation.
- The effects of core melt and relocation on the surrounding structures (such as the core plate and the core baffles) and on the lower head structures (such as the lower head itself, control rod guide tubes, instrument tube penetrations, and drain lines).
- The potential for recriticality as a result of changes in core geometry due to melting and the damage that occurs during core reflood.
- The coolability of a damaged or molten core, assuming reflooding can be accomplished.



These issues have varying degrees of importance, depending on whether the interest is in risk assessment, accident management, or recriticality. All of the issues are important, although not of equal importance, to the analysis of severe accidents and their consequences. A lesser number are important to the development of in-vessel accident management strategies. For the assessment of BWR recriticality only the following issues are important:

- The relative time of control blade and fuel rod melting (separation of the control blades from the fuel rods is what makes recriticality possible).
- The core geometry changes occurring during melting and core reflood (the reactivity of the damaged core depends on the debris mass, fuel particle shapes, and porosity).
- The nature of the reactivity transient (the ability to manage the recriticality event depends on whether it is a core-damaging or explosive transient event or is a benign event, which gradually increases to higher power levels).

#### 2.1.1 Control Blade Melting

The first issue deals with the timing of control blade melt and relocation. Two experiments have been performed that support early control blade melting (i.e., control blade melt and relocation prior to fuel rod melting): the DF-4 experiment (Ref. 2.1) by Sandia National Laboratory and the CORA 16 experiment (Ref. 2.2) by KfK (Karlsruhe, FRG). Figure 2.1 is a sketch showing the cross section of the DF-4 experiment and the arrangement of the fuel rods and the simulated channel box and control blade. The fuel length was about 19 inches. The CORA 16 experiment was of a comparable scale. Both experiments showed melting and relocation of the control blades to the bottom, leaving standing fuel rods behind. The CORA 16 experiment indicates the effective melting and relocation temperature of the control blades is approximately 2280°F, which is about 270°F below the stainless steel melting point (2550°F). This decreased effective melting temperature is due to alloying reactions with the B<sub>4</sub>C neutron absorber.

Calculations by Ott (Ref. 2.3) for the DF-4 experiment confirm that an assumed reduction of the control blade melting temperature by 200°F (to 2350°F) is necessary to explain the observed timing of the control blade melt relocation. Ott used a specially modified version of the BWR SAR code in his calculations. Special modifications were required because, in the experiment, nearly all of the heat losses were in the radial direction into the zirconia shroud. These radial heat losses are typically negligible and are not modeled in the normal full-sized core model. The modifications allowed the special experimental geometry to be accurately modeled. The DF-4 experimenters

# BWR CORE

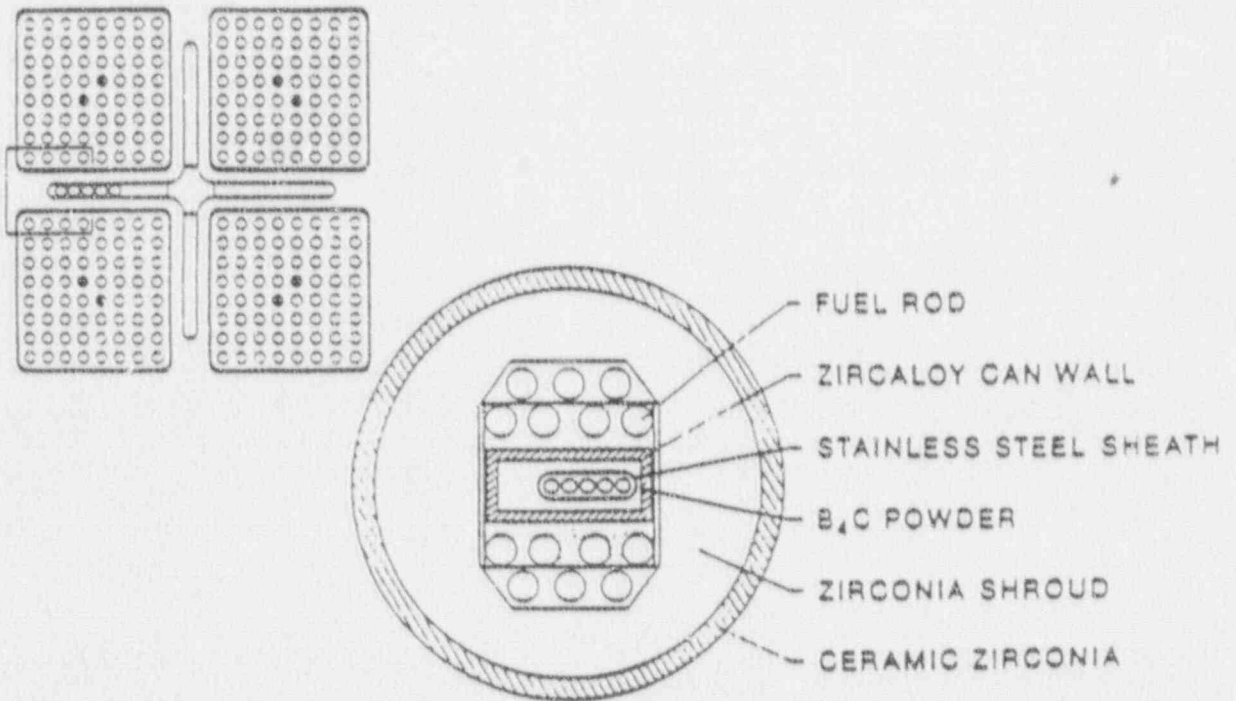


FIGURE 2.1. DF-4 Cross Section

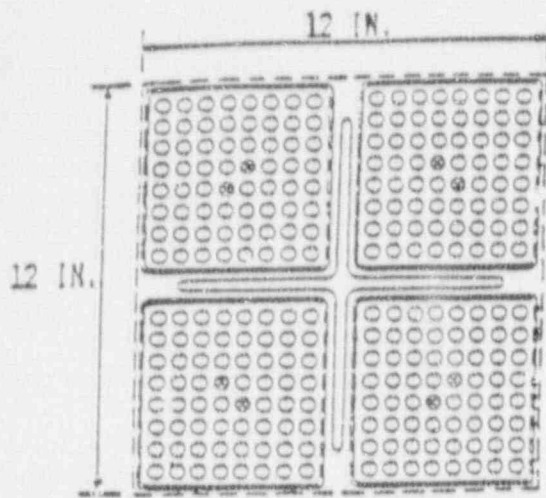
reported an "extensive" blockage was formed at the bottom from the relocated control blade and channel box melt. However, the blockage had little effect on the steam-zirconium reaction. The relocated materials continued to oxidize with about half the hydrogen produced after the melt relocation.

In conclusion, the DF-4 and CORA 16 experiments confirm the early melt relocation of the control blades. Also, the melt relocation temperature is believed to be somewhat (200-300°F) below the melting point of stainless steel. Because of the small size of the fuel assemblies used in the DF-4 and CORA 16 experiments, these experiments may not provide a complete picture of the melt and relocation phenomena associated with typical nuclear power plant fuel assemblies. The experiments provide little information on whether relocated blade melt would accumulate at the bottom of the core on the core plate or would simply pour through the existing flow holes. The extent of relocation would affect the location of blade remnants and other issues such as hydrogen generation, core slumping into the lower head, the lower head failure mode, and in-vessel accident management strategies. The planned FLHT-6 experiment in the NRU reactor will be 12 feet long and may give a better picture of length effects on blade and channel box melt relocation.

### 2.1.2 Core Geometry Changes

This section discusses the issues relating to the effects of core geometry changes which occur during melting and core reflooding. Figures 2.2 to 2.4 illustrate some of the theoretically possible types of fuel rod and core material rearrangements which could occur with core melting. These conceptual core conditions are based primarily on considerations of the material volumes and their possible relocations. Figure 2.2 illustrates that the potential water volume in the assembly could progressively increase from 58% to 67% by removal of the control blades and channel boxes and clad (by melting). Fuel rearrangements which increase the water content could have a higher neutron multiplication constant. Figure 2.3 is an illustration of how rod bowing could lead to fuel rearrangements. Figure 2.4 illustrates that relocation of the whole core in the form of a debris bed, with a porosity of 40%, would fill most of the lower head.

The illustrations do not take into account the core damage which is expected to occur during the reflood process. Because the core is severely overheated at the time of blade melting, reflood would be expected to result in fracturing and shattering of the fuel. A number of experiments have been performed which provide information on fuel rod shattering and the types of debris beds which might form after reflood. The principle experiments are those of Chung (Ref. 2.4) and Katanishi (Ref. 2.5). Two of the Severe Fuel Damage experiments (SFD Scoping Test and SFD-1) were also water-quenched; however, no specific evaluation of those tests for information on rod shattering is apparent. The Three Mile Island Unit 2 (TMI-2) accident also provides relevant information.



CORE HEATUP LEADS TO PROGRESSIVE  
RELOCATION OF UNIT CELL COMPONENTS

- ALL STRUCTURES INTACT

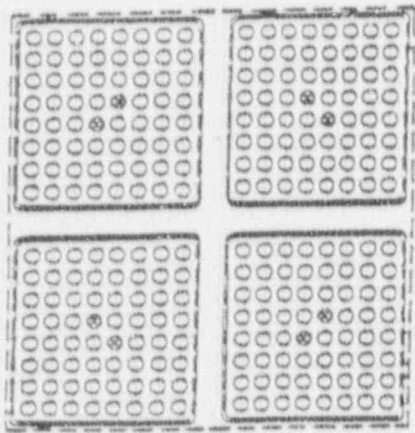
FLOW AREAS

FUEL ASSEMBLY 0.440

INTERSTITIAL 0.140

0.580

STRUCTURE CROSS SECTION 0.420



- LOSS OF CONTROL BLADE

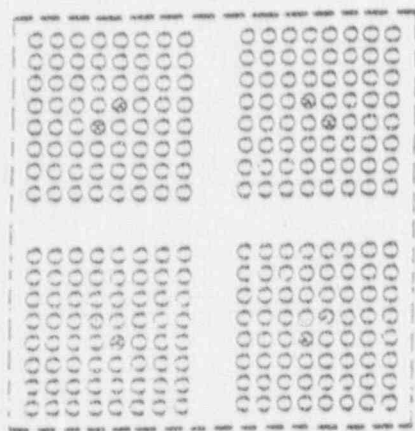
FLOW AREAS

FUEL ASSEMBLY 0.440

INTERSTITIAL 0.183

0.623

STRUCTURE CROSS SECTION 0.377



- LOSS OF CANISTER WALLS

FLOW AREA 0.670

STRUCTURE CROSS SECTION 0.330

FIGURE 2.2. BWR Flow Areas with Loss of Structures (ORNL)



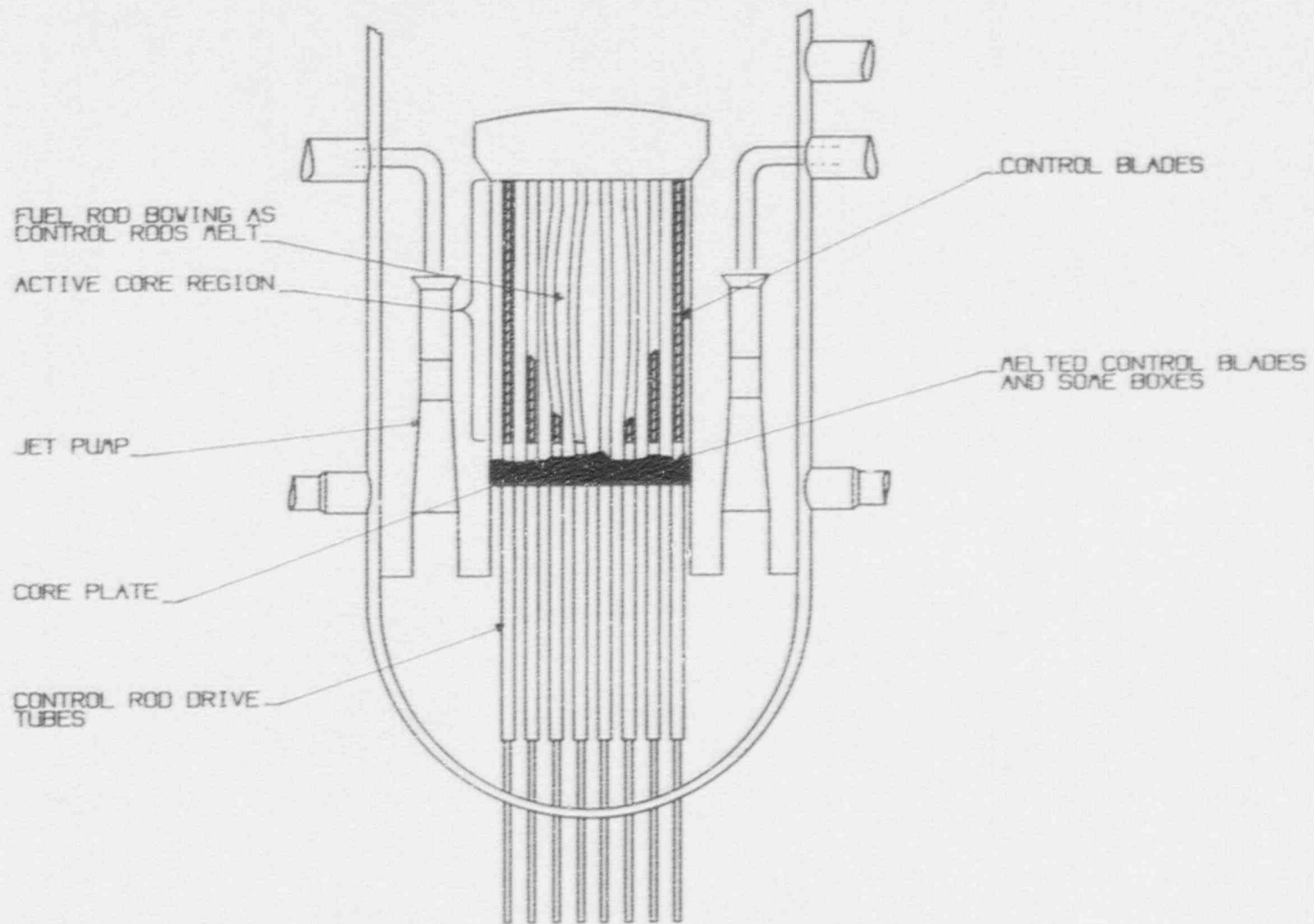


FIGURE 2.3. Sketch of Reactor Vessel and Core at Start of Melting

HEIGHT OF DEBRIS (POROSITY 0.40) IN LOWER PLENUM  
DEPENDS ON STATUS OF CONTROL ROD GUIDE TUBES.

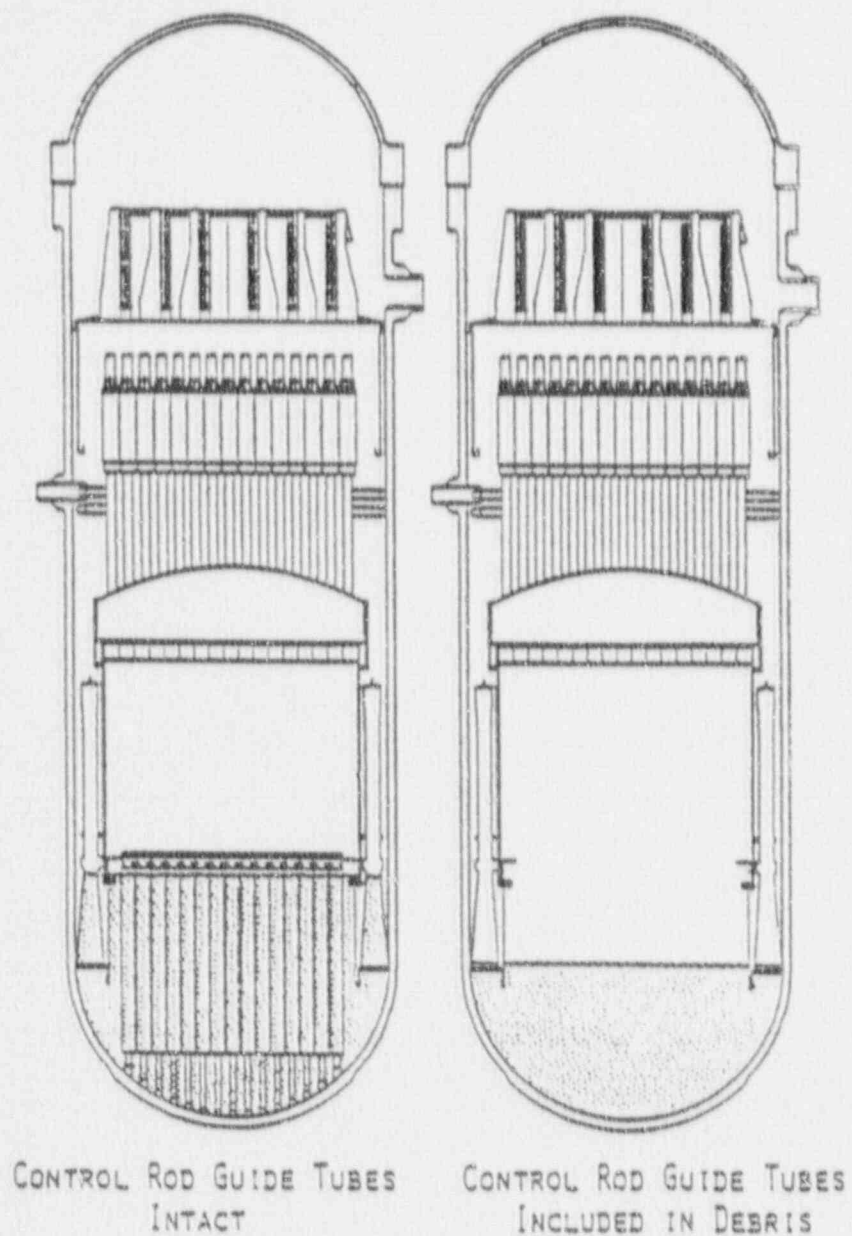


FIGURE 2.4. Volume of Lower Plenum Debris (ORNL)

Chung performed experiments to establish cladding embrittlement criteria during loss of coolant accident (LOCA) reflood. His experiments indicate that shattering depends on the extent of cladding oxidation. The experiments indicate that an equivalent cladding reaction of 30% produces BWR cladding failure (shattering) at approximately 2600°F. MARCH calculations generally indicate core-wide or average cladding oxidation of only a few percent at the onset of cladding melting (MARCH calculations will be discussed further in Section 2.2.1). Peak local oxidation is calculated to be about 25% to 35%. Depending on how much oxidation actually occurs during reflood, Chung's shattering criteria indicate shattering may be expected in some high oxidation regions of the core prior to the start of cladding melting.

Katanishi has reported experiments in which shattering was observed for fuel rods quenched from temperatures near 2300°F. The peak measured oxide layer thickness corresponded to oxidation of about 35% of the original zircaloy thickness of 0.024 inches. Thus, about 0.016 inches of unoxidized metal remained. Katanishi's results seem to be consistent with Chung's more rigorous criteria for fuel handling and transport but not with his LOCA reflood criteria.

Figure 2.5 diagrams the TMI-2 core end-state conditions (Ref. 2.6). Standing fuel rods were found in some regions at the periphery of the core. A bed of loose core debris was found above a region of previously molten material. Relocated core melt and a bed of loose debris were observed in the lower head. Clearly, significant fuel rod shattering occurred at some time in the accident. Unfortunately, the thermal transient experienced by the core is not well-known. From metallurgical evidence, a maximum core temperature of about 5120°F (Ref. 2.7) occurred at some time during the accident. Thus, the peak temperature was somewhat below the melting point of UO<sub>2</sub> (5150°F), but greater than the melting point of U-Zr-O ceramic (4700°F). About half the cladding is known to have reacted. Thus, the fuel rod shattering and debris bed formation observed at TMI-2 is not inconsistent with the observations of Chung and Katanishi discussed above.

Although fuel rod shattering has been observed in a number of experiments, there are little data on particle size distributions. This is unfortunate since porosity (water volume) and particle size information are required for both criticality and heat transfer analyses. Figure 2.6 plots particle sizes obtained in grab samples from TMI-2 core debris (Ref. 2.8). The mass-average (50% cumulative distribution value) particle size for these samples is seen to be about 2500 microns (0.1 inch). Particle dimensions on the order of an inch are seen for some of the resolidified melt which relocated to the lower head. For 3% enriched fuel particles in unbrated water, the maximum neutron multiplication is obtained with a particle size of about 0.8 inches and a bed porosity of 68% (see section 2.3.1). For uniformly shaped particles, a theoretical bed porosity of about 40% is obtained. This may be compared with a fuel assembly water volume of 56% in the intact core.

### Overview of the TMI-2 Accident

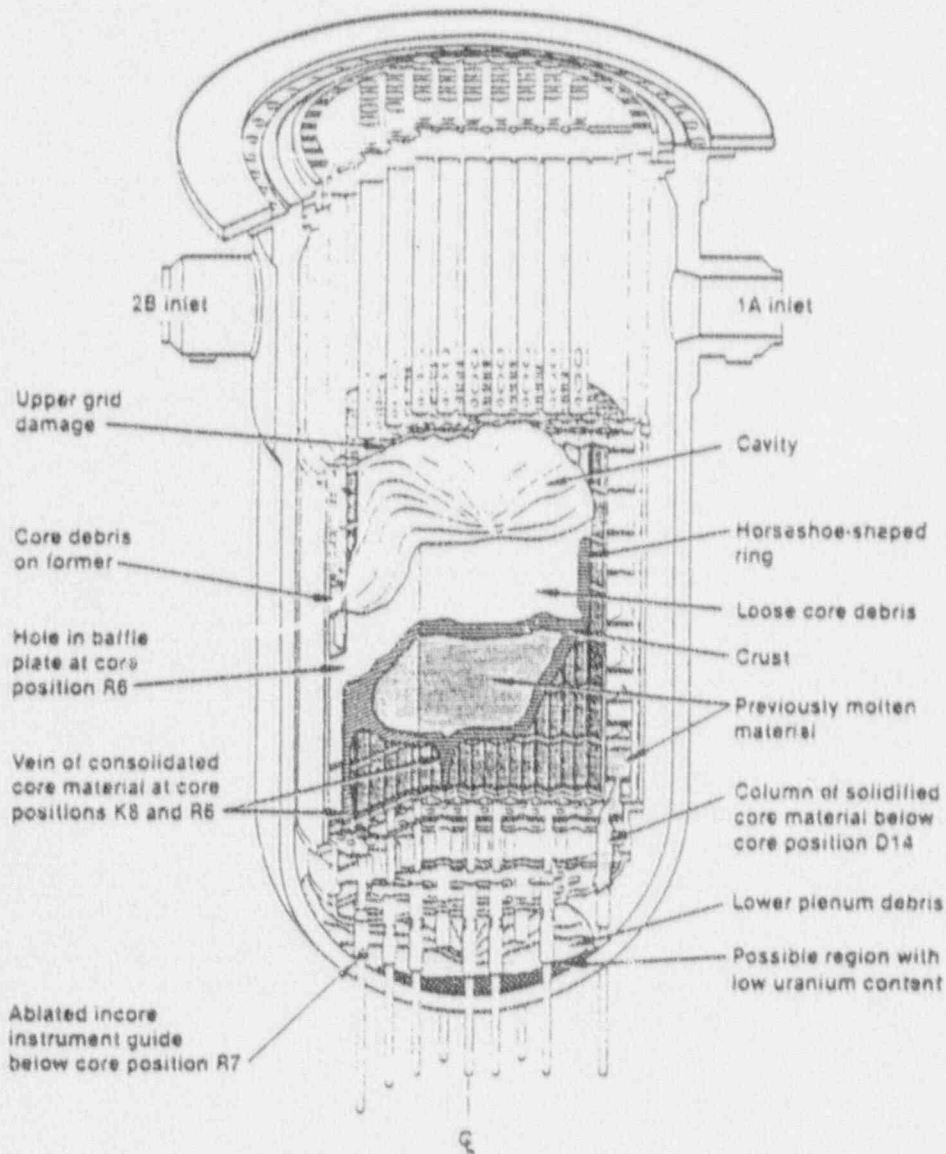


FIGURE 2.5. TMI-2 End-State Accident Configuration



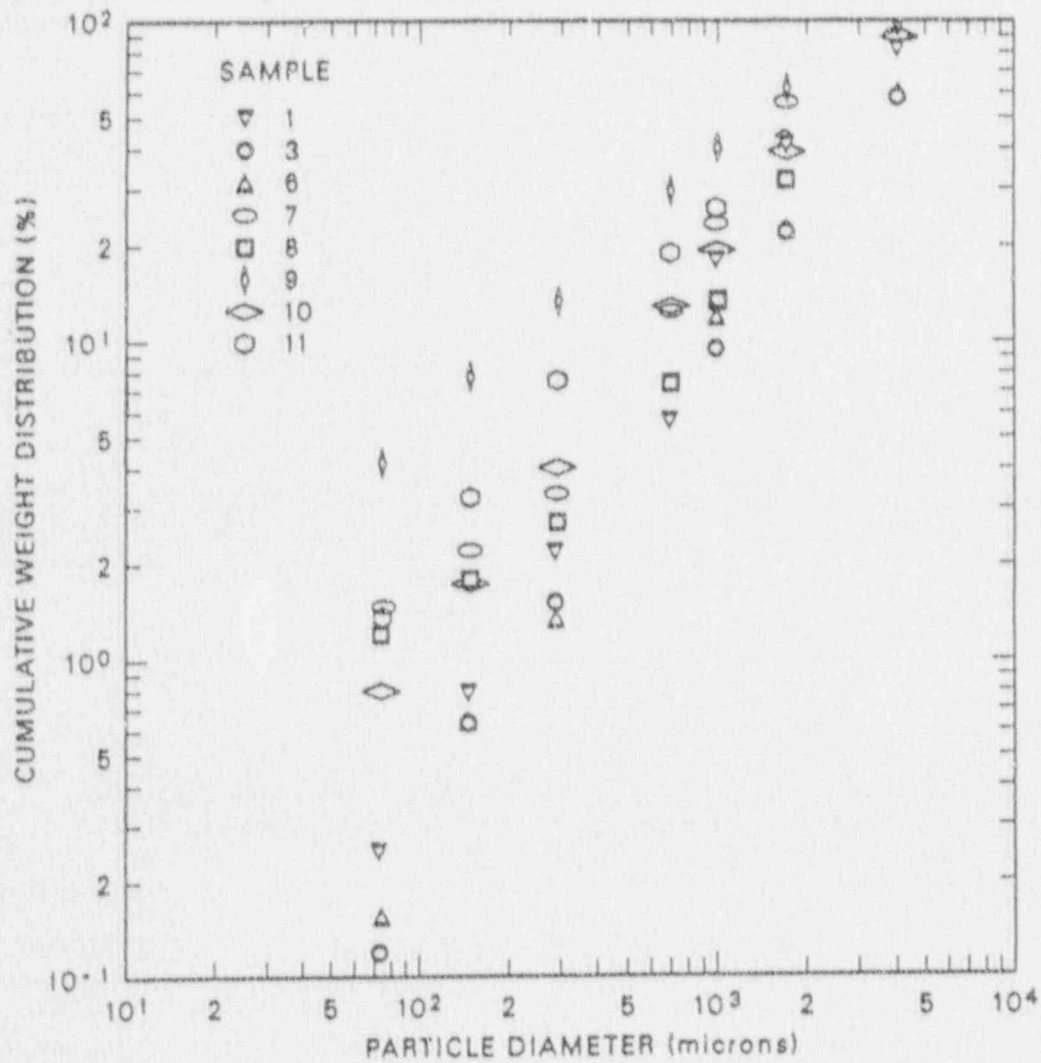


FIGURE 2.6. Logarithmic Plot of the Cumulative Weight Distribution for TMI-2 Core Debris Grab Samples

Based on this information, shattered fuel rods would be expected to form under-moderated debris beds.

Based upon the above discussion, there is a significant potential for fuel rod shattering and debris bed formation when an overheated core is reflooded with water. The shattering appears to be related to the extent of oxidation of the fuel rod cladding. It is also expected that debris beds, formed from shattered fuel rods and quenched core melt, will not be optimally moderated (i.e., they will be under-moderated and thus not a recriticality concern). Heat transfer aspects of debris bed criticality will be discussed in Section 2.3.3.

## 2.2 CORE MELT CALCULATIONS

The results of a number of computer code calculations of BWR core melt are presented in this section. This section provides:

- A discussion of the MARCH computer code analysis of the melt behavior of the control blades and control rods.
- Information on core melt timing for different accident sequences.
- Information on the relative timing of control blade and fuel rod melting.

The principle use for this information is to assess the potential for BWR recriticality. Thus, aspects of the evaluation which might be important to other issues such as hydrogen generation, core coolability, core relocation, or vessel failure are not emphasized. The accident scenarios considered include primarily those for which MARCH code results were available from previous Battelle work on NUREG-1150. Additional MARCH code calculations were performed for station blackout scenarios, and these results were used to provide more detailed information on the time of control blade melting.

### 2.2.1 MARCH Code Calculations

Table 2.1 lists Peach Bottom and Grand Gulf core melt accident scenarios for which MARCH code results were available from previous Battelle work on NUREG-1150. Also listed are a number of BWR scenarios for which MARCH calculations were performed to address station blackout scenarios specifically for this study. The calculations performed specifically for this study used a more recent version of the MARCH code (version V194) than was used in NUREG-1150 (i.e., version V192). The difference in code version accounts for the differences between sequences PBTBUX and PBTBO, which are similar cases.

TABLE 2.1. Summary of Key Accident Events

Case	Time Constants		Time of Core Uncovery min	Temp at Uncovery °F	Time of Blade Melt min	Time of Rod Melt min	Descriptions
	Tau min	Alpha °F/min					
<u>GROUP 1 (NUREG-1150)</u>							
GGTB1	33.9	21.8	483.0	571.9	552.0	579.0	Grand Gulf station blackout, late melt, no ADS
PBTBUX	18.8	42.6	67.0	577.4	109.0	134.0	Peach Bottom station blackout, early melt, no ADS
PBTB2	34.1	23.5	527.0	559.4	601.0	616.0	Peach Bottom station blackout, late melt, no ADS
PBTC3	16.1	49.7	34.0	850.6	53.0	58.0	Peach Bottom ATWS, no ADS
GGTPI	42.9	20.4	1536.0	322.8	(a)	1645.0	Grand Gulf, open valve, no RHR
GGTC	22.0	60.5	90.0	463.2	111.0	117.0	Grand Gulf, ATWS, no ADS
PBTW	71.0	18.7	2620.0	316.7	(a)	2748.0	Peach Bottom, no RHR
<u>GROUP 2 (NUREG-1150)</u>							
GGTBS	18.6	39.8	51.0	577.4	82.0	85.0	Grand Gulf station blackout, ADS at top of core
GG2E	9.6	83.4	6.0	593.7	(a)	28.0	Grand Gulf small LOCA, no makeup
PBAE	13.8	124.0	1.5	1197.0	15.8	12.0	Peach Bottom large LOCA, no makeup
PBV	17.9	44.7	3.1	1061.0	24.0	27.0	Peach Bottom LOCA outside containment
GGTQV	16.8	52.0	47.0	579.2	(a)	103.0	Grand Gulf transient, no makeup, ADS at 2 ft
<u>RECENT MARCH V194 CALCULATIONS</u>							
PBTB0	18.8	42.6	66.0	567.0	113.0	120.0	Peach Bottom station blackout, early melt, no ADS
PBTBS	34.1	23.5	530.0	564.0	649.0	716.0	Peach Bottom station blackout, late melt, ADS at 2 ft
PBEM2	18.8	42.6	65.0	567.0	127.0	132.0	Peach Bottom station blackout, early melt, ADS at 2 ft

(a) Information not available.

The NUREG-1150 accident scenarios in Table 2.1 are roughly divided into two groups, made partially for plotting convenience. The primary physical difference between the groupings is the vessel water level during core heatup and melt. For the cases in Group 1, the water level remains close to the bottom of the core. For the Group 2 cases, the water level is well below the core during core heatup. Generally, the sequences in Group 2 involve pipe break LOCAs, stuck-open valves, and cases where the automatic depressurization system (ADS) is activated. Figure 2.7 illustrates the differences in water levels as a result of ADS activation. Results are shown for Peach Bottom station blackout sequences PBTBO and PBTBS. For the PBTBS sequence in which the ADS is activated when the water level falls to 2.0 feet, the water level quickly falls well below the core. Generally, less metal-water reaction is predicted for the low water level cases.

The results in Figure 2.7 are displayed in terms of the dimensionless time after core uncovering:

$$(t - t_u)/\tau,$$

where,

- t = accident time, min
- t<sub>u</sub> = time at start of core uncovering, min
- τ = "boildown time constant," min

and

$$\tau = \rho \times A \times H \times H_{FG}/Q_{DK}$$

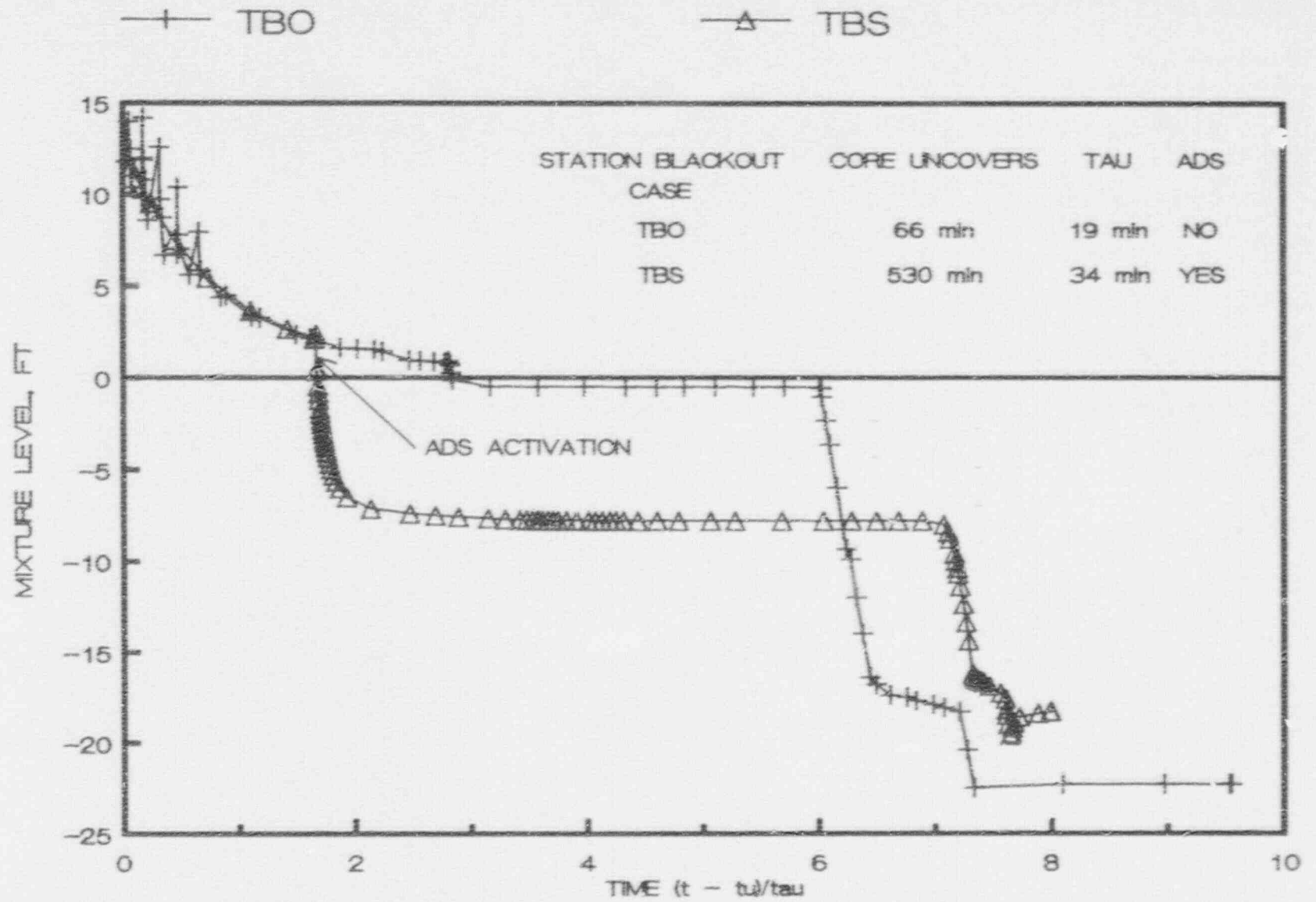
where,

- ρ = water density, lb/ft<sup>3</sup>
- A = vessel water area, ft<sup>2</sup>
- H = active core height, ft
- H<sub>FG</sub> = water heat of vaporization, Btu/lb
- Q<sub>DK</sub> = decay heat at start of core uncovering, Btu/min.

It is seen that the coolant water levels in Figure 2.7 prior to ADS activation are quite similar when displayed in this manner. Use of the dimensionless time parameter has been found to be convenient, and it will be frequently used in the following discussions to display the code results.

The MARCH calculations for NUREG-1150 were performed using the source term code package (STCP) or V192 version of the code. Although control blade melting was predicted for these calculations, actual control blade relocation was not modeled. The melted control blade nodes were assumed to remain in-place after melting. Since the control blade nodes have relatively low heat capacity compared to the rest of the core, this assumption has little effect





2.14

FIGURE 2.7. Mixture Level as a Function of Dimensionless Time  $(t - t_u)/\tau$  for Cases PBTBO and PBTBS

on the heatup of the core. However, for criticality evaluations it is desirable to model control blade relocation in addition to melting.

The more recent MARCH calculations in Table 2.1 were performed using version V194. The V194 version of the code contains a number of modeling enhancements, including a BWR control blade relocation model in which melted blade nodes fall either (input option) to the core plate below the core or into the water in the lower head. If there are solid control blade nodes above the melted nodes, the solid nodes are assumed to fall downward and replace the melted nodes. As before, the control blade melting temperature is specified by input.

Version V194 of MARCH also contains enhanced capability to calculate heat transfer and metal-water reaction during reflooding of a degraded core. The improved models were found to be necessary to explain the thermal behavior of the TMI-2 core. In addition, examination of the TMI-2 core debris indicated the core melting temperature used in the NUREG-1150 MARCH calculations ( $4130^{\circ}\text{F}$ ) was unrealistically low. Based on the TMI-2 data, a core melting temperature of  $4870^{\circ}\text{F}$  is more representative. The higher melting temperature was also used in the BWR core heatup calculations for the more recent MARCH calculations listed in Table 2.1.

All of the BWR scenarios in Table 2.1 are unmitigated meltdown accidents. That is, no makeup was assumed to be available after the start of core uncovering. The major potential for recriticality occurs if the core is reflooded with water in the time window between blade melting and fuel rod melting. No additional calculations were performed in the present study for BWR core reflood scenarios. Thus, the MARCH calculations have been used primarily to indicate that there is a time window during which a potential for recriticality exists due to the melting of control blades. Based on the Version V194 MARCH calculations, this window ranges from 5 to 67 minutes depending on the nature of the transient event.

### 2.2.2 Results of Calculations

Figures 2.8 and 2.9 display key event times for the MARCH calculations listed in Table 2.1. The event times range from minutes to over two days. Figures 2.10, 2.11, and 2.12 show the average core temperature from the MARCH calculation displayed as a function of the dimensionless time parameter discussed above.

Figures 2.13 and 2.14 are plots of the core melt fraction. Melting generally starts between 1 and 6 time constants after the start of core uncovering. Some of the larger melt start times can be explained in terms of the cooling from ADS activation or to the use of a higher assumed core (fuel rod) melt temperature. In general, however, there seems to be no simple correlation to pinpoint the time core melting starts. The best that can be

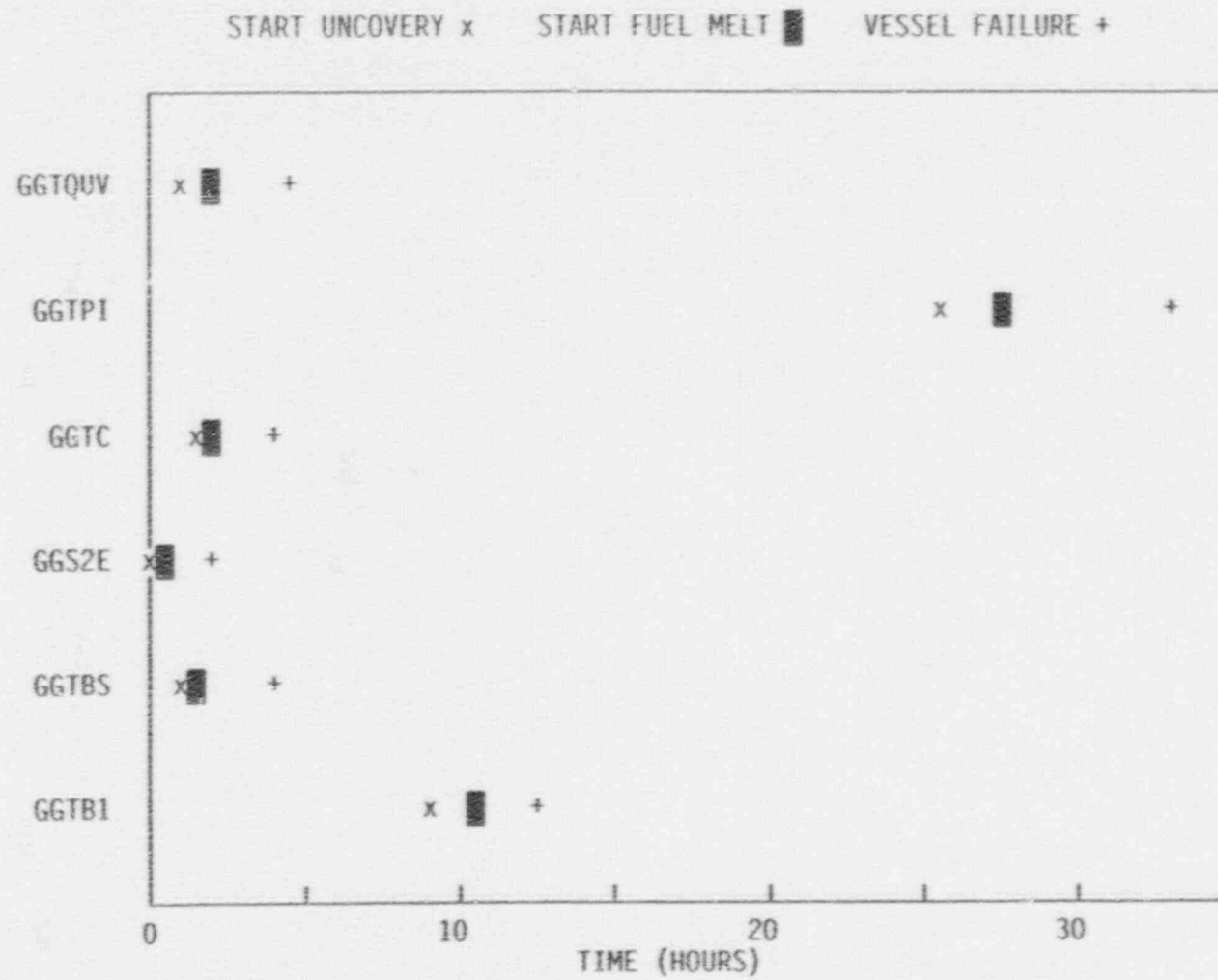


FIGURE 2.8. Grand Gulf Accident Event Timing

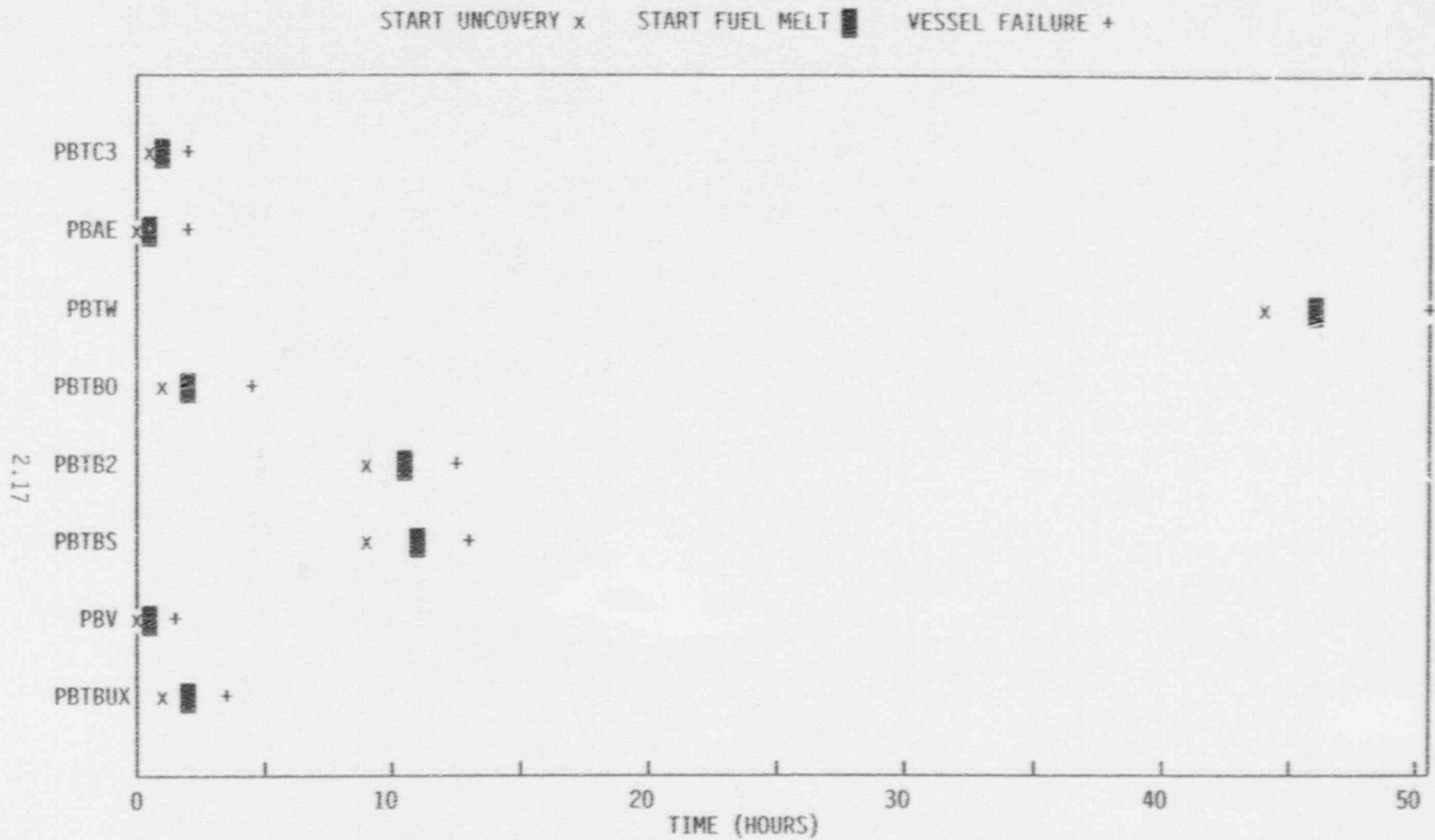


FIGURE 2.9. Peach Bottom Accident Event Timing

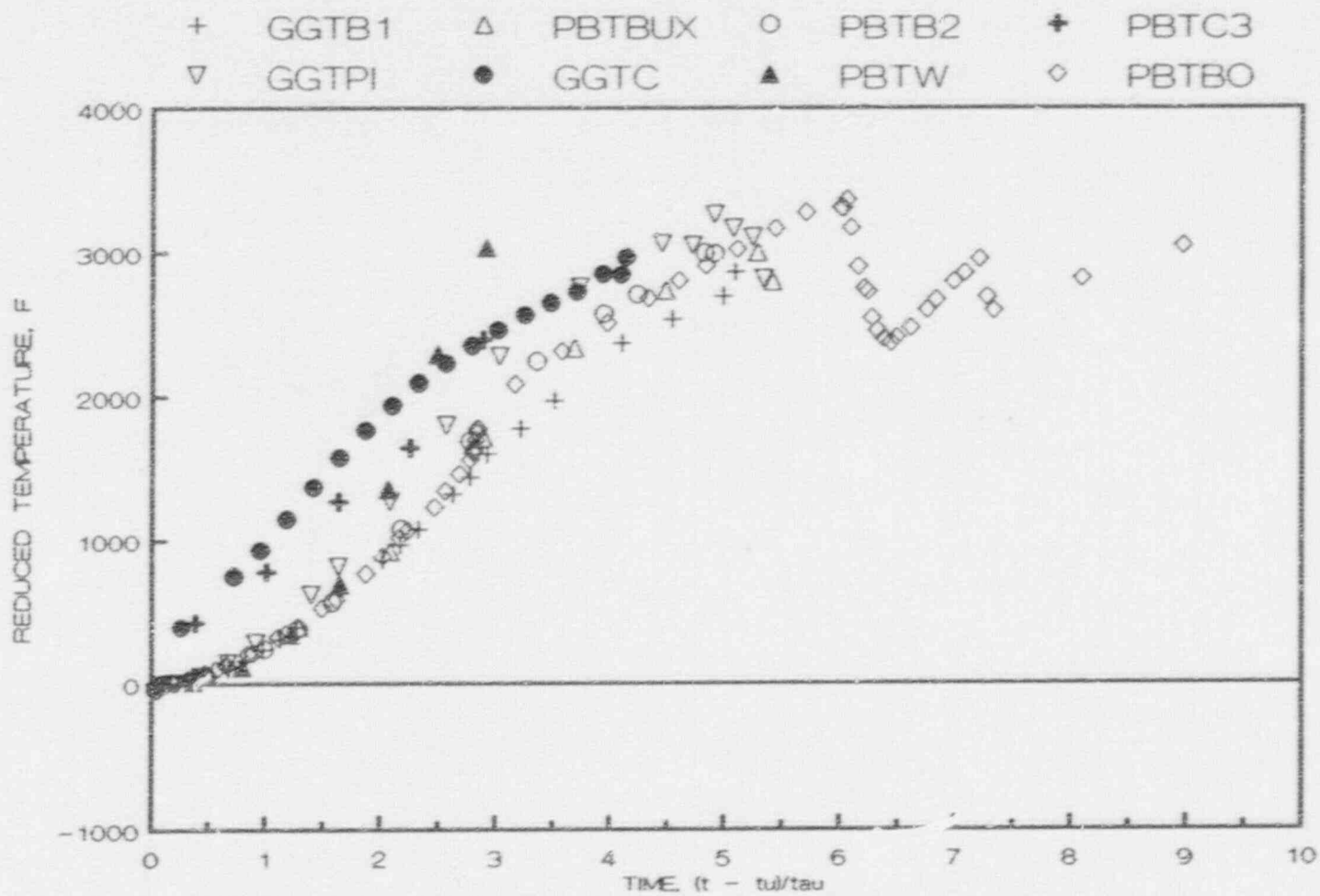


FIGURE 2.10. Average Core Temperature Change,  $(T - T_0)$ , as a Function of Dimensionless Time After Core Uncovery,  $(t - t_u)/\tau$ , for Group 1



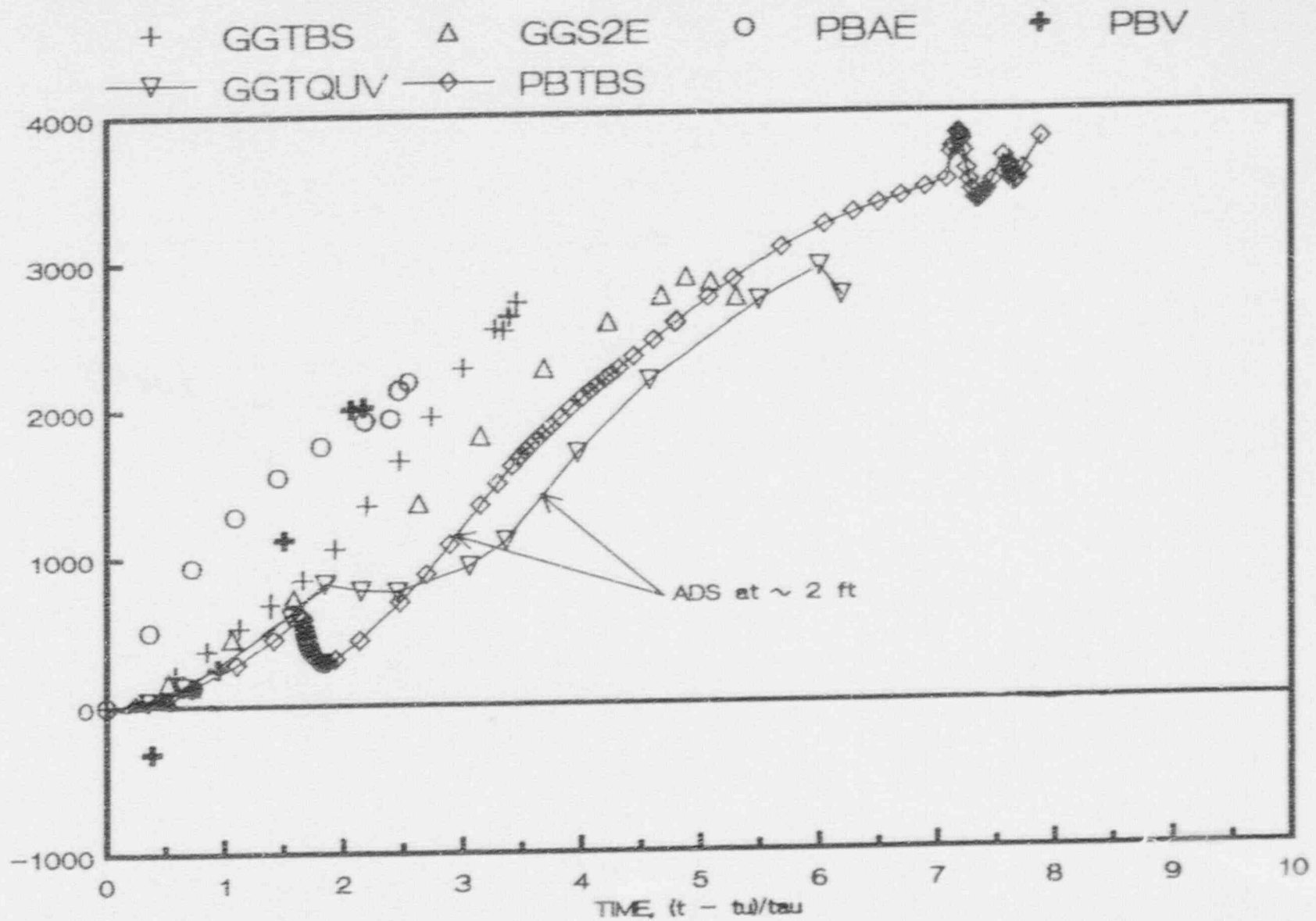


FIGURE 2.11. Average Core Temperature Change,  $(T - T_0)$ , as a Function of Dimensionless Time After Core Uncovery,  $(t - t_u)/\tau$ , for Group 2

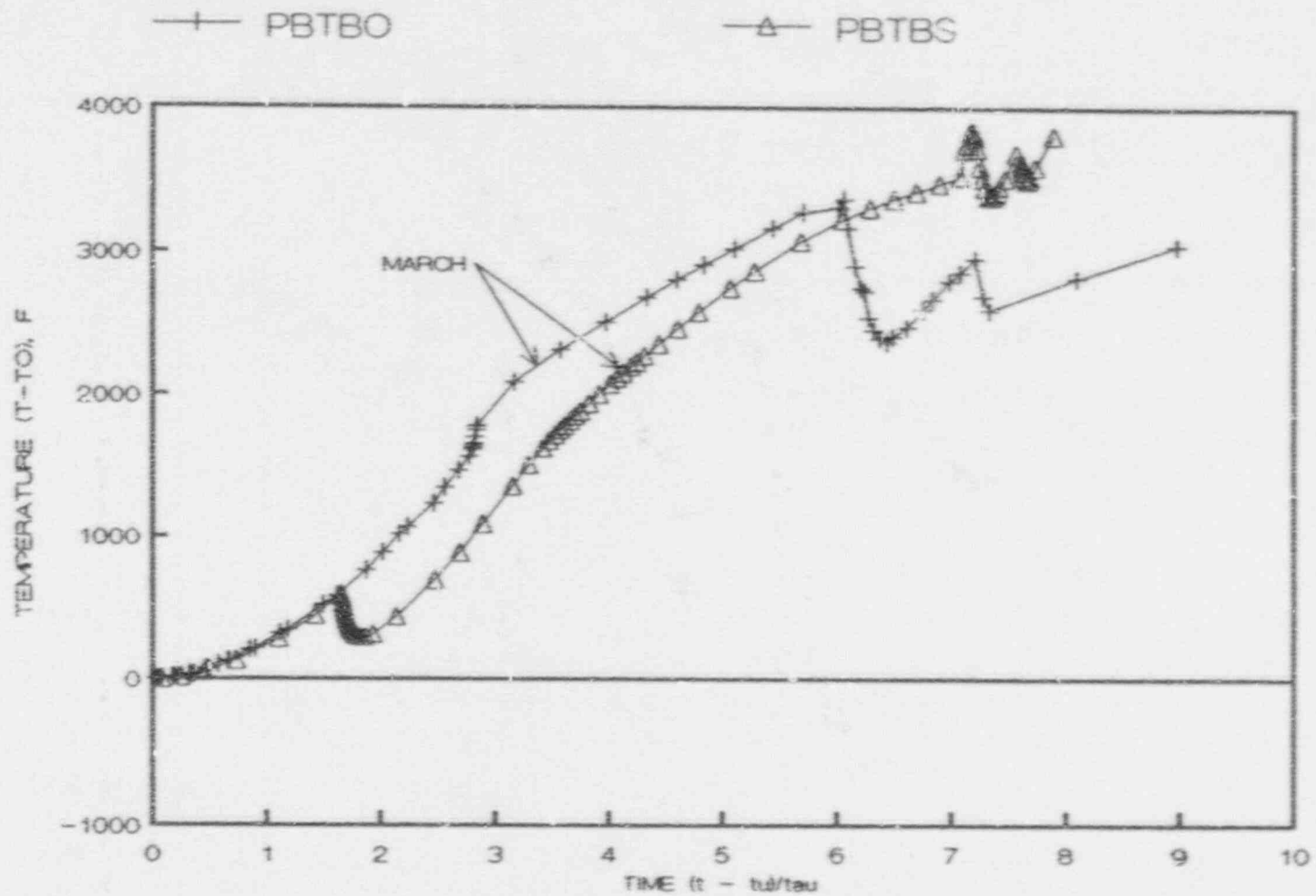


FIGURE 2.12. Average Core Temperature Change,  $(T - T_0)$ , as a Function of Dimensionless Time After Core Uncovery,  $(t - t_0)/\tau$ , for Cases PBTBS and PBTBO

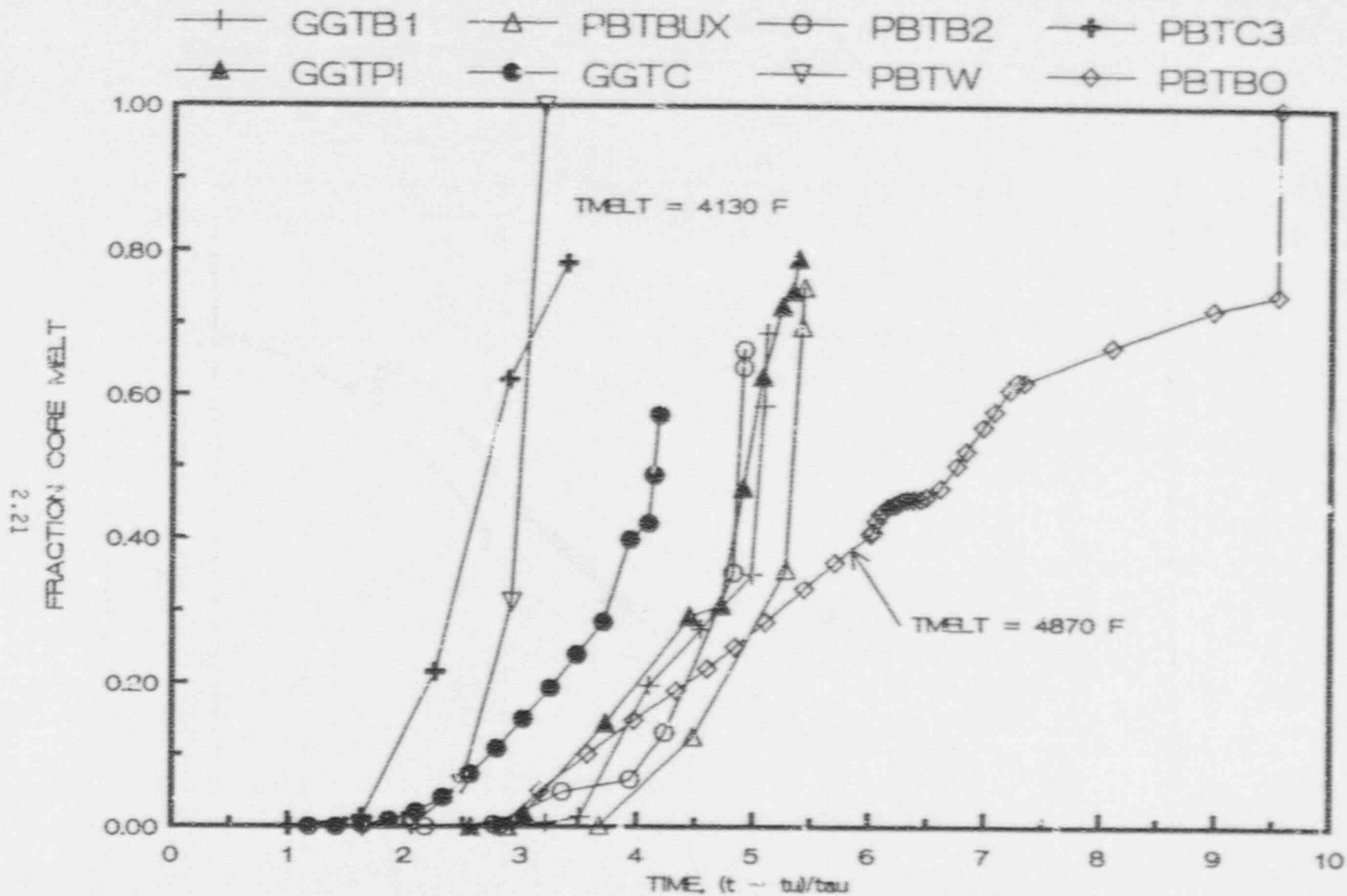


FIGURE 2.13. Fraction Fuel Rods Melted as a Function of Dimensionless Time After Core Uncovery,  $(t - t_u)/\tau$ , for Group 1

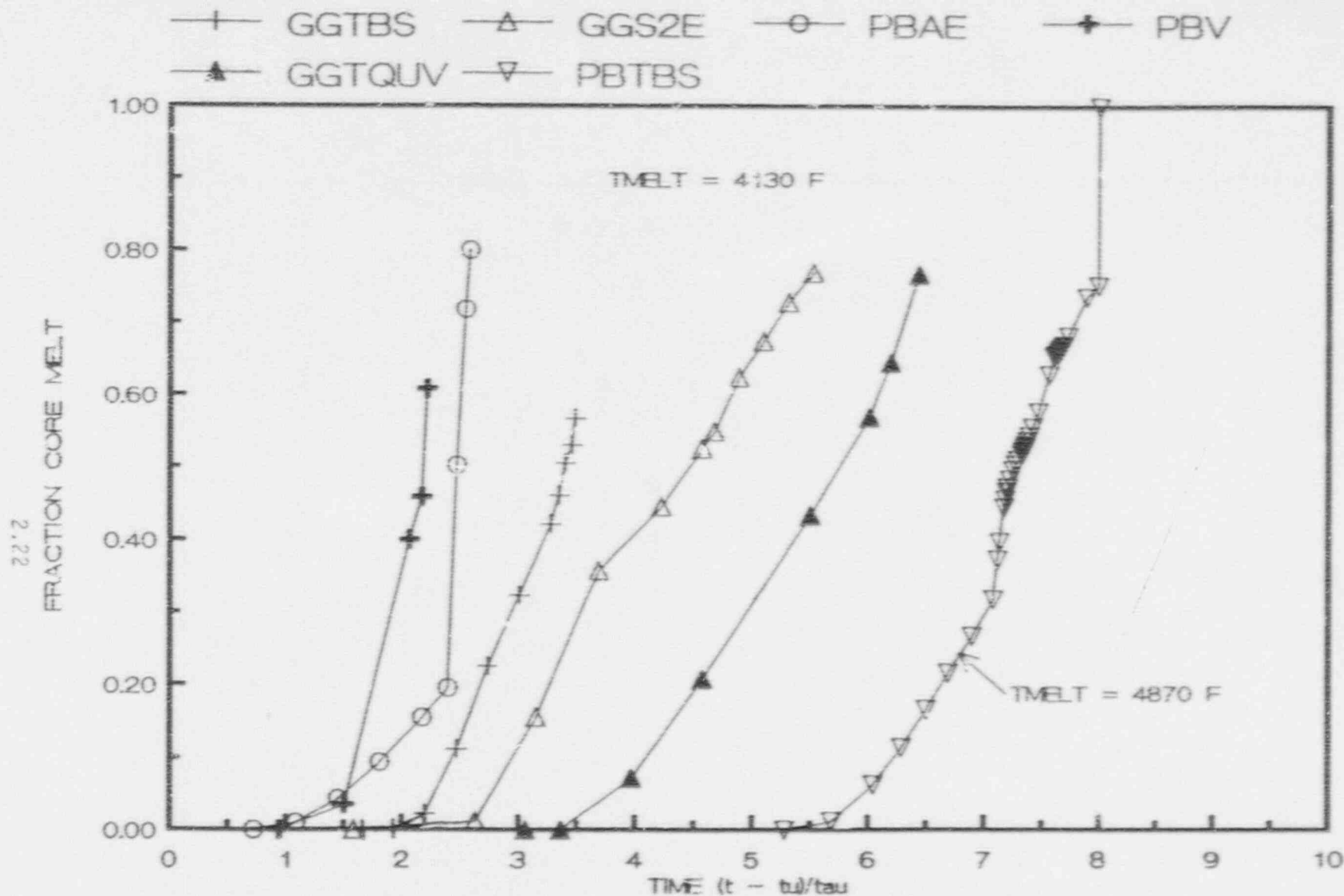


FIGURE 2.14. Fraction Fuel Rods Melted as a Function of Dimensionless Time After Core Uncovery,  $(t - t_u)/\tau$ , for Group 2

said is that core melting can be expected within a few time constants after the start of core uncovering.

Figure 2.15 indicates that control blade melting is strongly correlated to the average core temperature. Blade melting starts when the average core temperature increases to about 1500°F and about half of the blades have melted when the average core temperature increases to 2750°F. In principle, a calculational algorithm could be developed which uses the results in Figures 2.10 to 2.12 to define the core temperatures at a given time and the results in Figure 2.15 to define the blade melt fraction. In terms of practical plant operation, the control room operators have no direct instrumentation reading of the average core temperature. MARCH calculations indicate that the core exit gas temperature gives a rough indication of the average core temperature, except in periods of very low steam flow.

Figures 2.16 to 2.19 provide more detail on the time and spatial variation of control blade, channel box, and fuel rod melting for Peach Bottom cases PBTB0 and PBTBS. Melting temperatures used in these MARCH calculations were 2600°F for the blades, 3365°F for the boxes, and 4870°F for the rods. As discussed previously, a somewhat lower control blade melting temperature (about 2300°F) is currently believed to be more realistic. However, based on the relative timing of the blade and box melting seen in Figures 2.16 and 2.17, use of a blade melting temperature a few hundred degrees lower (or higher) would not be expected to significantly alter the results. The results in Figures 2.16 and 2.17 indicate about half of the control blades can be expected to melt before there is significant fuel rod melting. This is important because early melting of the control blades makes recriticality, during BWR core reflood with unborated water, a credible occurrence.

Figures 2.18 and 2.19 provide more detail on the spatial variation of the blade melting. Figure 2.18 indicates 60% control blade melting occurs in a very short time span in the central eight radial regions (about 75 volume percent) of the core. Melting in the two low power outer radial regions is delayed several time constants ( $\tau = 19$  min).

Figure 2.19 gives an indication of the blade melting as a function of core elevation and radius and the time (in minutes) after the start of core uncovering. The MARCH blade melt model, used in these calculations, assumes that melted blade nodes fall to the lower core plate, and are replaced by solid nodes, sliding down from above, if any exist. Thus, at 53 minutes after core uncovering the results in Figure 2.19 indicate that the control blades will have melted out of a central 6 foot diameter region of the core above the 6 foot elevation. Thus, large volumes of the core will contain no control blades. The results in Figure 2.16 indicate fuel rod melting begins at about the time half the blades are melted. Uncertainties in the relocation of the melted fuel rods also makes calculation of the blade melting somewhat uncertain after this point.



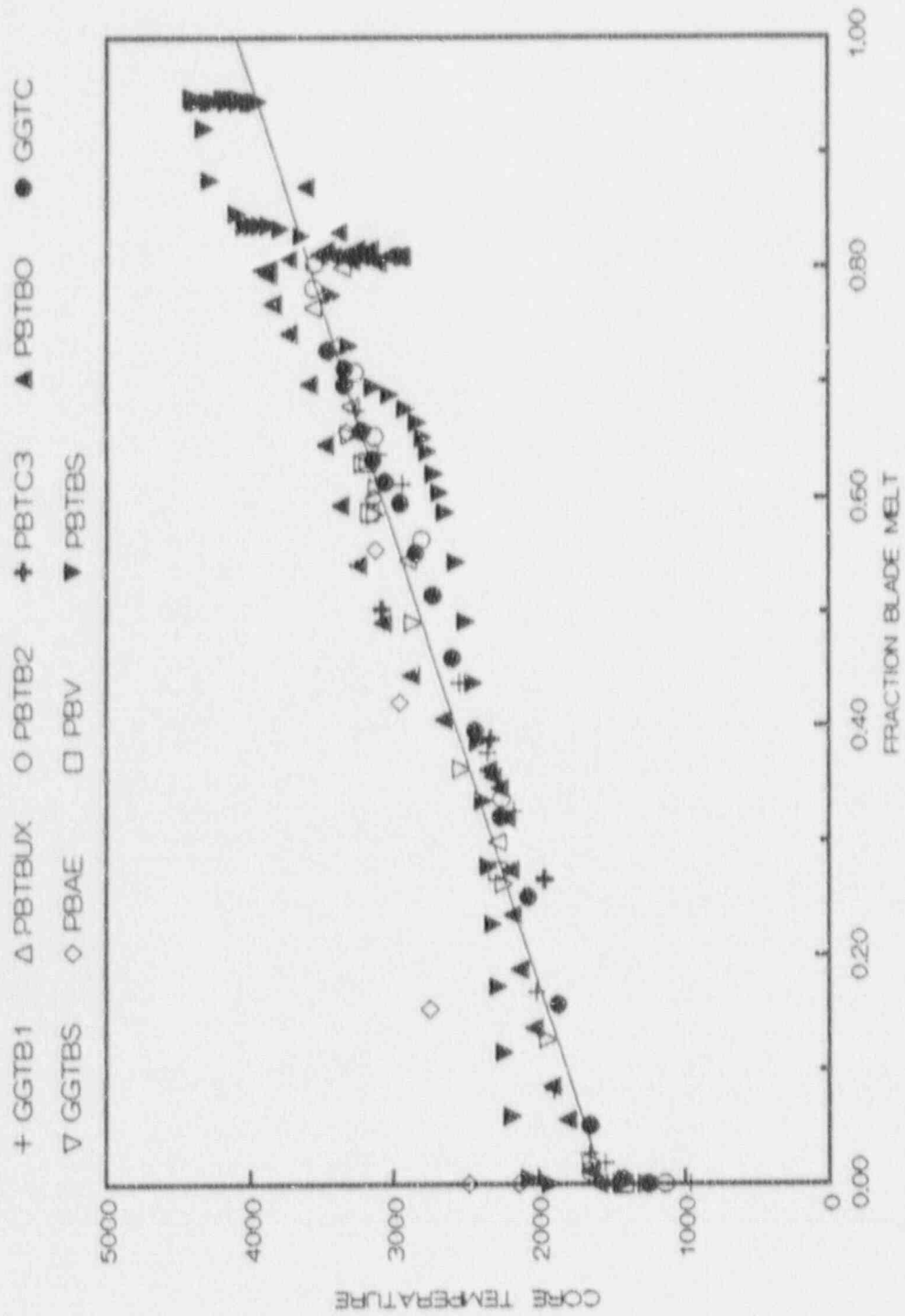


FIGURE 2.15. Fraction Control Blades Melted as a Function of the Average Core Temperature for All Cases

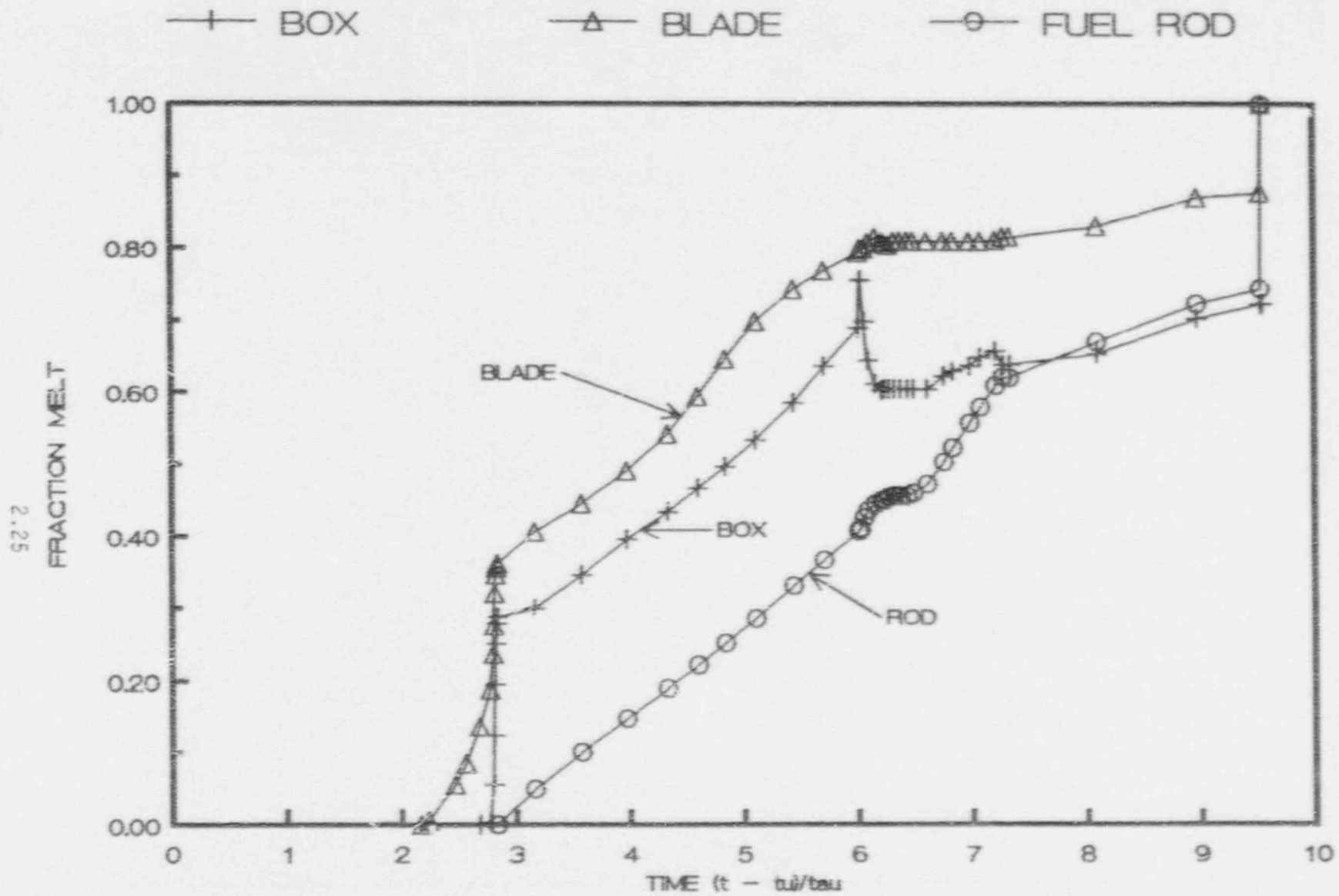


FIGURE 2.16. Fraction Control Blades, Channel Boxes, and Fuel Rods Melted as a Function of Dimensionless Time After Core Uncovery,  $(t - t_u)/\tau$ , for Case PBTB0

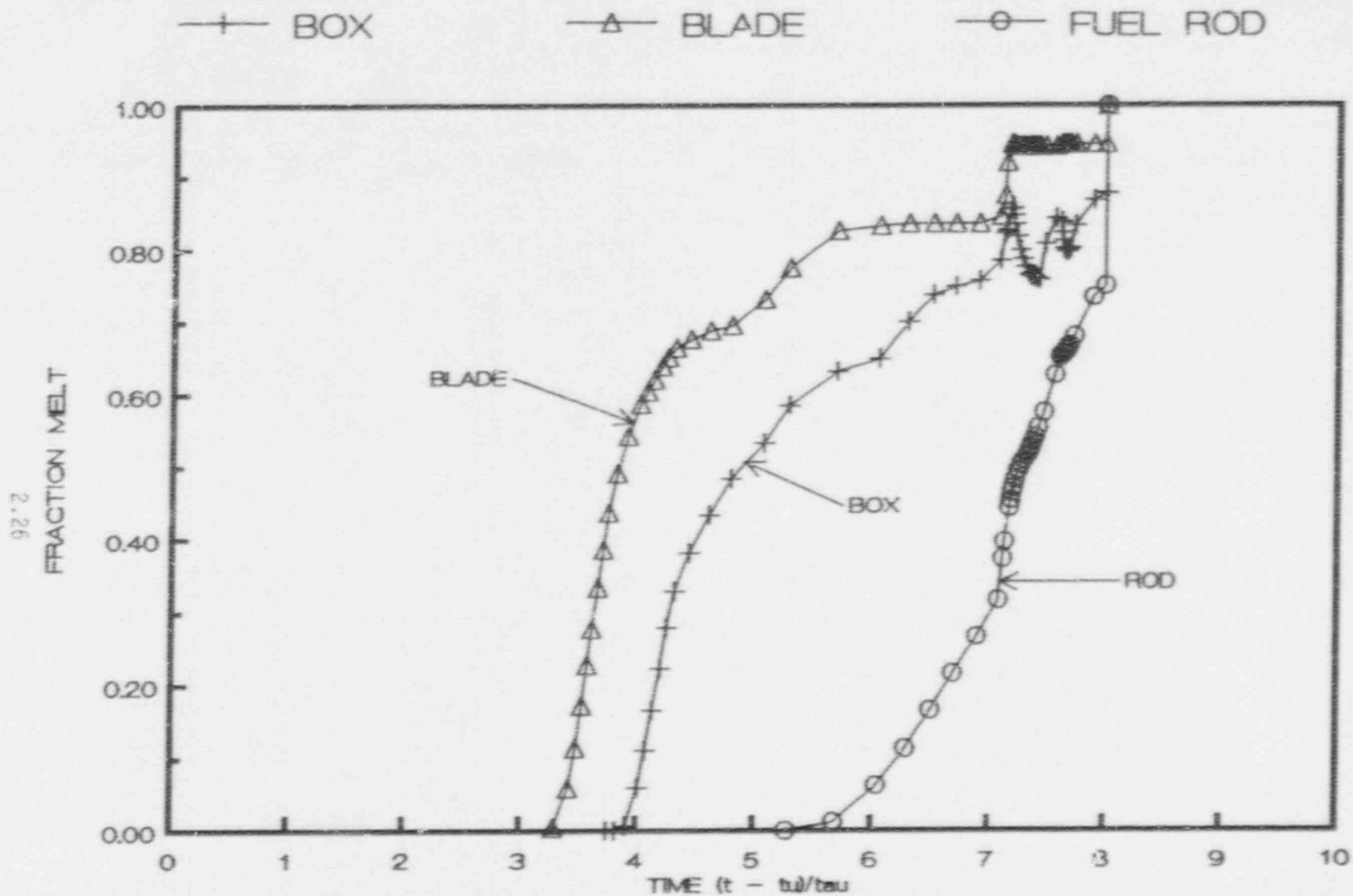


FIGURE 2.17. Fraction Control Blades, Channel Boxes, and Fuel Rods Melted as a Function of Dimensionless Time After Core Uncovery,  $(t - t_u)/\tau$ , for Case PBTBS

2.27

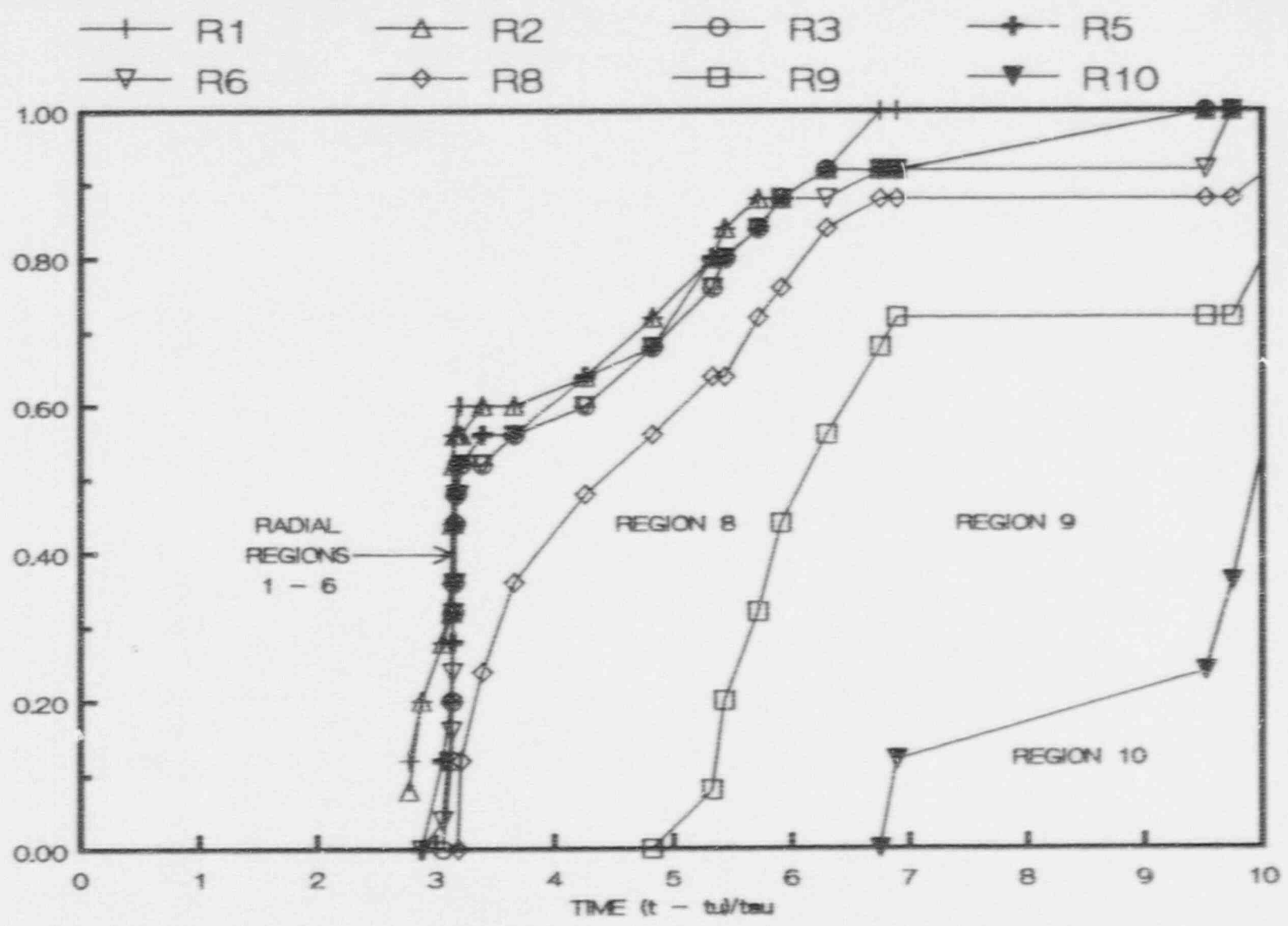


FIGURE 2.18. Fraction Control Blades, Melted by Radial Region as a Function of Dimensionless Time After Core Uncovery,  $(t - t_u)/\tau$ , for Case PBTB0

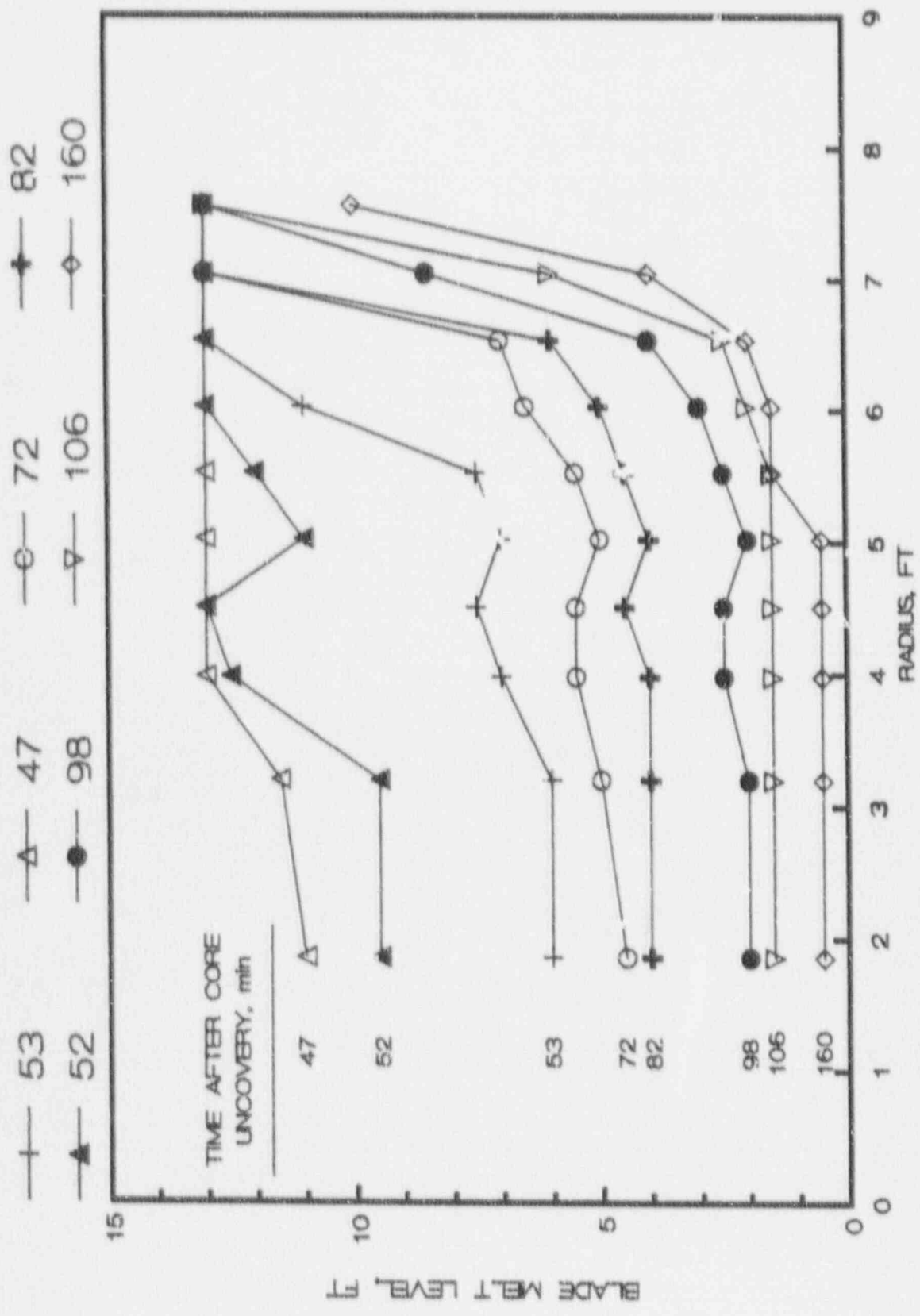


FIGURE 2.19. Highest Elevation of Unmelted Control Blade as a Function of Core Radius and Time After Core Uncovery, (t - tu), for Case PB1B0



Most of the code results discussed above were presented using the dimensionless time parameter as the time variable. This is a convenient way to present the results of many calculations and to display data trends and commonalities in the results. However, it is conceptually easier to think in terms of real time units (minutes) rather than the "buildup time constant" ( $\tau$ ) unit. For this reason, detailed real-time results for a Peach Bottom station blackout sequence with early melt are presented in the remainder of this section. The MARCH calculation is designated as case PBEM2. The sequence is briefly described below followed by a tabulation of the timing of key events.

There is no makeup in the scenario; and the core uncovers in about one hour. ADS valves are opened when the water level decreases to 2 feet above the bottom of the core. Blades are assumed to melt at 2600°F, channel boxes at 3365°F, and the fuel rods at 4870°F. The blade melt is assumed to flow through the core plate into the water in the lower head. Melted fuel rod nodes and the corresponding channel box nodes are retained in the core until the rod node at the 1 foot level melts. The slumped material is assumed to form a debris bed in the lower head, with cooling described by the Lipinski correlation (Ref. 2.18). Key accident events are sequentially given in Table 2.2. Times and locations for the start of control blade, fuel rod cladding, and fuel material melting are listed at the bottom of the table. Blade melting is seen to start towards the top of the core. The location of the initial fuel rod melting is shifted towards the lower part of the core due to the effects of metal-water reaction heating. Slumping of fuel rod material into the lower head is calculated to start at about 160 minutes.

Figures 2.20 to 2.25 provide graphical presentations of the MARCH calculations. Vessel pressure is shown in Figure 2.20. For computational convenience, valve cycling was not modeled prior to the start of core uncover. Thus, Figure 2.20 shows a smooth pressure trace prior to about 60 minutes. Pressure swings of 50 psia were assumed during the valve cycles after 60 minutes. At 95 minutes the pressure drops rapidly due to ADS activation. The two pressure spikes at 160 and 195 minutes are caused by slumping of molten fuel rod material into the water in the lower head. Slumping of melted control blade material into the lower head starts at 127 minutes. However, little effect is seen in the vessel pressure trace.

The steaming from the slumping of the control blade melt into the lower head increases the calculated hydrogen generation compared to the previous Peach Bottom PBTBO and PBTBS cases. In the previous calculations the blade melt was assumed to accumulate on the core plate rather than flowing into the lower head. The calculated fraction of the core zircaloy reacted is increased from about 30% to about 45% by the increased steaming.

The vessel collapsed liquid water level is shown in Figure 2.21. Activation of the ADS at 95 minutes is seen to decrease the water level about 4 feet below the core. Because of its low heat capacity, the blade slumping

TABLE 2.2. Early Melt Station Blackout Events (Case PBEM2)

<u>Time, Min</u>	<u>Event Description</u>
60	Collapsed liquid level falls below top of core.
65	Swollen level falls below top of core. Core heatup begins.
95	Liquid level falls to 2 feet. Peak core temperature about 1700°F. Three ADS valves are opened. One valve is assumed to remain open so the vessel pressure approaches the containment pressure. Five minutes after the ADS action, the peak core temperature has decreased to about 1450°F and the water level to about 3 feet below the core.
122	Control blade melting (2600°F) begins.
125	Melting of the fuel rod cladding (3365°F) begins.
127	Control blade slumping into the lower head starts.
132	Fuel rod melting (at 4870°F) begins.
133	Control blades are 40% melted and the fuel rods about 1% melted.
160-161	About 20% of the core falls into the lower head. The core is about half molten at this time.
196	An additional 10% of the core falls into the lower head.
197	Dryout of the lower head occurs.
208	The remaining core falls into the lower head. About 75% of the core has melted by this time. The average temperature of the debris falling into the lower head is about 4500°F. The average temperature of the debris in the lower head increases to about 3100°F.
288	Gross head failure occurs with about half of the head thickness melted.

	<u>blade melt</u>	<u>clad melt</u>	<u>fuel melt</u>
start melt time:	122 min	125 min	132 min
location	10 ft	5 ft	5 ft
melt at : ft	≈150 min	≈145 min	≈150 min

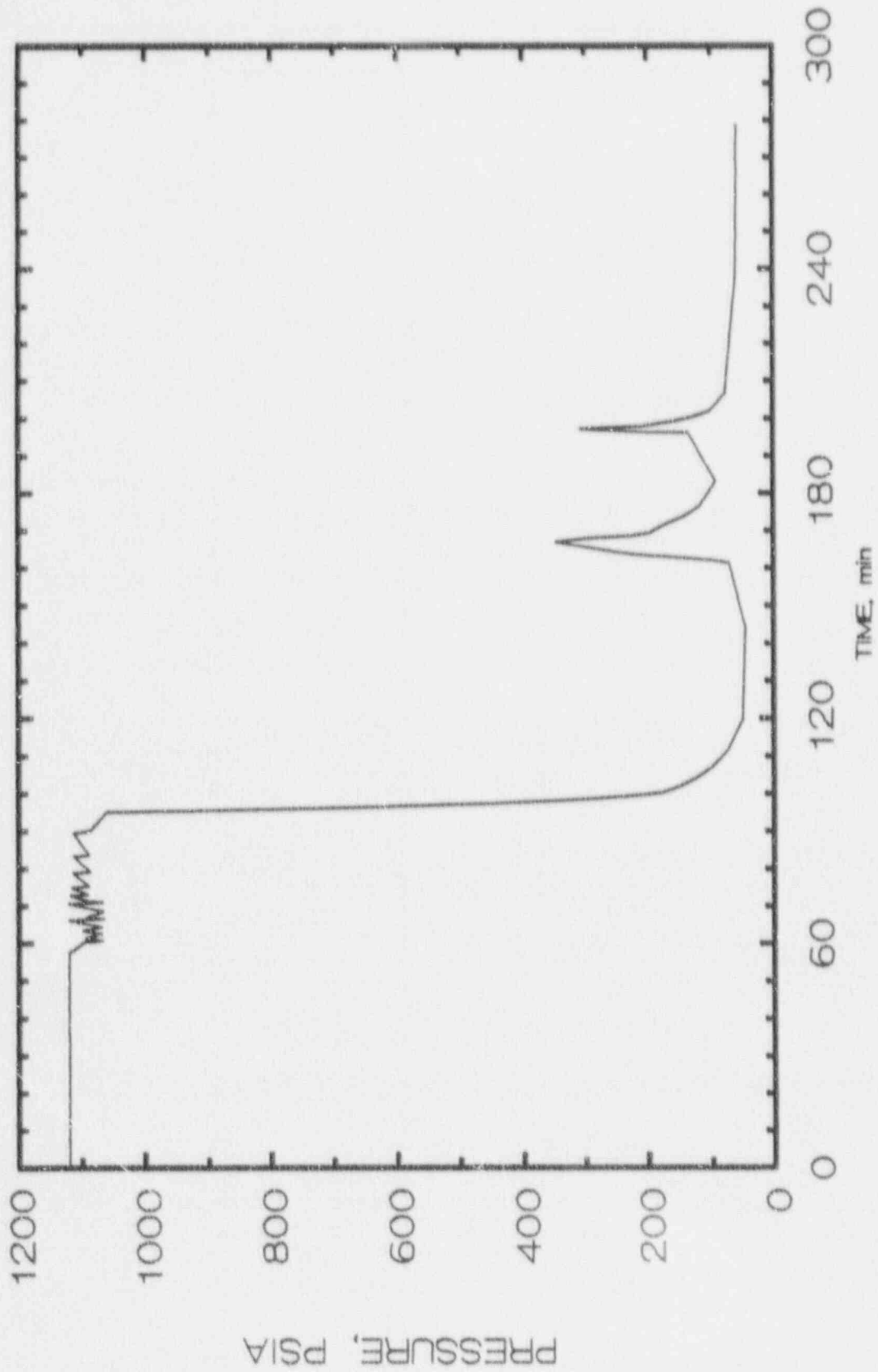


FIGURE 2.20. Vessel Pressure versus Time for Peach Bottom Early Melt Station Blackout (PBEM2)

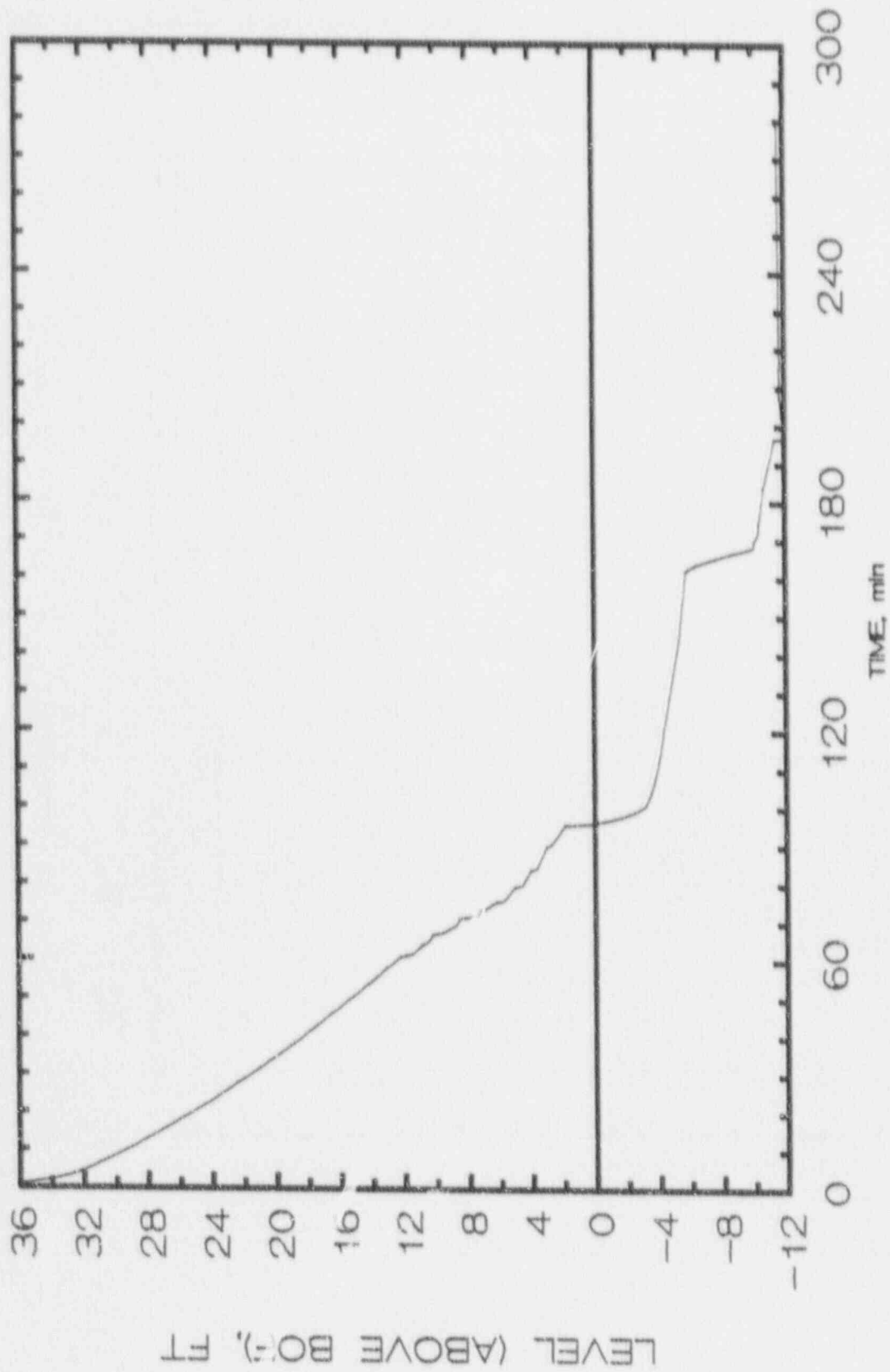


FIGURE 2.21. Reactor Vessel Water Level Versus Time for Peach Bottom Early Melt Station Blackout (PBEM2)

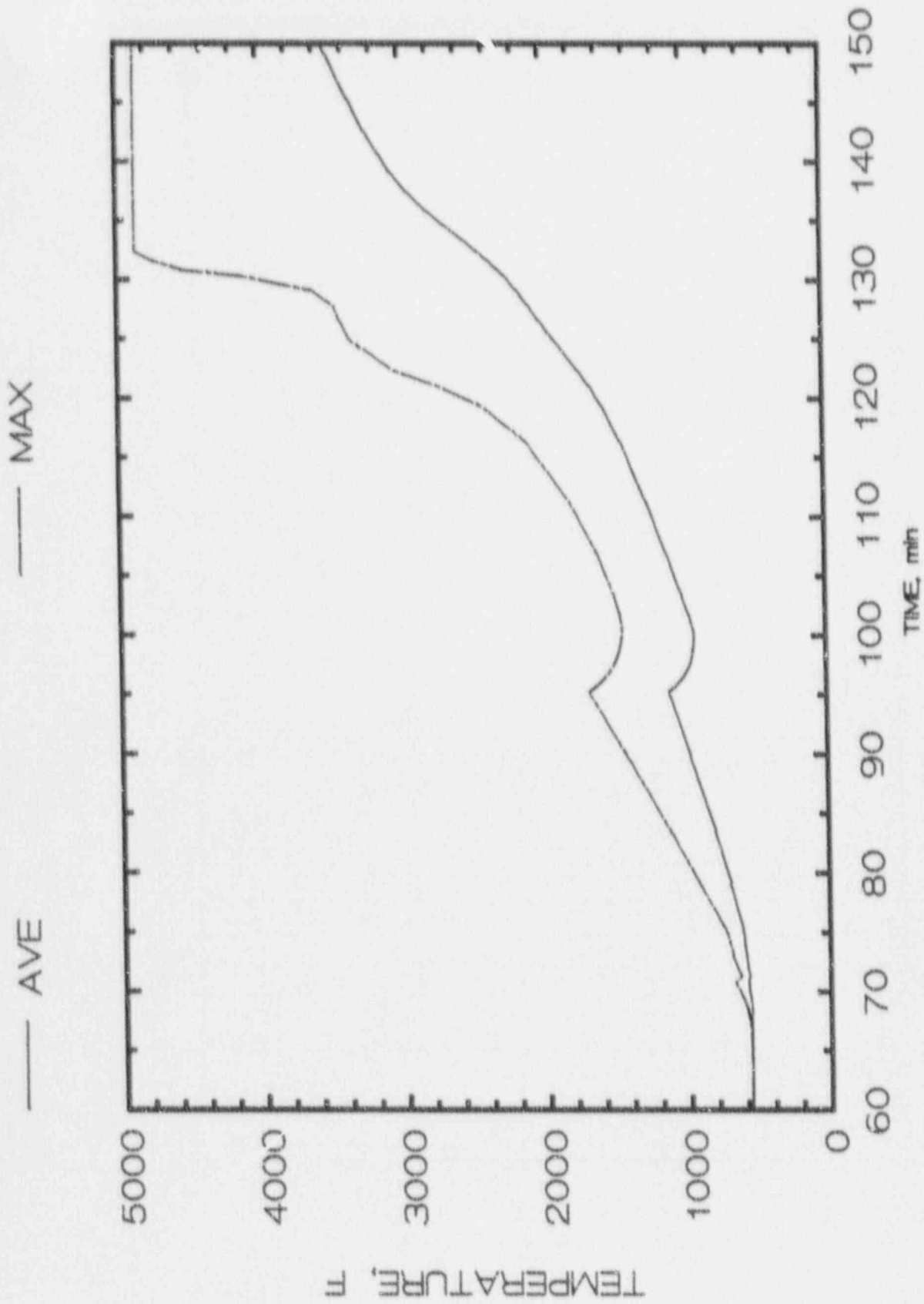


FIGURE 2.22. Core Temperature versus Time for Peach Bottom Early Melt Station Blackout (PBEM2)



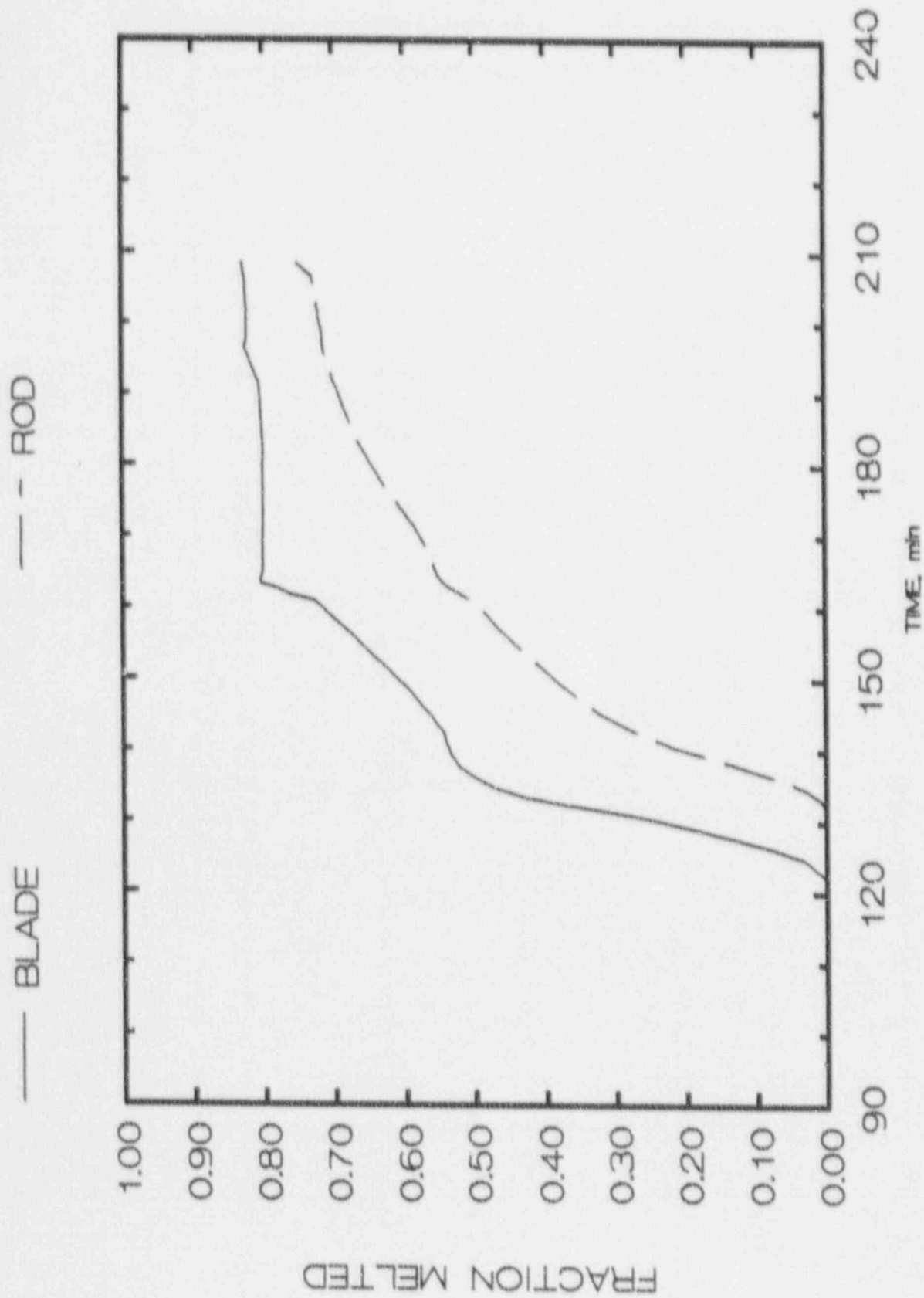


FIGURE 2.23. Melt Fraction versus Time for Peach Bottom Early Melt Station Blackout (PBEM2)

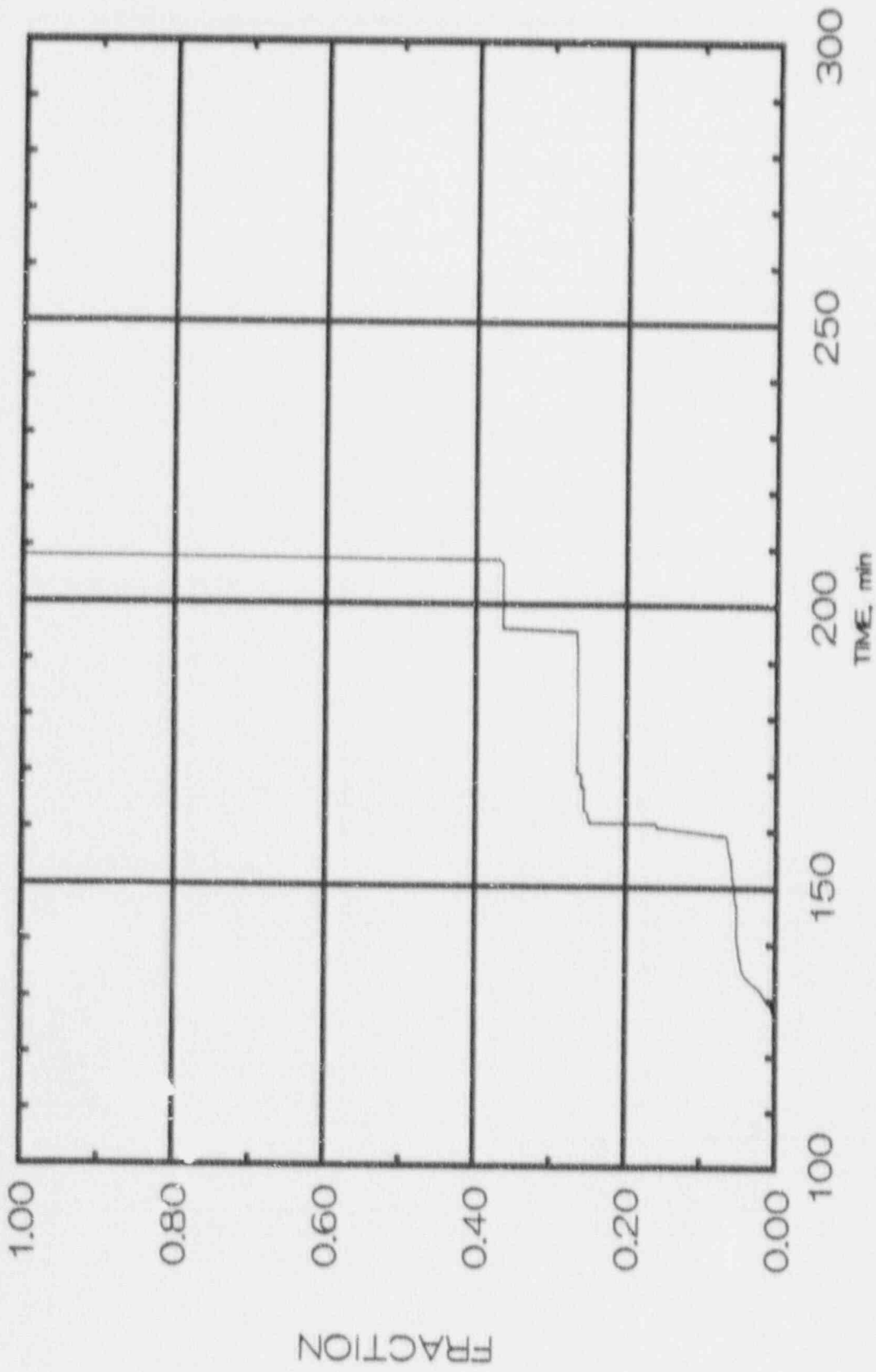


FIGURE 2.24. Fraction of Core in Lower Head versus Time for Peach Bottom Early Melt Station Blackout (PBEM2)

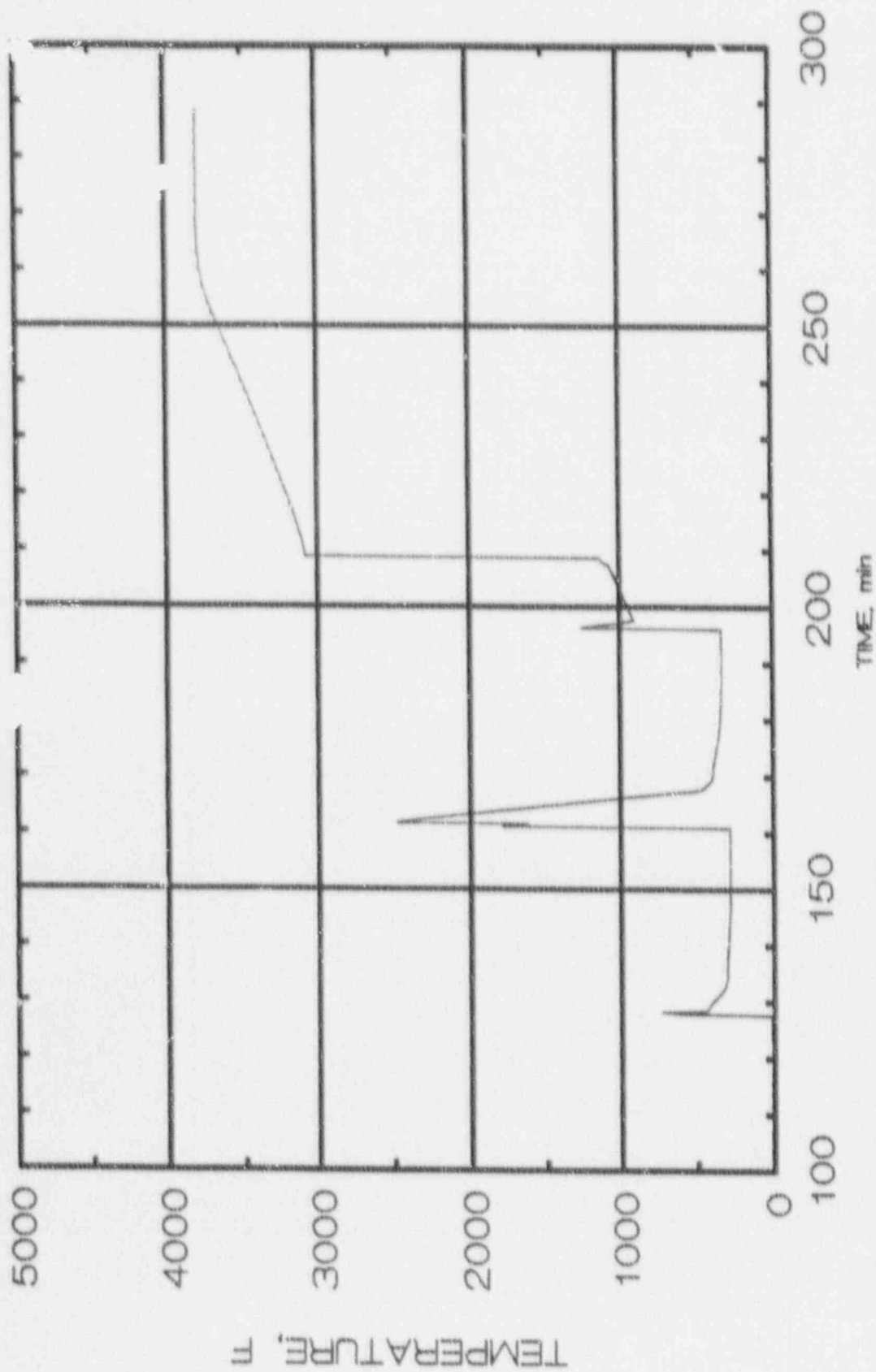


FIGURE 2.25. Lower Head Debris Temperature versus Time for Peach Bottom Early Melt Station Blackout (PBEM2)

starting at 127 minutes produces no large change in the water level. However, the fuel rod slumping occurring at 160 minutes and again at 195 minutes results in vessel dryout at 197 minutes.

Figure 2.22 shows core temperature decreases at 95 minutes due to the ADS activation. An additional 15 minute delay in the ADS activation, when core temperatures would have approached 2800°F, would likely increase steaming and accelerate the cladding-steam reaction, which would produce a different result.

Figure 2.23 shows that about half of the control blades are melted by the time fuel rod melting (at 4870°F) starts. This result is consistent with the previous conclusions.

Figures 2.24 and 2.25 illustrate the slumping of material into the lower head. From Figure 2.25 it can be seen that control blade material begins to arrive in the lower head at 127 minutes. Fuel rod material arrives at 160 minutes and again at 195 and 208 minutes. Figure 2.25 shows that the slumped control blade material quickly quenches the water temperature. The fuel rod material slump at 160 minutes produces a brief temperature spike to about 2500°F. The vessel pressure is relatively low (about 400 psia) at this time so high pressure melt ejection would be unlikely. After the core slump at 208 minutes, the debris temperatures are calculated to exceed the melting point of steel. Gross failure of the lower head with about 50% melt-through is calculated to occur at 288 minutes. Steam explosion phenomenon was not modeled in the code.

Based on the MARCH code analyses, it can be concluded that a time window may exist during a severe accident in which control blades start to melt out of a region of the core prior to the start of fuel rod melting. In Table 2.1 this window ranges from 5 to 67 minutes with control blade melting starting anywhere from 15.8 to 649 minutes after the initiation of the accident.

### 2.3 DOMAIN AND POTENTIAL CONSEQUENCES OF RECRITICALITY

Having concluded that an unpoisoned, degraded core is credible in a BWR severe accident (thus making recriticality possible), it becomes important to examine the range over which a recriticality is possible and the consequences of such an event. Knowledge of the domain of critical systems is necessary to ensure that adequate boron is present to prevent recriticality. If the potential consequences are very severe, it might be preferable not to reflood the core if the only available water supply is insufficiently borated.

The accident scenario of concern is a super prompt-critical excursion which would result in some vaporization of fuel, the dispersal of molten fuel debris, rapid molten fuel coolant interaction, and the production of a large pressure pulse capable of directly failing the vessel. As will be shown later

in this chapter, this type of scenario does not appear to be credible under the conditions of reflooding a hot, degraded core.

If a destructive excursion does not occur, the reactor will either achieve a quasi-steady power level or enter an oscillatory mode, perhaps similar to the predicted behavior of anticipated transient without scram (ATWS) sequences at low vessel pressure. If the core can be quenched and cooled, even though it is critical, boron addition may not be urgently required. However, a marginally coolable debris bed could become uncoolable with even a small addition of power. On the other hand, an increase in void fraction can effectively shut the core down. It is likely that there is a broad range of coolable conditions under which a balance is established between the power and the void fraction. A more likely constraint on the required timing for the addition of boron to reduce power is the challenge to containment integrity from the excessive heat load dumped to the suppression pool.

### 2.3.1 Domain of Critical Configurations

During a severe accident in which core cooling has been lost, substantial changes to the as-designed fuel geometry would be expected. Initially, the fuel consists of pellets arranged in coaxial cylindrical tubes forming fuel rods. The fuel rods are then grouped into assemblies, with a well defined, rectangular geometry. During an accident, the grid spacers and end fittings which define the rectangular spacing may melt or collapse, resulting in a loss of the regular geometry. Similarly, the fuel rod clad could melt or break releasing pellets in a random manner. The fuel pellets themselves may shatter, forming smaller, irregular shaped fuel particles, or they may melt, forming larger particles.

To conservatively model the unknown, ill defined geometry, a simplifying assumption was made: the particles were assumed to be spherical. To determine the optimum conditions, the spacing between the particles was varied (resulting in a varying water-to-fuel ratio or fuel volume fraction). Thus, the variables for the calculations were: spherical particle size (diameter), spacing (fuel volume fraction), and the boron concentration.

The standard computer codes NITAWL and XSDRNPM-S (Ref. 2.10) were used to calculate the k-infinity ( $k_{\infty}$ ) for each diameter, spacing, and boron concentration combination. The Dancoff self-shielding correction was calculated using the MCDAN (Ref. 2.11) program. To generate the large number of input data sets required, a semi-automated spreadsheet was developed. The spreadsheet calculated and arranged the data such as fuel enrichment, material densities, atomic weights, scattering cross sections, and the calculational variables into a form suitable for directly downloading as input to the neutronics computer codes. Appendices are included in this report which show the spreadsheet and typical output files (the case information print file and



the NITAWL and XSDRNPM-S input files). An additional appendix shows a typical MCDAN output and the calculated Dancoff corrections for all the cases calculated.

Four boron concentrations were analyzed: zero boron content, 200 ppm  $^{10}\text{B}$ , 500 ppm  $^{10}\text{B}$ , and 1000 ppm  $^{10}\text{B}$ . Major assumptions in all calculations were: uranium oxide density,  $10.4 \text{ g/cm}^3$  (95% of theoretical); enrichment, 3.0 wt%  $^{235}\text{U}$  (based on reloads projected for Peach Bottom and Grand Gulf); burnup, none; and temperature, cold (although a higher temperature case was calculated for comparison). The fuel volume fraction was varied to obtain the maximum  $k_{\infty}$ .

Table 2.3 shows the maximum  $k_{\infty}$  values for each spherical particle size and boron concentration. All  $k_{\infty}$  calculations for the spherical particles are listed in the appendices. The data is plotted in Figures 2.26 through 2.29, and an overall envelope for each boron concentration is shown in Figure 2.30. A significant result from these curves is that high reactivities are possible and even likely for low boron concentrations. At least 1000 ppm  $^{10}\text{B}$  is required to ensure subcriticality under all conditions. In general the curves are fairly "flat" in that  $k_{\infty}$  values near the maximum are calculated (for a specific boron content) over a broad range of spherical particle sizes and fuel volume fractions. For example, a change of the spherical particle size by a factor of two does not significantly change the maximum  $k_{\infty}$  point. The fuel volume fraction is slightly more sensitive, but even a change of 50% in fuel volume fraction (for a given size spherical particle) may only cause a  $1\% \Delta k/k$  change in  $k_{\infty}$ . In general, increasing the boron concentration will increase the spherical particle size and fuel volume fraction for the maximum  $k_{\infty}$ .

Given these high  $k_{\infty}$  values, the first question is, "How significant is the change from a 'pellet-like' size to the optimum spherical particle sizes calculated above?" As was indicated above, we don't expect a large change in going from pellet-equivalent particles to optimum spherical particles. Calculations were made for a spherical equivalent to a single pellet by conserving the surface-to-volume ratio. Since neutron escape from the pellet into the moderator is the most important effect in heterogenous systems, conserving the surface-to-volume ratio of the design pellet will enhance the  $^{238}\text{U}$  resonance self-shielding. For the two BWR fuel types of interest (i.e., GE 8x8 and GE 7x7) the resulting spherical radii are shown in Table 2.4. The calculated  $k_{\infty}$  values for these equivalent particles are also shown. Although there is a slight reduction in  $k_{\infty}$  (compared to the values in Table 2.3, as expected), all cases except 1000 ppm  $^{10}\text{B}$  are substantially supercritical.

The second question to be asked is, "What is the effect of temperature on these calculated reactivities?" Temperature effects are very important in reactivity calculations. It is well known that the Doppler broadening will decrease reactivity as temperature increases. To explore this effect a case was selected consisting of a fuel particle of radius 0.53 cm at a fuel volu

TABLE 2.3. Calculated Maximum  $k_{\infty}$  for Spherical Particles in Water

<u>Boron Concentration</u>	<u>Particle Radius (cm)</u>	<u>Fuel Volume Fraction</u>	<u>K-Infinity</u>
0	0.7	0.29	1.4070
0	1.0	0.32	1.4085
0	1.5	0.35	1.4015
200	0.7	0.44	1.2212
200	1.0	0.46	1.2250
200	1.5	0.49	1.2228
200	2.0	0.52	1.2152
500	1.0	0.56	1.1000
500	1.5	0.59	1.1017
500	2.0	0.62	1.0984
1000	1.5	0.68	0.9988
1000	1.8	0.69	0.9995
1000	2.0	0.69	0.9995

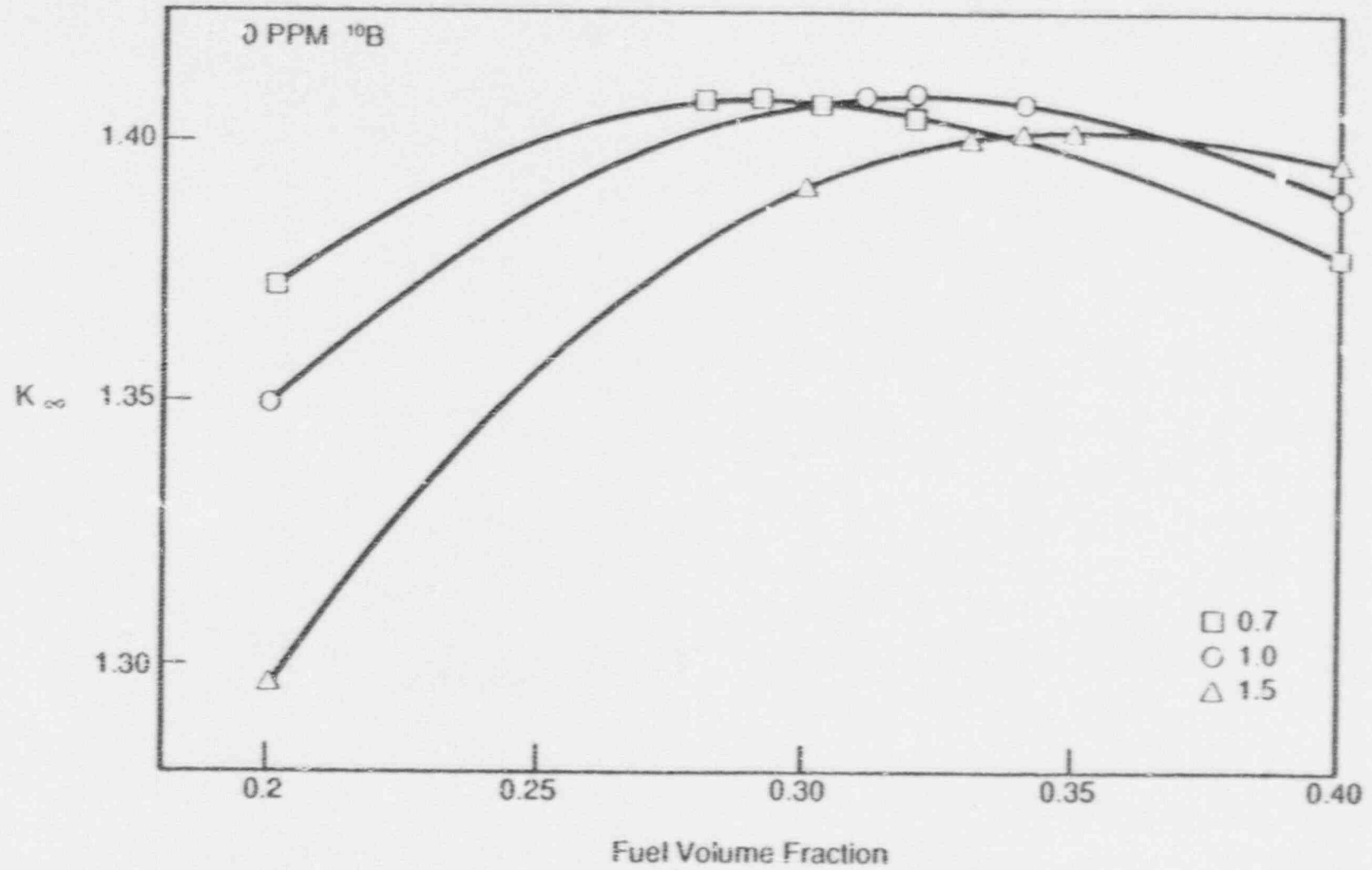


FIGURE 2.26. Calculated  $K_{\infty}$  for  $UO_2$  Fuel Particles in Water with 0 ppm  $^{10}B$

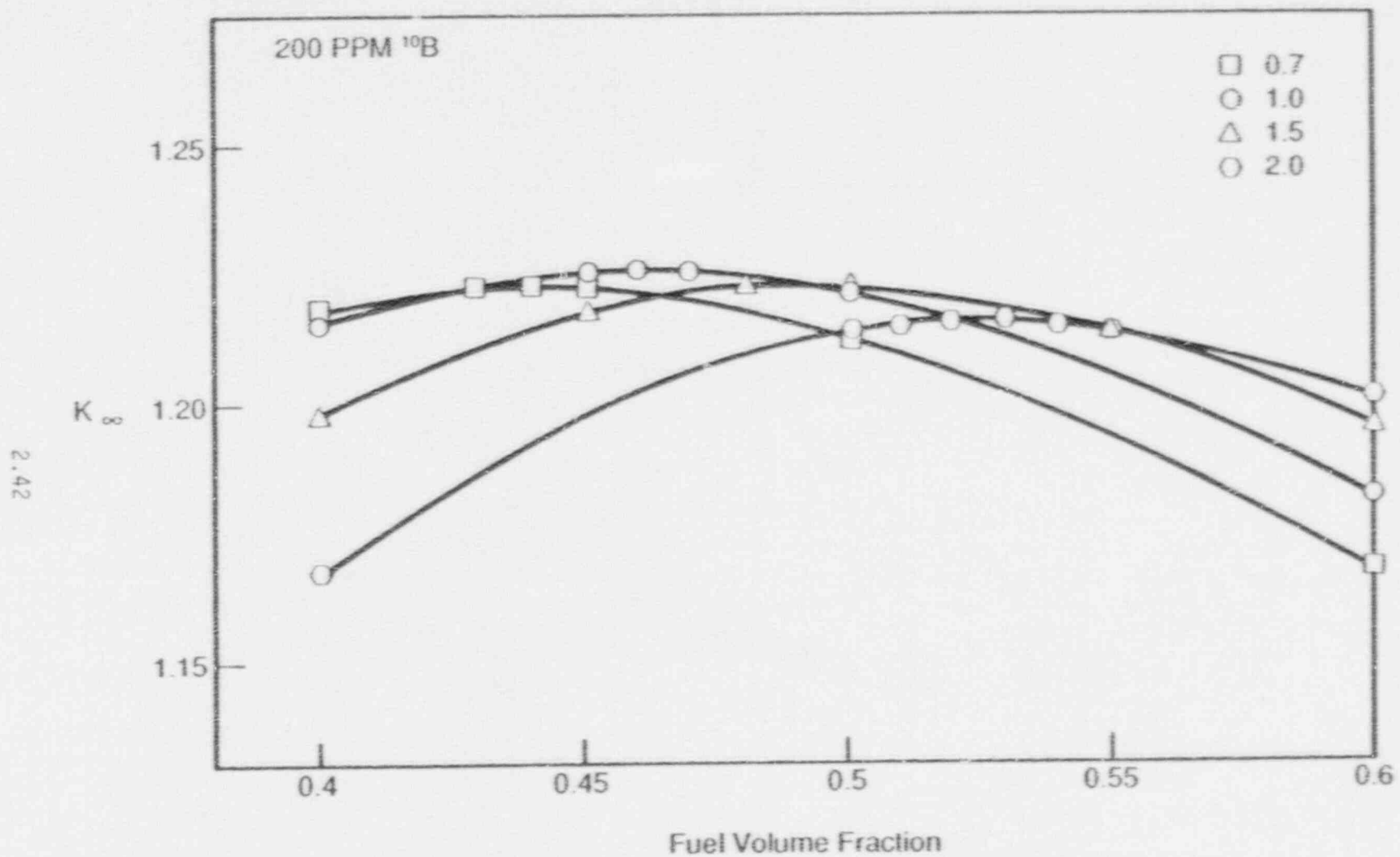


FIGURE 2.27. Calculated  $K_{\infty}$  for  $\text{UO}_2$  Fuel Particles in Water with 200 ppm  $^{10}\text{B}$

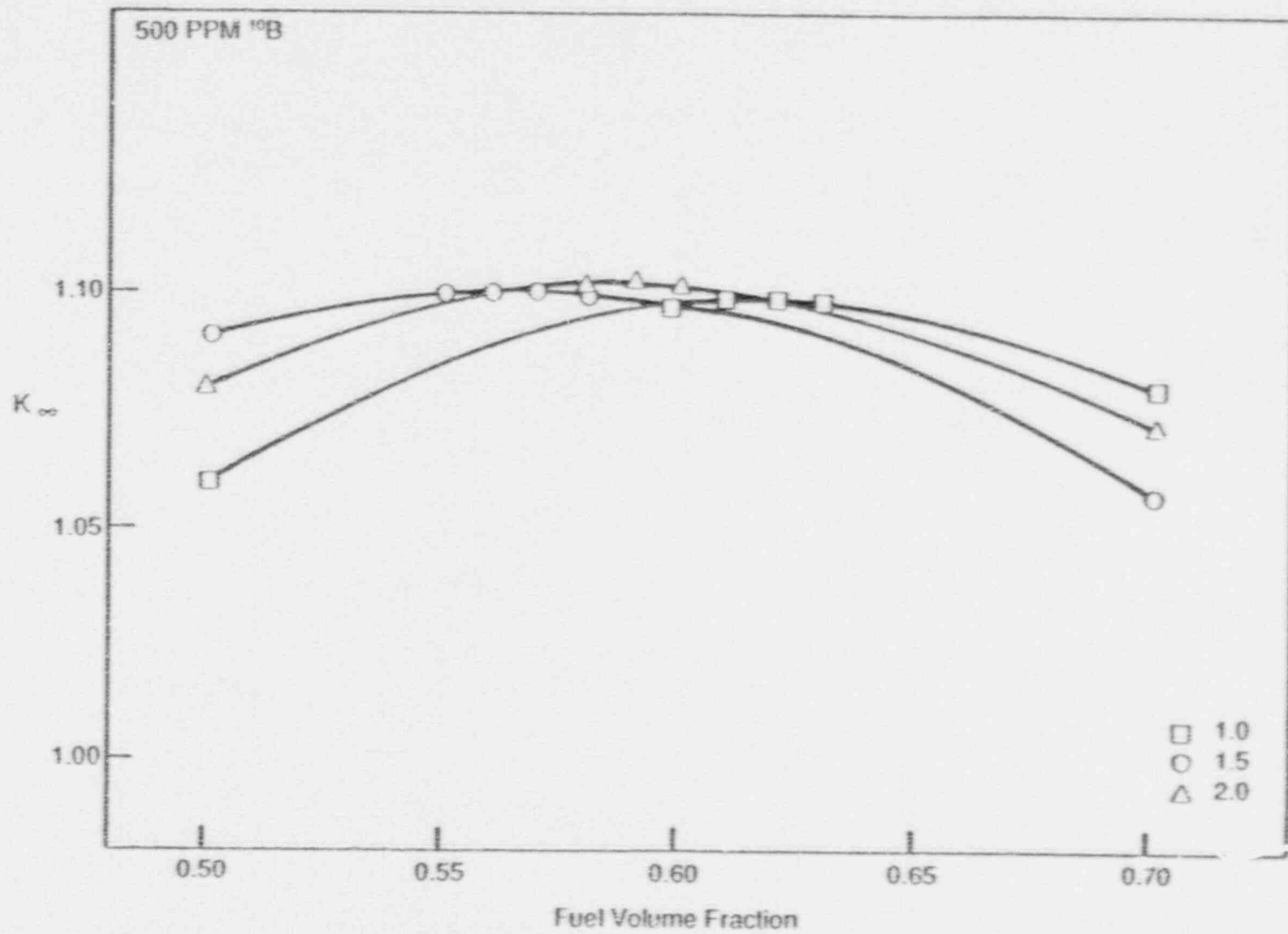


FIGURE 2.28. Calculated  $K_{\infty}$  for  $\text{UO}_2$  Fuel Particles in Water with 500 ppm  $^{10}\text{B}$



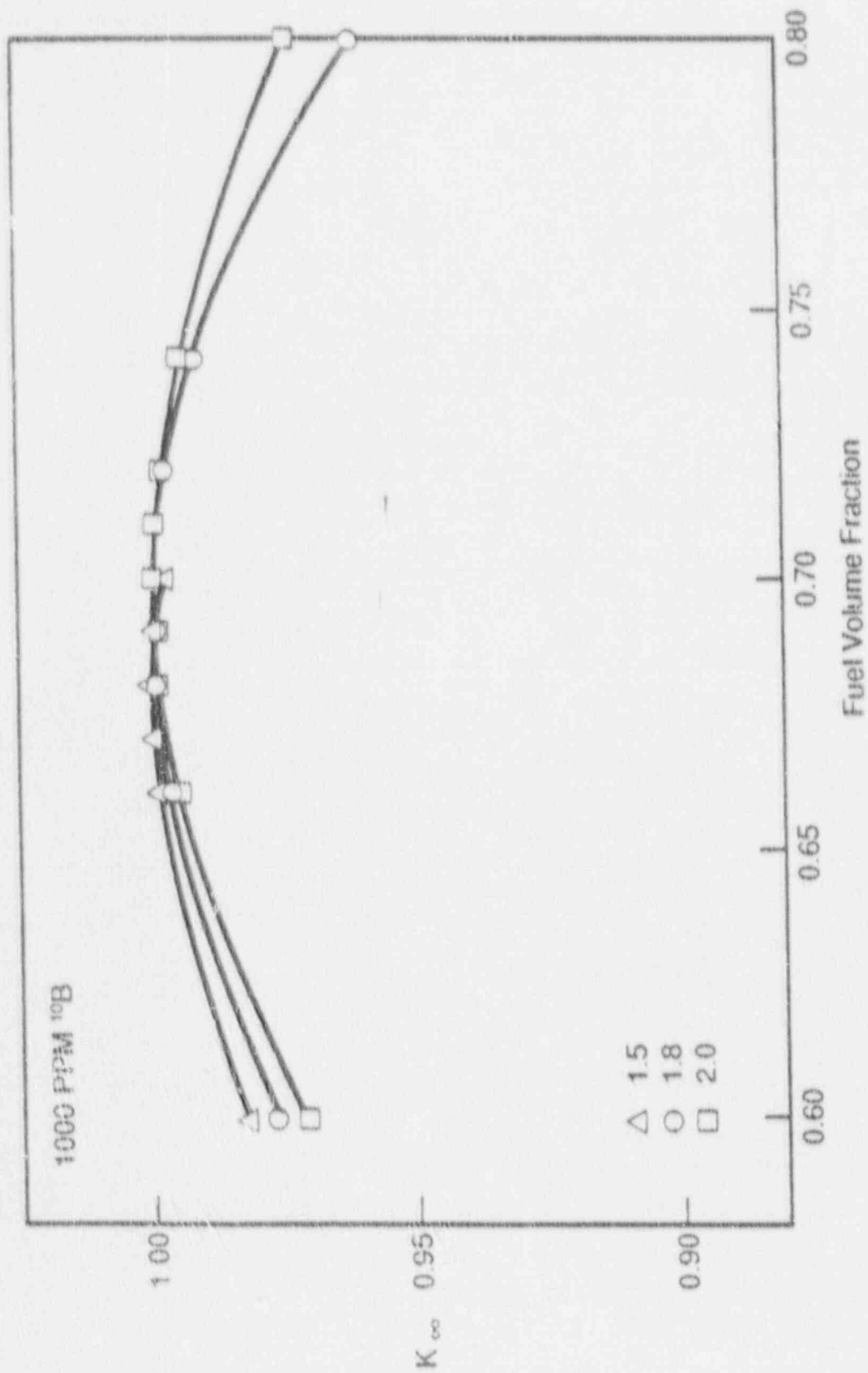


FIGURE 2.29. Calculated  $K_{\infty}$  for  $UO_2$  Fuel Particles in Water with 1000 ppm <sup>10</sup>B

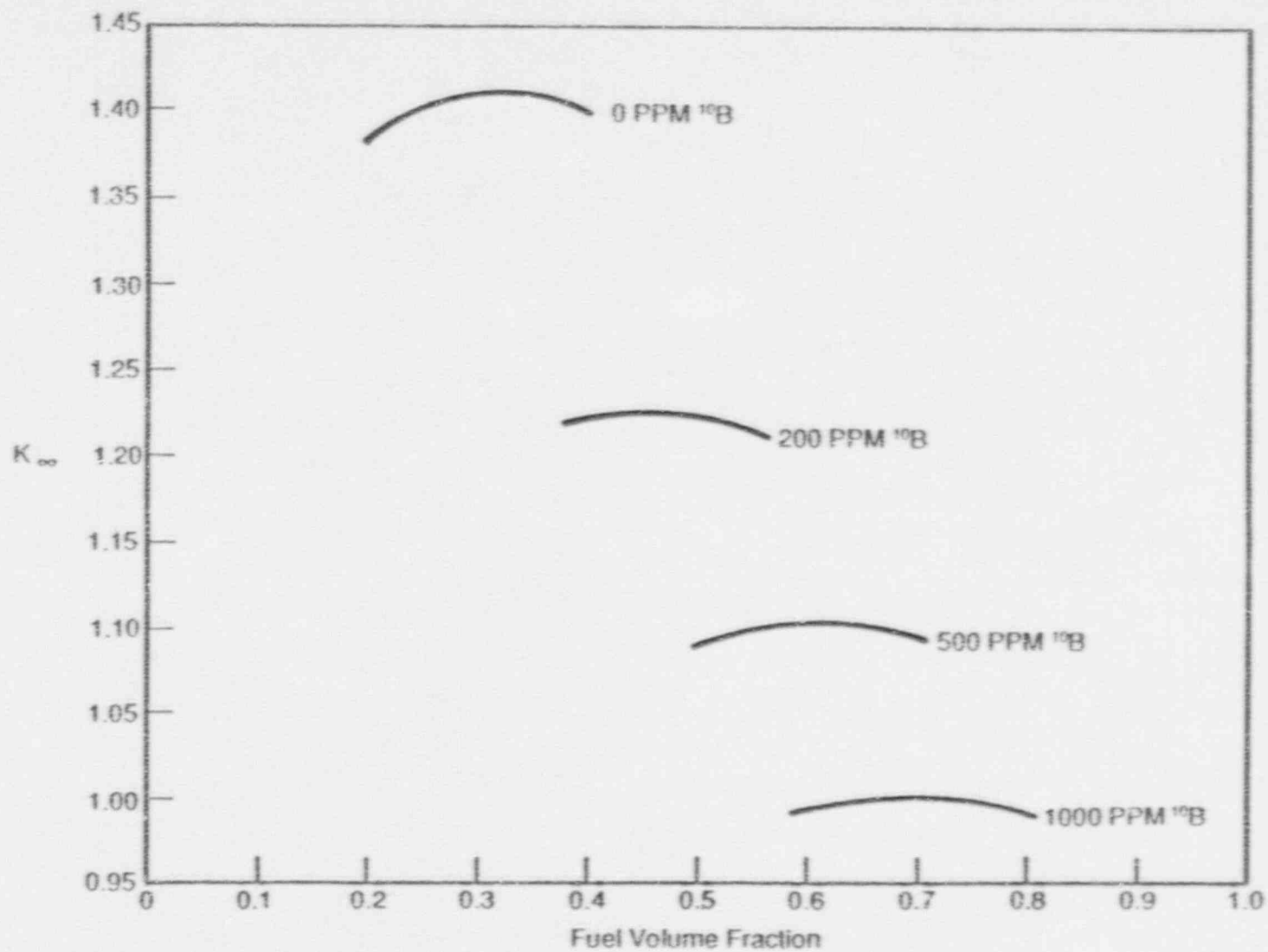


FIGURE 2.30. Envelope of Calculated  $K_{\infty}$ s for  $\text{UO}_2$  Fuel Particles in Water with  $^{10}\text{B}$  Concentrations of 0, 200, 500, and 1000 ppm

TABLE 2.4. Maximum Calculated  $k_{\infty}$  for Pellet Equivalent Particles in Water

<u>Boron Concentration</u>	<u>Particle Radius (cm)</u>	<u>Fuel Volume Fraction</u>	<u>K-Infinity</u>
0	0.5300 (8x8)	0.28	1.4034
0	0.6239 (7x7)	0.28	1.4061
200	0.5300 (8x8)	0.43	1.2160
200	0.6239 (7x7)	0.44	1.2192
500	0.5300 (8x8)	0.54	1.0890
500	0.6239 (7x7)	0.54	1.0925
1000	0.5300 (8x8)	0.64	0.9817
1000	0.6239 (7x7)	0.64	0.9850

fraction of 0.28 and no boron. A temperature of 3630°F was chosen. The calculated reactivity was 1.354 versus 1.403 for the cold condition. The  $5\% \Delta k/k$  reduction with temperature is large, but does not greatly change the results shown in Table 2.3. It would appear that temperature effects lower the boron concentration required to ensure subcriticality from about 1000 ppm  $^{10}\text{B}$  to perhaps 700 ppm  $^{10}\text{B}$ .

Another question which could be asked is, "How does the change in geometry when going from rods in an assembly to spherical particles affect the reactivity?" To answer this question, a series of  $k_{\infty}$  calculations were made for rods in a rectangular array. Two different rod/array combinations were calculated: a GE 7x7 and a GE 8x8. The pellet radius and pitch and resulting  $k_{\infty}$  values calculated are shown in Table 2.5. At zero boron the value is only slightly lower than that calculated for the optimum spherical particle size and volume fraction (since the reactor is designed to run at zero boron concentrations). At higher boron contents, however, the reactivity is lower than for optimum particles. It would appear that a boron concentration near 450 ppm  $^{10}\text{B}$  will ensure subcriticality. Unfortunately, under accident conditions, there is no guarantee that assembly geometry would be maintained.

The parameter calculated above was  $k$ -infinity. This results in two final questions, "How does the finite size of a reactor affect the results of the above analysis and what are the uranium masses required to achieve a critical system?" The leakage from a fuel volume the size of a reactor core will be at most a few percent. This will not significantly change the results unless the  $k_{\infty}$  is very close to unity. The critical volumes (and hence critical masses) were calculated for both the rods in a square array and the optimum spherical particle and pellet equivalent sphere cases (for those cases with  $k_{\infty}$  values greater than unity). The results are shown in Table 2.6. It must be recognized that these are not the minimum critical masses, only the critical masses calculated for the case with maximum  $k_{\infty}$ . Results show that a fairly large change in fuel volume fraction resulted in a small change in  $k_{\infty}$ . Thus, the minimum critical mass will occur for smaller fuel volume fractions than those calculated. However, the absolute minimum critical mass will occur for unrealistically low fuel volume fractions (i.e., the debris bed will compact to a greater density). These calculations indicate that only slightly more than 100 kg of uranium is necessary to achieve a critical configuration. The geometry and temperature effects noted in the  $k_{\infty}$  calculations result in a change in the critical mass of about 50%.

The calculations made in this section indicate that a critical core configuration can be obtained over a broad range of fuel particle sizes and fuel volume fractions for both unborated and fairly heavily borated reflood conditions. This indicates that further analysis of the consequences of a criticality accident should be performed.

TABLE 2.5. Calculated  $k_{\infty}$  Values for Fuel Rods at Assembly Pitch in Water

<u>Boron Concentration</u>	<u>Pellet Radius (cm)</u>	<u>Fuel Pitch (cm) [VF]</u>	<u>K-Infinity</u>
0	0.5283 (8x8)	1.6256 [0.3318]	1.4031
200	0.5283 (8x8)	1.6256 [0.3318]	1.1839
500	0.5283 (8x8)	1.6256 [0.3318]	0.9682
1000	0.5283 (8x8)	1.6256 [0.3318]	0.7556
0	0.6185 (7x7)	1.8745 [0.3420]	1.4028
200	0.6185 (7x7)	1.8745 [0.3420]	1.1845
500	0.6185 (7x7)	1.8745 [0.3420]	0.9704
1000	0.6185 (7x7)	1.8745 [0.3420]	0.7598



TABLE 2.6. Calculated Critical Masses for Spherical Particles and Pellets in Water

Boron Conc.	Particle or Pellet		Critical Radius(cm)	Critical Volume(cm <sup>3</sup> )	Critical Fuel Volume(cm <sup>3</sup> )	Uranium Critical Mass(kg)
	Radius	Vol. Frac.				
0 <sup>1</sup>	1.0	0.32	21.72	42040	13740	126
200 <sup>1</sup>	1.0	0.46	31.86	135400	62290	571
500 <sup>1</sup>	1.5	0.59	52.67	612100	361100	3310
0 <sup>2</sup>	0.5300	0.28	21.48	41520	11630	107
0 <sup>3</sup>	0.5300	0.28	22.83	49840	13950	128
200 <sup>2</sup>	0.5300	0.43	33.78	161500	69440	637
500 <sup>2</sup>	0.5300	0.54	54.59	681500	368000	3370
0 <sup>2</sup>	0.6239	0.28	21.46	41390	11590	106
200 <sup>2</sup>	0.6239	0.44	31.91	136100	59880	549
500 <sup>2</sup>	0.6239	0.54	53.42	638600	344900	3160
0 <sup>4</sup>	0.5283	0.3318	23.43	53870	17880	164
200 <sup>4</sup>	0.5283	0.3318	34.43	171000	56730	520
0 <sup>4</sup>	0.6185	0.3420	21.91	44060	15070	138
200 <sup>4</sup>	0.6185	0.3420	34.54	172500	59010	541

- Notes:
- 1 Spherical particles with maximum  $k_{\infty}$
  - 2 Spherical particles equivalent to pellets (S/V) with maximum  $k_{\infty}$
  - 3 As above except at 3630°F
  - 4 Cylindrical pellets at actual assembly design pitch

### 2.3.2 Excursion Analysis

The first step in the excursion analysis is to estimate the reactivity addition rate corresponding to the maximum core reflood rate. The high flow rate, low pressure flooding systems at Peach Bottom are the low pressure coolant injection (LPCI) (10,000-40,000 gpm) and low pressure core spray (LPCS) (3,125-12,500 gpm) systems. With all four pumps operating in each system, the core could be reflooded at a maximum flow rate of 52,500 gpm. For a total flow area of approximately 144 ft<sup>2</sup> within the core region of the vessel, this corresponds to a flooding rate of 49 ft/min.

The Peach Bottom SAR (Ref. 2.12) indicates that the core can go critical with two neighboring control blades removed. For the purpose of treating a specific core configuration, a small region of the core will be considered as being highly reactive in the following excursion analysis. A parallelepiped region will be used which is 2 feet on each side and 4 feet high. The region, which represents one-third of the height of 16 adjacent assemblies, is assumed to have no control blades and to be near optimum lattice conditions for criticality. At a flooding rate of 49 ft/min this region can be reflooded in approximately 5 seconds.

From the Criticality Handbook (Ref. 2.13), the minimum critical infinite length cylinder diameter for 3 wt% enriched uranium is about 11 inches. The maximum material buckling occurs for rods which have a 0.635 cm radius and a water-to-fuel volume ratio of 2.4 (a fuel volume fraction of 0.29). Within the channel box in an 8x8 BWR assembly with two unfueled rod locations the water-to-fuel ratio is 1.9 (a fuel volume fraction of 0.34) and the pellet radius is 0.53 cm. Thus, in the cold reflooded condition, the system is close to optimum. Fuel fragmentation or an increase in the water-to-fuel ratio would result in less reactivity. The effect of leakage on reactivity from a parallelepiped two feet on a side is approximately 10% and will be neglected (a conservative assumption).

The amount of reactivity that can potentially be added to the core by reflooding this region can be estimated by examining the reactivity coefficients of the intact core. The largest reactivity coefficient in the BWR is the void coefficient associated with steam bubbles. From the normal operating condition of approximately 40% voids to 0% voids the reactivity increases by  $\Delta k/k \approx 5.6 \times 10^{-2}$  (based on Fig. 3.6.9 of PBSAR). Since  $\beta = 0.0056$  (at 10,000 MWD/T), a reasonable estimate of the maximum reactivity addition is \$10.00 within a 5 second period (the minimum reflooding period).

Doppler feedback (broadening of <sup>238</sup>U absorption resonances with increased temperature) is the principle feedback mechanism for terminating rapid transients in low enriched uranium-water systems. In the 1960s a number of tests were performed on systems of this type in the SPERT facility at Idaho National Engineering Laboratory (INEL) (Ref. 2.14). Using a simple model developed by INEL engineers for a ramp insertion of reactivity and assuming

linear energy feedback, the energetics of a maximum reflood excursion will be estimated and then compared with those of the SPERT tests as an experimental benchmark.

The linear energy model is in the form (Ref. 2.15)

$$\frac{\dot{\phi}}{\phi} = at - bE(t) \quad (1)$$

where,

- $\dot{\phi}$  = change in core power with time (Mw/sec)
- $\phi$  = core power (Mw)
- $a$  = reactivity insertion rate in \$/sec multiplied by  $\beta/l$
- $t$  = time (sec)
- $b$  = Doppler reactivity feedback in \$ per Mw·sec multiplied by  $\beta/l$
- $E(t)$  = energy release (Mw·sec) as a function of time  $t$
- $\beta$  = delayed neutron fraction = 0.0056
- $l$  = neutron lifetime = 49 $\mu$  sec

This simple model predicts qualitatively the step-burst and ramp-burst behavior for a wide variety of reactors, both fast and thermal, with a wide range of shutdown coefficient values, and with a variety of quenching mechanisms. It is useful for estimating reactor behavior, particularly when specific details regarding shutdown mechanisms are not known.

The energy release function,  $E(t)$ , is in the form of a quotient of exponential function in  $t$ . Until the time of maximum reciprocal period the power shape behaves as if there were no shutdown effects operating. This is followed by the rise to maximum power and Doppler feedback induced shutdown. The energy released from the excursion (integrated over the excursion time so that time is not a variable) is approximately:

$$E_f = \frac{2[2a(\ln \left[ \frac{a}{b \phi_0} \right] - 1)]^{\frac{1}{2}}}{b} \quad (2)$$

For a \$2.00/sec ramp insertion rate  $a = 229$  \$/sec<sup>2</sup>. The Doppler coefficient at 0% voids is  $8.4 \times 10^{-6}$   $\Delta k/k/^\circ F$ . If it is assumed that the energy is deposited adiabatically in a cosine shape across each of the three dimensions of the assembly (an importance weighting of  $(4/3)^3 = 2.37$ ), the coefficient  $b = 2.23$  \$/(Mw·sec<sup>2</sup>).

The initial fission power level of the core segment depends on the magnitude of the spontaneous neutron source. The total energy produced in the excursion is not strongly sensitive to this value. The spontaneous neutron source can be calculated using the ORIGEN code (Ref. 2.16), which computes time-dependent concentrations and source terms of a large number of isotopes, with generation and depletion through transmutation, fission, and radioactive decay. Using ORIGEN results to estimate the spontaneous fission and  $(\alpha, n)$  source strength of irradiated fuel, the initial power,  $\phi_0$ , is estimated to be  $1 \times 10^{-8}$  Mw.

Substituting these values into Equation 2,  $E_f = 90$  Mw·sec. The average energy deposition in the fuel is 19 cal/g and the peak, assuming a cosine distribution in each dimension, is 73 cal/g, which corresponds to an approximately 1300°F temperature rise in the fuel. The peak energy deposition calculated above conservatively assumes zero voids. In an actual event it is expected that steam voids would form, thus lowering the actual energy deposition in the fuel. In reactivity insertion accident tests, it is found that, in order to obtain bursting of the fuel and dispersal of molten fuel droplets into the coolant, energy densities substantially greater than 280 cal/g (Ref. 2.17) must be added to the fuel. In the present example, however, the fuel may already be at a high temperature when the excursion starts. Thus, less energy deposition in the fuel may be sufficient to cause fuel bursting, which may occur if the fuel is already near its melting point. Based on Table 2.2, the fuel rod cladding begins to melt at approximately 3365°F. If the reflood excursion event occurs near this point in time, with the fuel near this temperature, the peak fuel temperature will be about 4665°F including the 1300°F temperature rise calculated above. Since the fuel rods are not expected to begin to melt until a temperature of 4870°F is reached, the energy deposition in the present example is probably not sufficient to result in bulk melting of the oxide. If the initial fuel temperature was higher than 3365°F, substantial clad melting will occur, making the presence of an intact standing core unlikely.

These temperatures are calculated by the MARCH code and are subject to the uncertainties of the code. If more accurate results are desired, more detailed and accurate codes should be used.

Two tests were performed in the SPERT I facility which were similar to the above example. The SPERT facility had steel clad oxide fuel with higher enrichment (4 wt%  $^{235}\text{U}$ ) than a BWR. The height of the fuel was 67 inches and the total mass of uranium dioxide was similar to that in the BWR reflood excursion example. The first test involved a \$2.70 step in reactivity and the second test involved an initial ramp followed by a step to \$3.30. The minimum periods for the two cases were 2.2 msec and 1.55 msec, respectively, in comparison with 10 msec for the BWR example. Total energies of 160 Mw·sec and 165 Mw·sec were observed in the two tests.



In the tests, two fuel rods failed, disintegrated, and formed steam through the rapid transfer of heat from the fine fuel particles. It is thought that these two fuel rods had become waterlogged prior to the start of the test. However, since numerous fuel rods were involved in the tests (and only two failed), the tests are considered valid and applicable to this discussion. The maximum pressure rise resulting from rod failure was 135 psig. The peak fuel surface temperature measured in the first test (30 msec after the peak power) was 1000°F above ambient. Premature rupture, rapid disintegration, and resulting steam formation of the waterlogged fuel in the second test was probably a factor in limiting the energetics of the excursion. The failed fuel rods had maximum energy densities of up to 220 joules/g (53 cal/g) although they were not in the highest flux zone in the experimental core.

The two SPERT tests provide support to the conclusions of the BWR reflood excursion analysis. In an actual excursion, steam generation and void formation would play a role in limiting the energy release and terminating the transient. Doppler feedback in itself, however, is adequate to limit the energetics of reflood recriticality to a level below which the vessel would be threatened by a pressure pulse.

### 2.3.3 Debris Bed Dryout Power Limits

If the reactor remains critical following an initial excursion at the time of reflooding, it will either enter an oscillatory mode in which water periodically enters and is expelled from the core debris or it will approach a quasi-steady state. In either case, the average power level achieved will be determined by the balance between the reactivity added and the feedback mechanisms.

The energy required to heat and boil the coolant water being added to the vessel provides an upper bound to the time-averaged power in the core. Debris bed dryout limits can also impose a limit on the amount of heat generated in a critical debris bed. The argument is similar to that made under more normal ATWS situations. Higher power levels will result in more boiling, hence a higher void fraction and eventually under-moderation of the fuel. The under-moderated condition will reduce reactivity and the power level. As the bed power decreases, voids will collapse allowing more water to enter the bed. With this increase in moderation the reactivity and the bed power will increase. Under steady-state conditions, the bed power will be expected to stabilize at the bed dryout power level which will balance the power level to the rate of moderator incursion into the bed.

Debris bed dryout is a relatively well understood phenomenon. At the dryout limit, a balanced vapor and liquid counter-flow situation is established. Under steady-state conditions, the hydrostatic head of the water trying to enter the bed is balanced by the steam pressures produced by



vaporization of the water. Bed dryout has been measured by a number of investigators. Figure 2.31 shows typical results (reproduced from Ginsburg, Ref. 2.18), and illustrates the dependence of the dryout heat flux on the bed particle size at atmospheric pressure. The data scatter is seen to be about a factor of two.

Comparison of the Lipinski correlation (Ref. 2.19) with the data in Figure 2.31 indicates the correlation falls on the low side of the data for larger particles. However, the correlation is found to provide a good representation of the data over a wide range of parameters, and is frequently used in reactor safety analyses. Figure 2.32 shows debris bed dryout heat fluxes using the Lipinski correlation for pressures between atmospheric and 2000 psia and particle diameters of 0.1 and 0.5 inches. Particle diameters between 0.1 and 0.5 inches are representative of the sizes expected for scattered fuel rods in reflooded cores. It is seen from Figure 2.32 that the dryout heat flux increases rapidly above atmospheric pressure, but is relatively insensitive to pressures above 200 psia.

A debris bed porosity (water volume fraction) of 0.4 was assumed for the calculations in Figure 2.32. A water volume fraction of 0.4 is less than that in the original core, but the analyses reported in Section 2.3.1 indicate that such a system would be critical.

Figure 2.5 shows the TMI-2 core end-state conditions. Debris beds are observed above the region of previously molten materials and in the lower head. Primarily for the sake of convenience, a hemispherical-shaped debris bed will be assumed in the present calculations. It is assumed that all the heat is released through the top (circular) surface of the bed. However, since there is scatter in the data and uncertainties in the correlations, the bed geometry, and the heat transfer area, a multiplier is used as an adjustable sensitivity parameter. A relation can be used to compare debris bed dryout power limits with the bed decay heat and assumed fission power levels.

It is instructive to note that very large debris beds are required to enclose more than a few percent of the core. Figure 2.33 shows the fraction of the core that can be contained in a hemispherical debris bed. A bed porosity of 0.4 was assumed in the calculations. An 8 foot diameter hemispherical debris bed can hold only 11% of the core fuel material. A hemispherical bed diameter of nearly 17 feet is required to hold the whole core. For comparison, the diameter of the lower head of the Peach Bottom reactor is about 21 feet while the diameter of the lower head of the Duane Arnold reactor is about 15 feet.

Figure 2.34 shows power densities expected in critical debris beds for expected particle sizes and pressures. In order to simplify the calculations, constant debris bed dryout heat fluxes were assumed for pressures above 200 psia ( $Q_{DB} = 1.06 \times 10^6$  and  $2.79 \times 10^6$  Btu/hr·ft<sup>3</sup> for particle diameters of 0.1 and

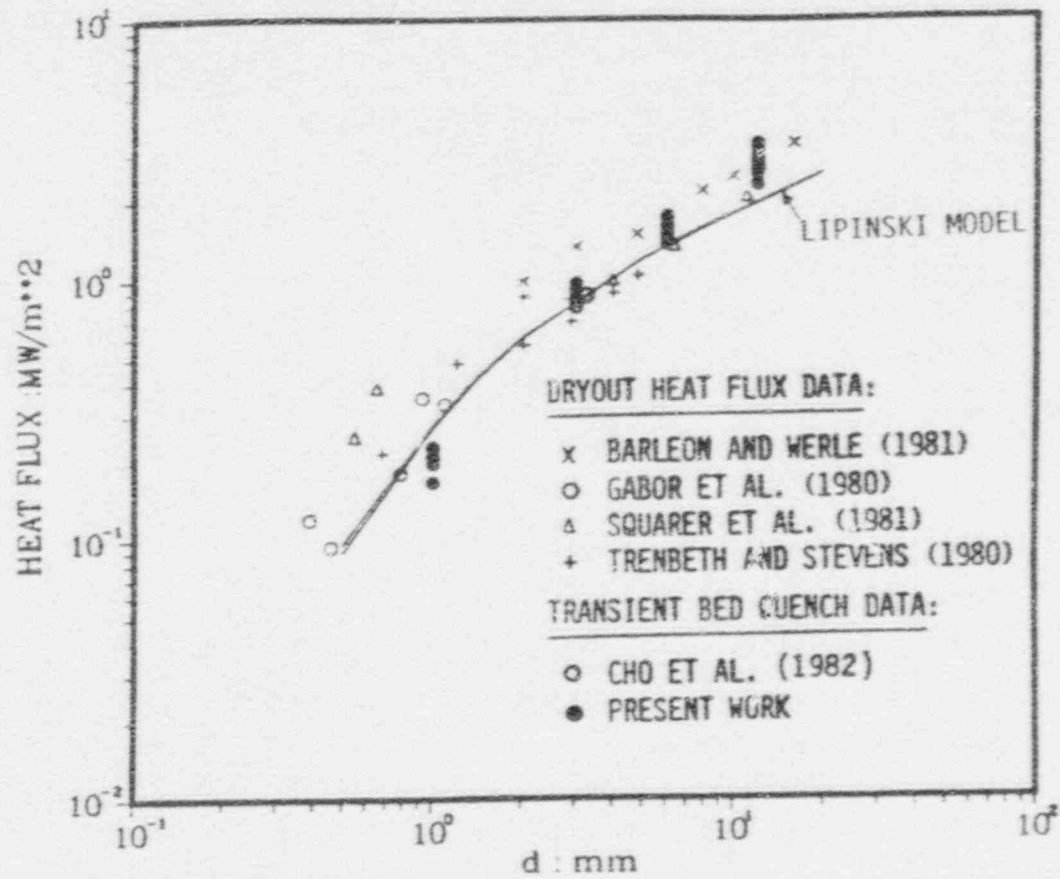


FIGURE 2.31. Steady-State Dryout Heat Flux and Bed Quench Heat Flux Data Compared With Steady-State Lipinski Model ( $P=0.1$  MPa,  $e=0.4$ ) (From References 2.17 and 2.18)

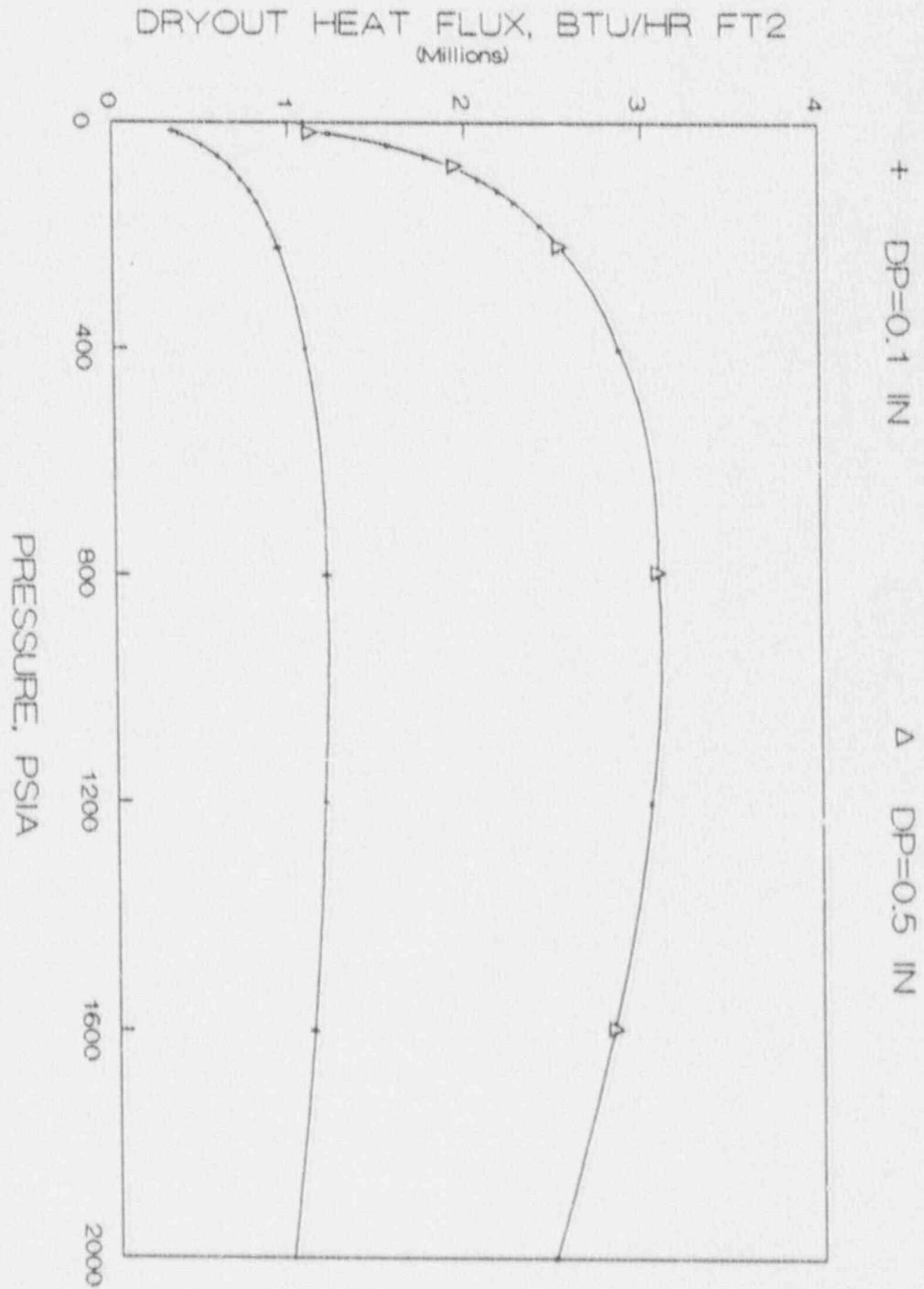


FIGURE 2.32. Lipinski Correlation of Debris Bed Dryout Heat Flux (Ref. 2.18)

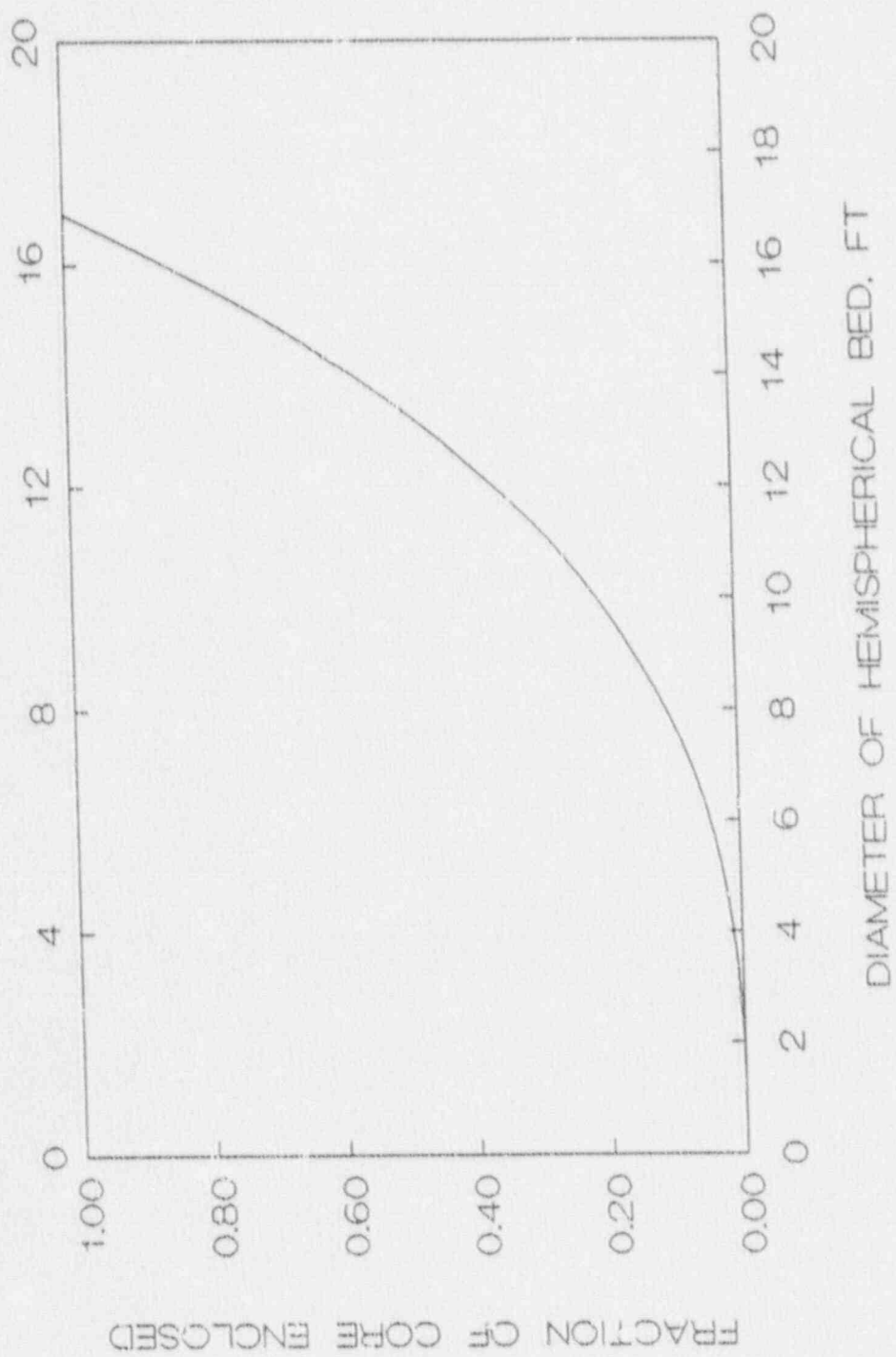


FIGURE 2.33. Fraction of Core Enclosed in Debris Bed as a Function of Bed Diameter



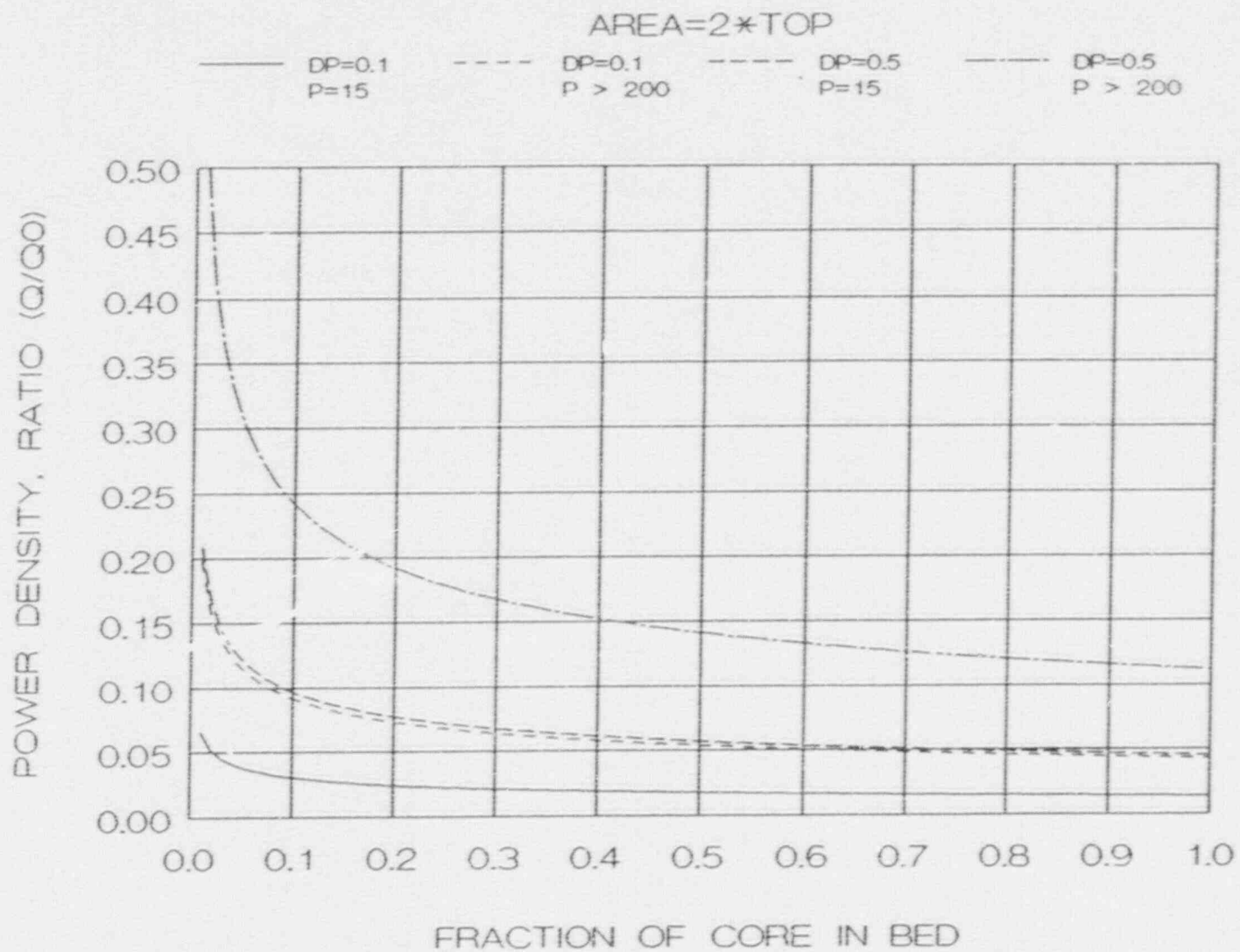


FIGURE 2.34. Debris Bed Dryout Power Density Limit at 15 and 200 psia for 0.1 and 0.5 inch Particle,  $F_A = 2.0$



0.5 inches, respectively). Also, a sensitivity multiplier of  $F_A = 2.0$  is assumed to partially account for correlational bias and the possibility of larger heat transfer areas.

The results in Figure 2.34 indicate that debris bed dryout would be expected to limit power densities to relatively low levels for small particles and low pressures. Power densities less than 5% of the operating density are generally predicted. The core decay heat falls below 2% at about 15 minutes after shutdown. Thus these rates are roughly comparable to decay heat levels. However, for large particles and high pressures, the power densities may be a significant fraction of the normal operating power density. For small debris beds in particular, the power densities may approach full operating power densities.

The results in Figure 2.34 were formulated in terms of the fuel power density, that is, the fuel volumetric power. Figure 2.35 shows the debris bed powers expressed as a fraction of the normal core power level rather than the particle power density (the bed power level is obtained by multiplying the power densities by the fraction of the core in the bed). As before, it is seen that for large particles at high pressure, bed power levels significantly above the decay heat level (2% at 15 minutes) may be obtained due to recriticality.

It is also instructive to consider how much makeup water is required to compensate for the coolant boiloff rates implied by the bed powers in Figure 2.35. Figure 2.36 shows the makeup which must be supplied to the debris bed to prevent dryout and support the criticality. These boiloff rates may be compared with the capacity of typical BWR makeup pumps listed in Table 2.7. Depending on what makeup systems are available and the size of the critical debris bed, the makeup may be inadequate to support criticality under steady-state conditions. If insufficient makeup is available, a recurrent "chugging" phenomena would be expected. Water would enter an under-moderated, shutdown core. Eventually sufficient water would exist to allow criticality. The additional heat produced would void the core, shutting the nuclear reaction down. Water would again enter, repeating the process.

The results in Figures 2.35 and 2.36 do not consider the heat generation in the remainder of the core; that is, the portion not in the debris bed. The remaining portions of the core could conceivably be composed of intact fuel rods or be in the configuration of a molten mass. Decay heat will add up to 0.02 (15 minutes after shutdown) to the results shown in Figure 2.35.

Dryout provides an upper limit to the power which can be generated in a critical debris bed. The expected power is generally well below normal operating power levels, however, the power may significantly exceed decay heat levels. The higher power levels are encountered at high pressures for large particles. For small particles and low pressures, the power is expected to be comparable to decay heat levels.

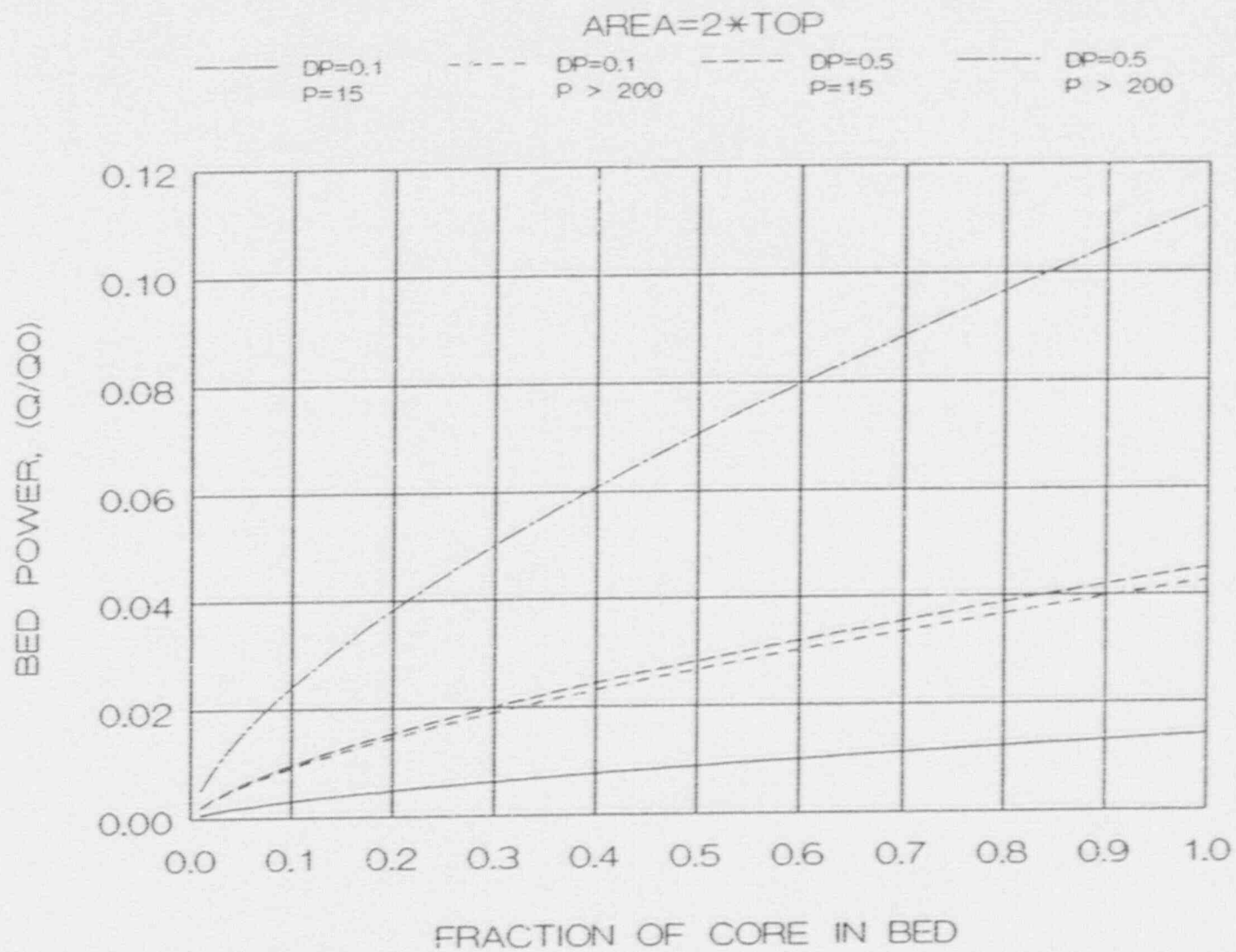


FIGURE 2.35. Ratio of Debris Bed Power to Core Operating Power

2.61

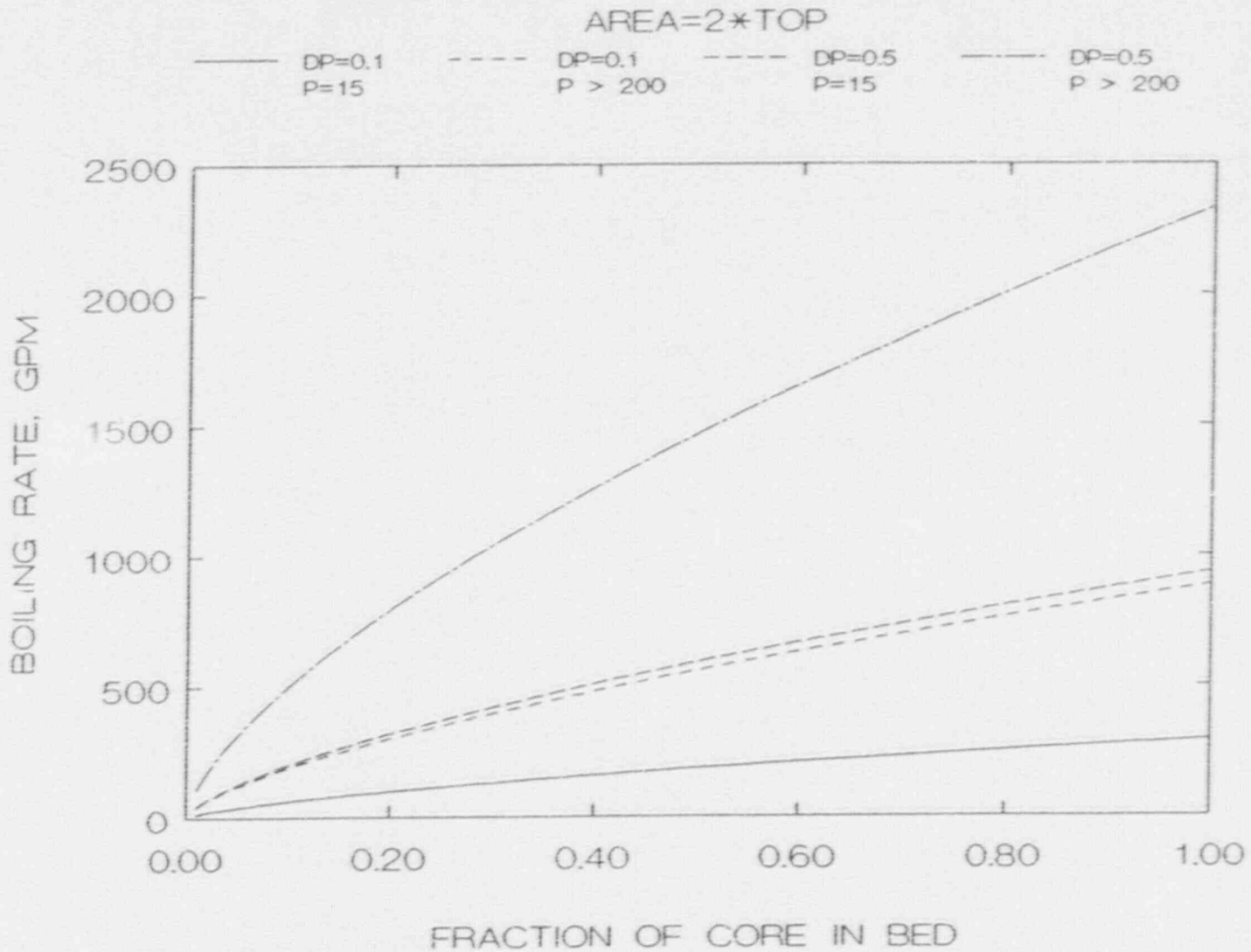


FIGURE 2.36. Coolant Boiloff Rate From a Critical Debris Bed

TABLE 2.7. Capacity of BWR Makeup Pumps

<u>Pump</u>	<u>Capacity, GPM</u>	<u>Pressure operating range, psi</u>
RCIC	600	1120 > p > 150
HPCI	5000	1120 > p > 100
RWCU	162 each (3 pumps)	p < 1450
SLC	56	p < 1120
CRD	55 to 90 each, depending on pressure (2 pumps)	p < 1055
LPCI	10000 each (4 pumps)	p < 295
LPCS	3125 each (4 pumps)	p < 290

Criticality in debris beds is unlikely to produce power levels much above 10% of normal power. At these power levels, either the high or low pressure makeup systems would provide adequate coolant to remove the heat being generated within the debris bed. This does not imply, however, that the interior of the bed will remain cooled. A dried region could become molten and relocate. Whether the relocated melt would eventually become coolable, as at TMI-2, is speculative. The effect of melting and relocation would almost certainly be to reduce the criticality of the bed, however.

#### 2.3.4 Containment System Effects

The nature of the recriticality event occurring following BWR core melting and reflood has been established. The arguments presented in Section 2.3.2 indicate an explosive response is unlikely even under conditions of maximum reflood rate. A steady-state power level would be established which could be elevated above the normal decay heat power levels. The response of the containment to these elevated, but steady-state, power levels is considered in this section of the report. Time windows are calculated where emergency boration and reactor shutdown would have to be established in order to prevent containment over-pressure failure. Also, the results of previous studies of containment venting during ATWS scenarios are discussed.

#### Core Power

In general, the power levels achieved during recriticality would depend on the core damage state, the coolant makeup rate available, the pressure in the reactor vessel, and the water level maintained in the core. If the core geometry is severely degraded and a packed debris bed forms after reflood, the results in Section 2.3.3 indicate debris bed dryout considerations would limit the power to 10% to 20% of operating power. A simple hand calculation indicates a coolant makeup rate of about 2500 gpm is required to compensate for the boiloff at a 10% core power level. This makeup rate may be compared with the pump capacities listed previously in Table 2.7. It is apparent that only the high flow rate high pressure coolant injection (HPCI), LPCI, and LPCS pumps would be able to support steady-state core power levels above 10%. If the core is not severely damaged, ATWS calculations performed for intact cores can be used to give an indication of the expected power levels. It is quite unlikely that a degraded core will be more reactive than an unbladed core in its normal geometry. ATWS calculations (Ref. 2.20, 2.21, and 2.22) indicate that reduction of the primary system pressure and maintenance of a water level near the top of the core will result in core powers between 8% and 13% of full power. In conclusion, it is expected that either naturally occurring debris bed dryout considerations or operator actions can limit core power levels to less than about 20%.



## Suppression Pool Heatup and Containment Pressure

Table 2.1 listed a number of severe accident scenarios. For some of the accidents the containment fails (e.g., GG1P1, PBTC, and PBTW) or is bypassed (e.g., PBV) prior to core melt. For these accidents emergency boration obviously cannot prevent containment failure. However, reduction of core power would still be desirable to minimize the driving force for dispersal of fission products. For the remaining accidents, the containment is intact during the core melt. These accidents can be divided into two categories, depending on the suppression pool temperature at the time of core melt. For LOCAs and station blackout cases with early emergency core cooling (ECC) failure, the MARCH calculations predict suppression pool temperatures between 122 and 155°F during the core melt but prior to core collapse and head failure. Sequences of this type include PBTBUX, PBTBO, GGTBS, GGS2E, and GGTQUV. For some ATWS and station blackout sequences in which the ECC initially functions and keeps the core covered for several hours, pool temperatures between 215 and 237°F are calculated. Sequences of this type include GGTB1, PBTB2, PBTBS, and PBTB3. For calculational convenience, initial suppression pool temperatures of 140°F and 225°F will be assumed for the two categories at the start of recriticality.

Based on NUREG/CR-2442 (Ref. 2.23), the containment failure pressure is estimated to be about 132 psia, corresponding to a pool saturation temperature of 348°F. This study was based on the Browns Ferry containment. A more recent analysis of the Peach Bottom containment has predicted a failure pressure of 174 psia (Ref. 2.24). In the NUREG-1150 assessment, 132 psia corresponds to approximately the 5th percentile and 165 psia corresponds to the 50th percentile of the containment failure distribution. The median failure pressure for Grand Gulf, given in NUREG-1150, is 70 psia, corresponding to a pool saturation temperature of 303°F. Both suppression pools contain about 9,000,000 lb of water. For reference, the (adiabatic) suppression pool heatup rate is about 130°F/hr for a steam input rate corresponding to 10% of full power. Using an appropriate heatup rate and the initial pool temperatures discussed above, curves were constructed to define the time following recriticality to reach the Peach Bottom and Grand Gulf containment failure pressures. The results are shown in Figure 2.37.

Since suppression pool cooling may be available in addition to coolant makeup, the energy input to the suppression pool is defined in terms of that in excess of residual heat removal (RHR) cooling. The rated capacity of all four RHR heat exchangers corresponds to about 2.5% of full power. As the suppression pool temperatures increase, the capacity of the heat exchangers also increases. At the temperatures corresponding to containment failure (303 to 348°F), the RHR capacity is estimated to increase to about 7% of full power. Since the core power is likely to be below 10% to 20% of full power, RHR cooling may have a significant effect on the containment pressurization.

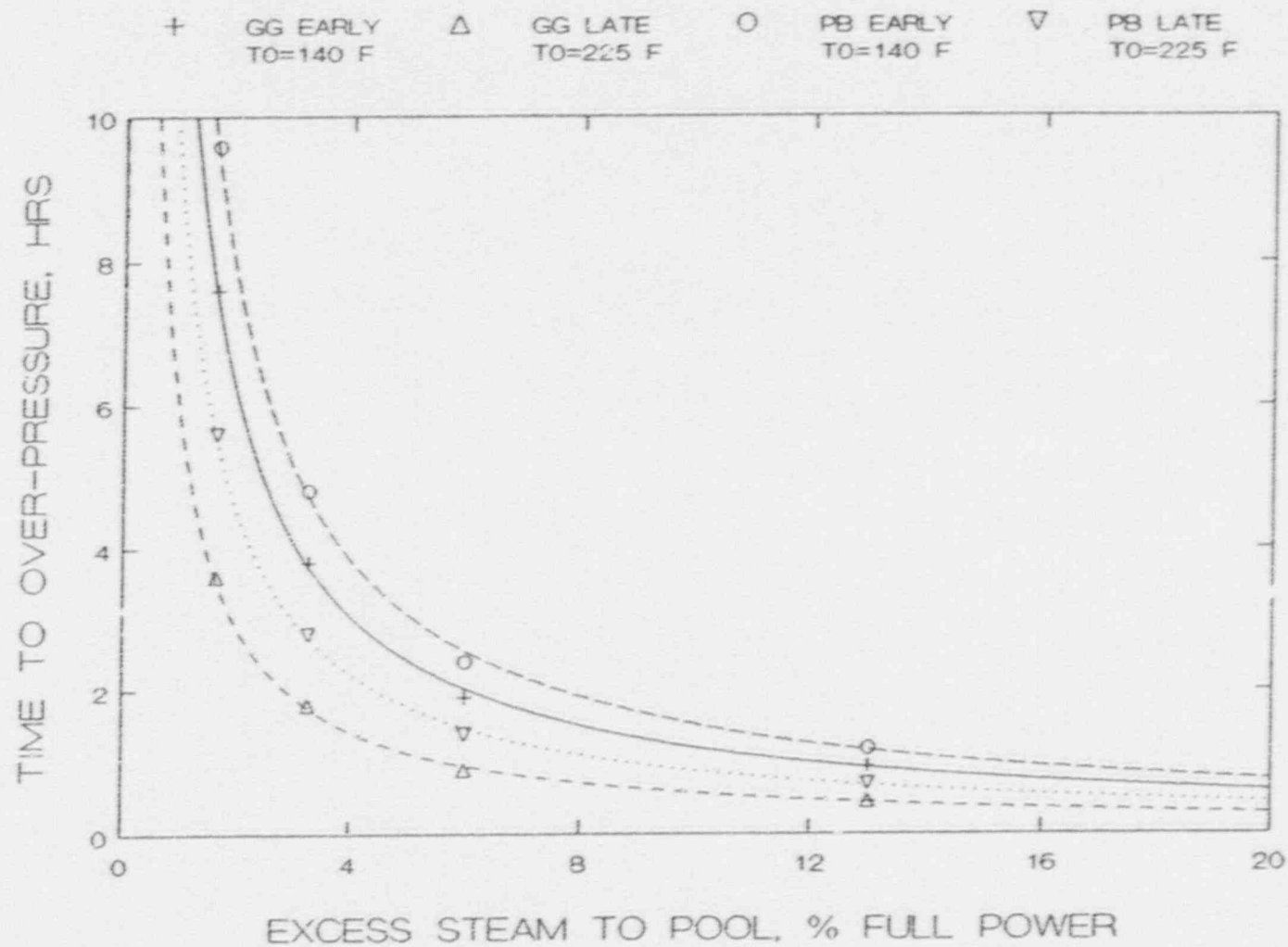


FIGURE 2.37. Containment Over-pressure Time as a Function of Energy to Pool

### Emergency Boration

The results in Figure 2.37 indicate that if the excess steam is limited to about 3% of full power, over two hours are available to establish core shutdown by boration. However, if the excess steam corresponds to 13% of full power, only about a half hour may be available for the cases considered. These times may be compared with the time required to establish boration to terminate the recriticality accident.

The present standby liquid control (SLC) system is designed to provide boration in one-half to two hours, depending on the boration pump flow rate. Depending on the resulting  $^{10}\text{B}$  concentration in the reactor vessel, this may be adequate to bring the core to cold shutdown in the absence of control blades. Based on the results in Figure 2.37, the boration rate would seem to be marginally adequate to avoid containment over-pressure, assuming boration is adequate and actuated at the same time as core reflood.

### Containment Venting

Containment venting in ATWS sequences prior to core damage for the Peach Bottom reactor is discussed in Ref. 2.21. The venting calculations indicate over-pressure failure of containment can be avoided under steady-state conditions at 13% of full power provided all four RHR systems are operating and two 18 inch containment vents are opened. In station blackout cases, however, it is necessary in the present system to make manual alignments in the reactor building to establish torus venting. However, high temperatures and radiation levels are expected to be present locally if prior venting or core damage has occurred. Thus, in the present Peach Bottom system, establishment of the 18 inch vent path may not always be feasible. It is also not clear that the vent could be re-closed if desired.

## 2.4 REFERENCES

- 2.1 J. V. Walker, editor, "Reactor Safety Research Semiannual Report, July-December 1987, Reactor Safety Research Program," NUREG/CR-5039, Sandia National Laboratories, November 1988.
- 2.2 P. Hofmann, M. Markiewicz, and J. Spine, "Reasons for the Low-Temperature Failure of BWR Absorber Elements," KfK, Karlsruhe, FRG, SFD Partners Meeting, April 1989.
- 2.3 L. J. Ott, "Boiling Water Reactor Severe Accident Response (BWRSAR) Post Test Analysis of the ACRR DF-4 Experiment," ORNL, SFD Partners Meeting, April 1989.

- 2.4 H. M. Chung and T. E. Kassner, "Embrittlement Criteria for Zircaloy Fuel Cladding Applicable to Accident Situations in Light Water Reactors: Summary Report, NUREG/CR-1344, ANLJ-79-48, January 1980.
- 2.5 Katanishi, et al., "Fuel Rod Behavior in Reflooding Phase Under Severe Accident Conditions," JAERI, Japan, SFD Partners Meeting, April 1989.
- 2.6 J. M. Broughton, et al., "A Scenario of the TMI-2 Accident," ANS Transactions, October 1988 Meeting, Vol. 57, TANSO, 395, 1988.
- 2.7 P. Bottomley, and M. Coquerelle, "Metallurgical Examination of Bore Samples from the TMI-2 Reactor Core," ANS Transactions, October 1988 Meeting, Vol. 57, TANSO, 403-4, 1988.
- 2.8 G. E. Muller, and A. Sozer, "Thermal-Hydraulic Characteristic Models for Packed Debris Beds," NUREG/CR-5689, December 1986.
- 2.9 R. S. Denning, et al., "Verification Test Calculations for the Source Term Code Package," NUREG/CR-4656, July 1986.
- 2.10 "SCALE: A Modular Code System for Performing Standardized Computer Analyses for Licensing Evaluation," NUREG/CR-0200, Oak Ridge National Lab, 1982.
- 2.11 J.P. McNeece, T.J. Trapp, and J.K. Thompson, "MCDAN - A Monte Carlo Computer Code for Calculating the Dancoff Correction Factor for Spheres and Rods," PNL-3086, 1979.
- 2.12 Philadelphia Electric Company, "Final Safety Analysis Report, Peach Bottom Atomic Power Station Units No. 2 and 3," Docket 50-277, 50-278.
- 2.13 W.A. Blyckert, et al, Criticality Handbook, ARH-600, Vol. III, p.IV.B.7-2, 1971.
- 2.14 T.J. Thompson, "Accidents and Destructive Tests," The Technology of Nuclear Reactor Safety, Reactor Physics and Control, The MIT Press, Cambridge, Vol. 1, pp 684-685, 1964.
- 2.15 W.E. Nyer, "Mathematical Models of Fast Transients," The Technology of Nuclear Reactor Safety, Reactor Physics and Control, The MIT Press, Cambridge, Vol. 1, pp. 420-423, 1964.
- 2.16 M. J. Bell, "ORIGEN - The ORNL Isotope Generations and Depletion Code," ORNL-4628, CCC-217, Oak Ridge National Laboratory, Oak Ridge, TN, 1973.
- 2.17 P.E. MacDonald, et al, "Assessment of Light Water Reactor Fuel Damage During a Reactivity-Initiated Accident," Nuclear Safety, Vol. 21, No. 5, Sept.-Oct. 1980.



- 2.18 T. Ginsburg, et al, "An Experimental and Analytical Investigation of Quenching of Superheated Debris Beds Under Top-Reflow Conditions," NUREG/CR-4493, January 1986.
- 2.19 R.J. Lipinski, "A Coolability Model for Post-Accident Nuclear Reactor Debris," Nuclear Technology, Vol. 65, pp. 53-66, 1984.
- 2.20 R.M. Harrington, Letter Report to T.J. Walker (NRC), "The Effect of Reactor Vessel Pressure and Water Level on Equilibrium BWR Core Thermal Power During MSIV-Closure-Initiated ATWS," Severe Accident Sequence Analysis Program, Oak Ridge National Laboratory, January 10, 1986.
- 2.21 D.J. Hanson, et al, "Containment Venting Analysis for the Peach Bottom Atomic Power Station," NUREG/CR-4696, EGG-2464, December 1986.
- 2.22 BWR Owners Group calculations quoted in R.M. Harrington and S.A. Hodge, "ATWS at Browns Ferry Unit One-Accident Sequence Analysis," NUREG/CR-3470, ORNL/TM-8902, July 1984.
- 2.23 Ames Laboratory, "Reliability Analysis of Steel Containment Strength," NUREG/CR-2442, June 1982.
- 2.24 Chicago Bridge and Iron Company, "Mark I Containment Severe Accident Analysis," April 1987.



### 3.0 ACCIDENT SEQUENCES

According to NUREG-1150 (Ref. 3.1), which is based on the NUREG/CR-4550 analyses (Ref. 3.2), the risk dominant accident sequences for internally initiated events at Peach Bottom Unit 2 are of two types:

1. Station blackout (SBO) events (i.e., loss of all ac power, except that which is dc-powered through an inverter), which account for 86% of the plant risk of core damage.
2. Anticipated transient without scram (ATWS) events, which account for 12% of the plant risk of core damage.

No other accident types contribute more than 1% to the plant core damage frequency.

Substantial activities were conducted at Peach Bottom to reduce the risks identified by earlier PRA results by making changes in hardware and improving training, procedures, and testing and maintenance at the plant. These changes and improvements mean that this plant may not be entirely characteristic of all BWRs. However, other BWRs should also be dominated by the same events as Peach Bottom, rather than by other events such as loss of coolant accidents (LOCAs). This observation is based upon the multiplicity and diversity of water supplies typically available in BWRs for coolant injection, which makes most transients and LOCAs with a loss of coolant injection a small contributor to the plant risk of core damage, except for the SBO events where all ac power is lost. The observation is also consistent with results identified in NUREG-1150 for Grand Gulf, where SBO events account for 99% of the plant risk of core damage and ATWS events account for the remaining 1%.

The following sections discuss these internally initiated events and their base-case event trees, sequences, and dominant cutsets. The majority of the information used in the following sections has been obtained from the analysis conducted in NUREG/CR-4550.

#### 3.1 STATION BLACKOUT (SBO)

A station blackout is defined as the loss of all ac power, except that which is powered through an inverter from the station batteries. As such, a station blackout involves the loss of both the normal ac power source from the offsite grid and the emergency ac power source from the onsite diesel generators. The loss of offsite power (LOSP) can occur as an initiating event or subsequent to another event, such as a generator trip. The loss of onsite power can occur from the combination of a multitude of system and/or

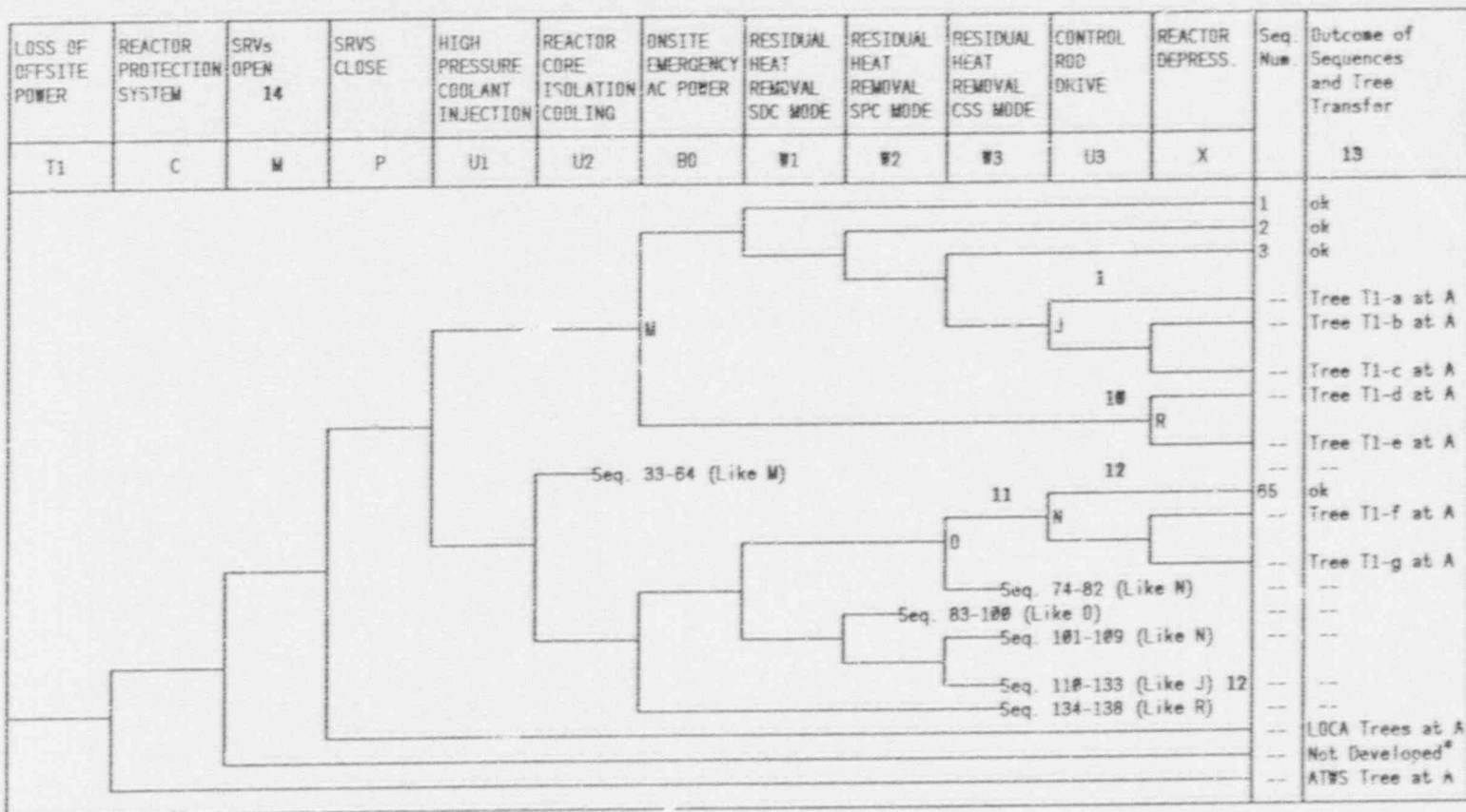
supporting system failures. The logic that depicts the sequence of events involved in a station blackout at Peach Bottom Unit 2 is shown in the NUREG/CR-4550 loss of offsite power event tree, provided as Figure 3.1. This event tree logic applies to all loss of offsite power events, regardless of the actual initiator. It should be noted that the power conversion system, feedwater system, and condensate system are not modelled in the event tree since a loss of offsite power would prevent the operation of these systems. If offsite power were restored, these systems could be used to mitigate and/or terminate the event.

Event tree sequences 28-32, 60-64, and 134-138 (in Figure 3.1) represent the SBO sequences. There is an equivalent set of sequences involving a stuck-open safety relief valve (SRV) that is not explicitly modelled, but is considered in the analysis. The SBO sequences can be divided into two groups based on the timing to core damage. The first group consists of those sequences (134-138) where core damage occurs within 1 hour and are referred to as short-term station blackout (SSBO) sequences. The other group consists of those sequences (28-32 and 60-64) where core damage occurs after 1 hour, typically 9 to 12 hours later. These sequences are referred to as long-term station blackout (LSBO) sequences.

The primary difference between these sequence groups is the period at which the station batteries become depleted. If all the station batteries are depleted when a loss of offsite power occurs due to some common cause failure, the diesel generators will be unable to start and provide emergency onsite ac power and all ac- and dc-powered equipment required for coolant injection/makeup will be failed. Under these circumstances, core damage is estimated to begin within 30 to 40 minutes. If the station batteries are initially functional and the diesel generators fail by some mechanism other than common cause station battery failure, dc power and ac-powered vital instrumentation, which receives power from the station batteries through an inverter, are available to power systems that provide coolant injection and makeup. However, the station batteries are expected to be depleted approximately 6 hours after initiation if they are not recharged. It takes another 3 hours after station battery failure for core damage to commence.

The timing to station battery depletion also affects the amount of time available to restore offsite ac power and thus bring the plant to a safe stable state without core damage. Offsite ac power is less likely to be recovered during a SSBO sequence due to the short time available (< 1 hour) than during a LSBO sequence, which has available many hours to repair and restore the offsite ac power.

The SSBO sequences make up 56% and the LSBO sequences make up 30% of the plant core damage frequency. The loss of offsite power event tree headings are described below, followed by a discussion of SSBO and LSBO dominant sequences and the potential for a recriticality event to occur.



\*Negligible Probability, Not Analyzed.

Figure 3.1. Peach Bottom Loss of Offsite Power Event Tree (Tree T1).

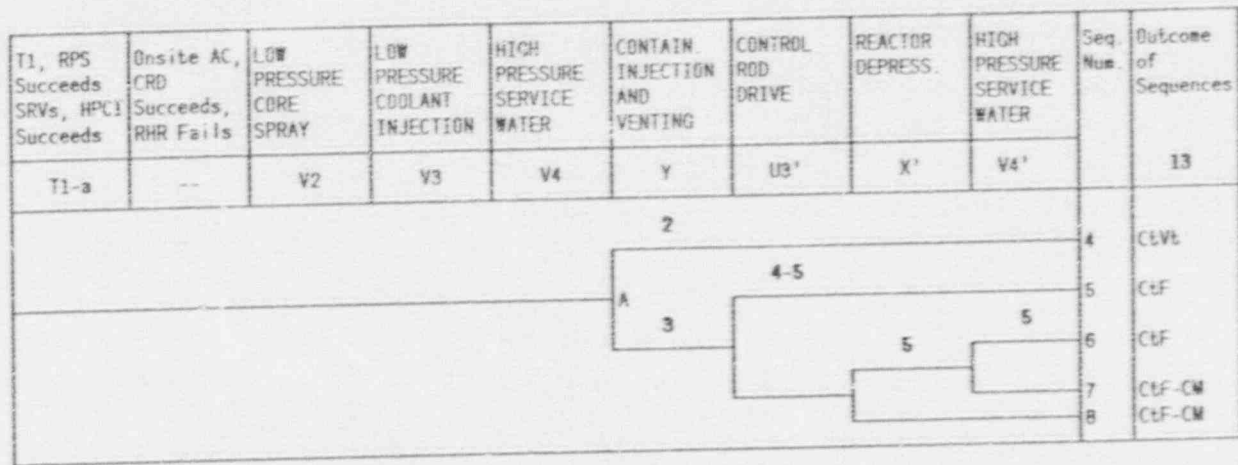


Figure 3.1. Peach Bottom Loss of Offsite Power Event Tree (Tree T1-a).

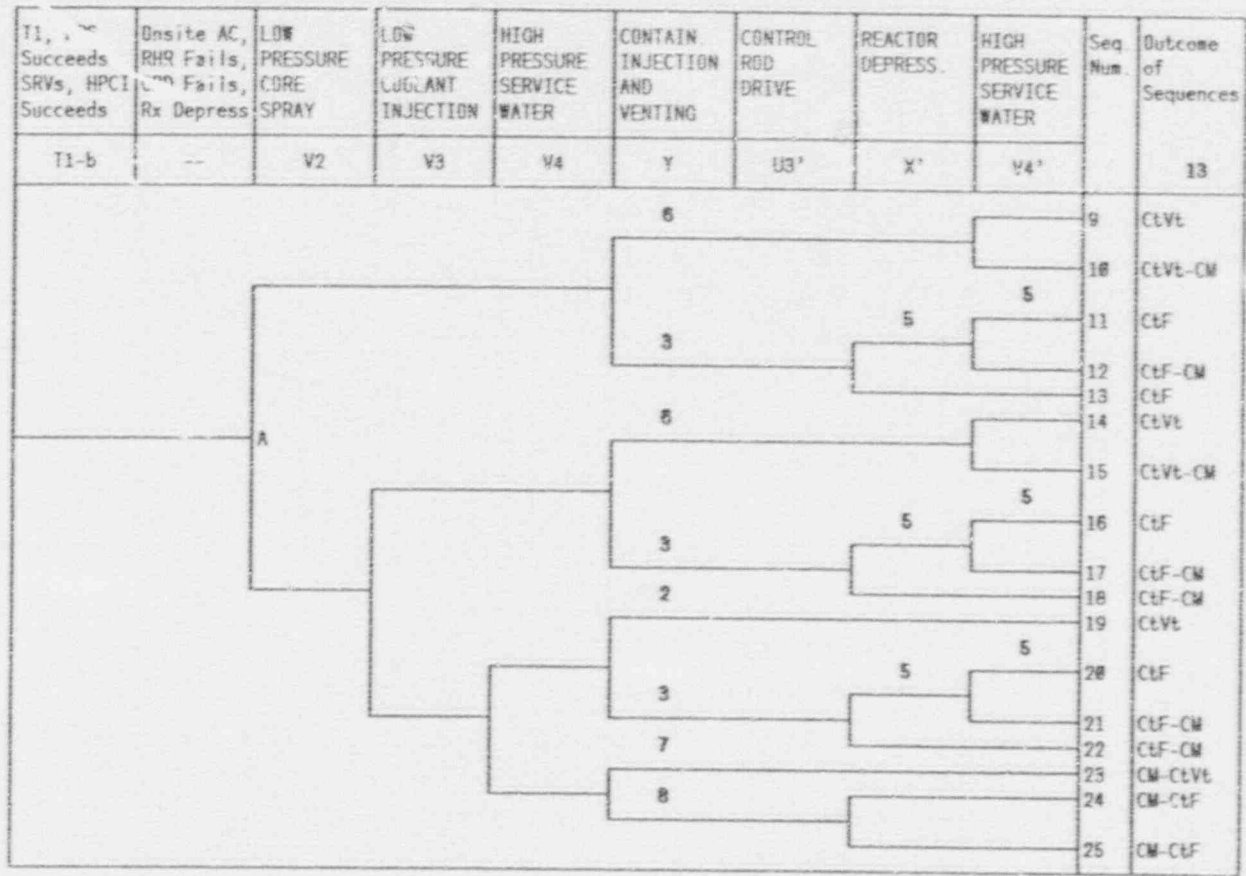


Figure 3.1. Peach Bottom Loss of Offsite Power Event Tree (Tree T1-b).



T1, RPS Succeeds SRVs, HPCI Succeeds	Onsite AC, RHR & CRD & Depress Fail	LOW PRESSURE CORE SPRAY	LOW PRESSURE COOLANT INJECTION	HIGH PRESSURE SERVICE WATER	CONTAIN. INJECTION AND VENTING	CONTROL ROD DRIVE	REACTOR DEPRESS.	HIGH PRESSURE SERVICE WATER	Seq. Num.	Outcome of Sequences		
T1-c	--	V2	V3	V4	Y	U3'	X'	V4'		13		
									7	26	CM-CtVt	
									A	9	27	CM-CtF

Figure 3.1. Peach Bottom Loss of Offsite Power Event Tree (Tree T1-c).

T1, RPS Succeeds SRVs, HPCI Succeeds	Onsite AC, Fails, Reactor Depress.	LOW PRESSURE CORE SPRAY	LOW PRESSURE COOLANT INJECTION	HIGH PRESSURE SERVICE WATER	CONTAIN. INJECTION AND VENTING	CONTROL ROD DRIVE	REACTOR DEPRESS.	HIGH PRESSURE SERVICE WATER	Seq. Num.	Outcome of Sequences		
T1-d	--	V2	V3	V4	Y	U3'	X'	V4'		13		
										28	CM-CtVt	
									A		29	CM-CtF
											30	CM-CtF

Figure 3.1. Peach Bottom Loss of Offsite Power Event Tree (Tree T1-d).

T1, RPS Succeeds SRVs, K <sub>2</sub> CI Succeeds	Onsite AC and Depress. Fail	LOW PRESSURE CORE SPRAY	LOW PRESSURE COOLANT INJECTION	HIGH PRESSURE SERVICE WATER	CONTAIN. INJECTION AND VENTING	CONTROL ROD DRIVE	REACTOR DEPRESS.	HIGH PRESSURE SERVICE WATER	Seq. Num.	Outcome of Sequences
T1-e	--	V2	V3	V4	Y	U3'	X'	V4'		13
									31	CM-CtVt
									32	CM-CtF

Figure 3.1. Peach Bottom Loss of Offsite Power Event Tree (Tree T1-e).

T1, RPS Succeed SRVs Succeed	HPCI & RCIC Fail Onsite AC Succeeds	RHR & Depress. Succeed, CRD Fail	LOW PRESSURE CORE SPRAY	LOW PRESSURE COOLANT INJECTION	HIGH PRESSURE SERVICE WATER	CONTAIN. INJECTION AND VENTING	CONTROL ROD DRIVE	REACTOR DEPRESS.	HIGH PRESSURE SERVICE WATER	Seq. Num.	Outcome of Sequences
T1-f	--	--	V2	V3	V4	Y	U3'	X'	V4'		13
									66	ok	
									67	ok	
									68	ok	
									69	CM-CtVt	
									70	CM-CtF	
									71	CM-CtF	

Figure 3.1. Peach Bottom Loss of Offsite Power Event Tree (Tree T1-f).

T1, RPS & SRVs Succeed	HPCI & RCI Fail Onsite AC Succeeds	60R Succeeds Dep Fail	LOW PRESSURE CORE SPRAY	LOW PRESSURE COOLANT INJECTION	HIGH PRESSURE SERVICE WATER	CURTAIN INJECTION AND VENTING	CONTROL ROD DRIVE	REACTOR DEPRESS.	HIGH PRESSURE SERVICE WATER	Seq. Num	Outcome of Sequences
T1-g	---	---	V2	V3	V4	Y	U3*	X*	V4*		13
7											
A 9											
										72	OM-CUWL
										73	OM-CGF

Figure 3.1. Peach Bottom Loss of Offsite Power Event Tree (Tree T1-g).

Notes for Figures 3.1, 3.2, 3.3, and 3.4

---

- (1) One CRD pump operation is considered here since HPCI (or RCIC) operation would cool the core for  $\approx 8$  hours or more before HPCI/RCIC fail on high pool temperature. By this time, the decay heat load is low and there is no significant breach of the primary system.
  - (2) With no containment heat removal, venting is eventually required. When successful venting occurs, the LPCS/LPCI/RHR pumps are assumed to fail. The cooling system operating before venting takes place should not be affected by venting operation; hence, no other event choices are shown.
  - (3) Containment fails by overpressure. The suppression pool achieves saturated conditions failing LPCS/LPCI/RHR. Since survivability of other previously operating systems is in question, choices are provided following this point in the tree for previously successful systems. Also note that since air capacity to the SRVs for depressurization is  $\approx 100$ - $125$  psig and containment failure is at  $\approx 150$  psig, loss of SRV control is expected until containment failure occurs.
  - (4) Since containment failure has occurred, success or failure of continued CRD operation is considered due to possible phenomenological effects (e.g., damage to the system as a result of containment failure) or failure to run considerations. CRD is operating earlier in sequence.
  - (5) One CRD pump or depressurization with one HPSW pump operation is considered to be adequate to continue successful core cooling.
  - (6) With venting success (at  $\approx 60$  psig in containment), continued depressurization success is assumed since air pressure to SRVs is  $\approx 100$ - $125$  psig. With assumed LPCS/LPCI failure at pool saturated conditions, only HPSW is available for success.
  - (7) Core damage occurs. Venting can only save the containment.
  - (8) Core damage and containment failure occur. Depressurization success or failure (X' event) only provides information as to vessel pressure conditions at vessel breach.
-

Notes for Figures 3.1, 3.2, 3.3, and 3.4 (Continued)

---

- (9) Like NOTE 8 except depressurization has already failed and is assumed to remain failed.
- (10) Station blackout leads to core damage. Depressurization choices only provide information as to vessel pressure at time of breach and venting choices depict whether containment is vented or failed.
- (11) W3 event is given a choice even though another mode of RHR is successful so as to consider fission product removal capability of sprays for subsequent sequences leading to core damage.
- (12) Two CRD pump operation is considered here since no other successful coolant injection has occurred and it is still early in the sequence when decay heat loads are relatively high.
- (13) "Outcome" Key:
- OK = successful mitigation
  - CtVt = containment is vented, no core damage
  - CtF = containment fails, no core damage
  - CtV = containment vulnerable
  - CM = core damage begins; core melt will result if not mitigated
  - CM-CtF = core damage leading to core melt precedes containment failure
  - CM-CtVt = core damage leading to core melt, containment vented  
(other similar combinations also exist)
- (14) SRV demands are assumed on a loss of offsite power to control any initial pressure rise in the primary system.
-



### 3.1.1 Loss of Offsite Power Event Tree Headings

The following event tree headings are discussed in the order that they appear in the loss of offsite power event tree. Station blackout impacts are discussed for those functions that are dependent on ac power.

#### Event T1

This event tree heading represents the occurrence of a loss of offsite power. It is shown as an initiating event, but the event tree logic would also apply if the offsite power loss occurred after another event, such as a generator trip.

#### Event C

Operation of the reactor protection system (RPS) to scram the reactor is modelled under this event tree heading. Success implies the automatic scram by the control rods, while failure implies an ATWS event has occurred. The failure logic is handled by the ATWS event tree analysis and is not analyzed further here.

#### Event M

This event tree heading models the automatic operation of the SRVs to provide overpressure protection for the reactor coolant system (RCS). Success implies the prevention of RCS overpressure, and thus the integrity of the primary system is maintained, by opening SRVs. The probability of a substantial number of these valves failing to open to relief pressure is negligibly small and was not modelled further.

#### Event P

Once the SRVs open to relief pressure, there is an additional concern that the valves will stick open, essentially resulting in a loss of coolant accident (LOCA) coincident with the loss of offsite power. This event tree heading addresses this concern. Success implies that all SRVs reclose when the vessel pressure drops below their closure setpoints. Failure implies that a valve or multiple valves have failed to close. The event tree logic transfers to the LOCA event tree for further analysis. However, if a station blackout occurs the sequence of events will be the same regardless of the LOCA occurrence. For a station blackout sequence, the only impact of a stuck-open SRV is to depressurize the primary system.

#### Event U1

This event tree heading models the operation of the high pressure coolant injection (HPCI) system. Success implies the initial operation of the

HPCI system so as to maintain sufficient coolant injection. Failure implies the HPCI system was not functional and coolant injection must be provided by another means.

#### Event U2

This event tree heading models the operation of the reactor core isolation cooling (RCIC) system as an alternate means of injection, given that the HPCI system has failed. Success implies the initial operation of the RCIC system so as to maintain sufficient coolant injection. Failure implies the RCIC system was not functional and operation of the residual heat removal (RHR) system must be initiated to avoid core damage.

#### Event B0

This event tree heading models the operation of the onsite ac power source (i.e., the diesel generators and associated equipment and emergency buses) in response to the loss of offsite power. Success implies the diesel generators provide sufficient electrical power so that ac-powered mitigating systems and equipment can be utilized and a station blackout has been averted. Failure implies a station blackout has occurred and ac-powered equipment is unavailable. Depending on the type of failure, the station blackout may occur almost simultaneously with the loss of offsite power or may occur many hours after the loss of offsite power.

#### Events W1, W2, and W3

These event tree headings address the operation of the RHR system in various operational modes to remove the decay heat generated in the core. However, this system is dependent upon ac power and is thus not functional in station blackout sequences.

#### Event U3

This event tree heading addresses the operation of the control rod drive (CRD) system as an alternate injection source. However, like the RHR system above, this system is dependent on ac power and is not functional in station blackout sequences.

#### Event X

Primary system depressurization is addressed by this event tree heading. Depressurization can be achieved by automatic or manual operation of the ADS or by manual operation of other SRVs. Operation of the SRVs either by the ADS system or by manual actions by the operators requires the availability of dc power. Manual actuation of the ADS system is accomplished by pushing a control room button while manual actuation of an individual SRV is

accomplished by positioning a control room switch (direct local actuation of these valves is not possible since they are located within the primary containment). Event success implies automatic or manual operation of the automatic depressurization system (ADS) or manual operation of other SRVs such that two or more valves are opened to allow low pressure injection. Failure implies the primary system is not depressurized and remains at a high pressure, thus not allowing low pressure injection to function. For station blackout sequences, the question of depressurization only determines the vessel pressure at the time of breach (i.e., containment failure or venting) and is not a factor in averting core damage, since the low pressure injection function is dependent on ac power.

#### Events V2, V3, and V4

These event tree headings address the operation of the low pressure core spray (LPCS), low pressure coolant injection (LPCI), or high pressure service water (HPSW) systems, respectively, to inject into the reactor vessel through a LPCI line. However, these systems are dependent on ac power and are thus not available during the station blackout sequences.

#### Event Y

This event tree heading models the venting of the containment. Success implies that the 6" integrated leak test line or larger size line is open so as to prevent over-pressurization of the containment. Failure implies that the containment is not vented and over-pressurization will eventually occur. Both success and failure of containment venting potentially leads to saturated conditions in the suppression pool, which were conservatively assumed to result in the loss of all systems using the pool as the injection source. Neither success nor failure of this event impacts the potential for core damage. Rather, it provides information on the containment integrity and potential releases from the containment following core damage.

#### Events U3', X', and V4'

These event tree headings are the same as those defined above for U3, X, and V4, respectively. The only difference here is that they occur after an attempt to vent the containment. The systems that provide these functions are the only ones that do not use the suppression pool as the injection water source and are thus the only systems potentially available following an attempted containment venting. However, for station blackout sequences only depressurization (X') is possible since the other functions are dependent on ac power.

During a station blackout, many of the functions modelled in the event tree are not available due to a reliance on ac power. A station blackout event tree, which is a simplified version of the loss of offsite power event

tree, has been developed and is provided as Figure 3.2. This simplified event tree only models the events that are addressed for station blackout sequences and eliminates the event tree headings that depict functions that are not available during a station blackout.

### 3.1.2 Short-term Station Blackout (SSBO)

Short-term station blackout sequences are Sequences 134-138. The progression of events common to all SSBO sequences is: a loss of offsite power occurs, the control rods scram the reactor, and the SRVs open to relieve the initial primary system pressure increase. The next event in the sequence addresses the potential for a SRV to stick in the open position. If a SRV fails to reclose after the pressure reaches its closure setpoint, essentially a LOCA is initiated. However, the sequences involving a stuck-open SRV are not explicitly modelled since the events that follow are the same as those without a stuck-open SRV. The only impact a stuck-open SRV has on the SSBO sequences is to cause the primary system to become depressurized.

Following the SRV reclosure event, HPCI and RCIC fail to provide coolant injection to the RCS and the onsite emergency ac power source (i.e., diesel generators) fails. The primary cause of failing HPCI, RCIC, and the diesels is the common cause failure of station batteries. Such a failure would fail the ability to start the diesels to provide ac power and fail the dc power to control the equipment not dependent on ac power (e.g., HPCI and RCIC turbine-driven pumps and SRVs). This common cause failure would also prevent reactor depressurization via the ADS since it is dependent on dc power and cause the loss of all vital instrumentation. Independent failures of HPCI, RCIC, and the diesels could also cause a station blackout without a means for coolant injection. Under these conditions, ADS and vital instrumentation might be available. If offsite power is not restored within 30 to 40 minutes, core damage begins due to a loss of primary inventory.

The remaining events in the event tree do not address the concern for core damage, but rather address the potential for atmospheric release. The release to the atmosphere is dependent on the status of the primary system pressure and the integrity of the containment. For the SBO sequences, the primary system can be at a high or low pressure and the containment can be over-pressurized or vented. The five SSBO sequences are as follows:

- 134 Reactor depressurization succeeds and the containment is vented.
- 135 Reactor depressurization succeeds, containment venting fails, and the reactor remains depressurized after containment failure.

3.15

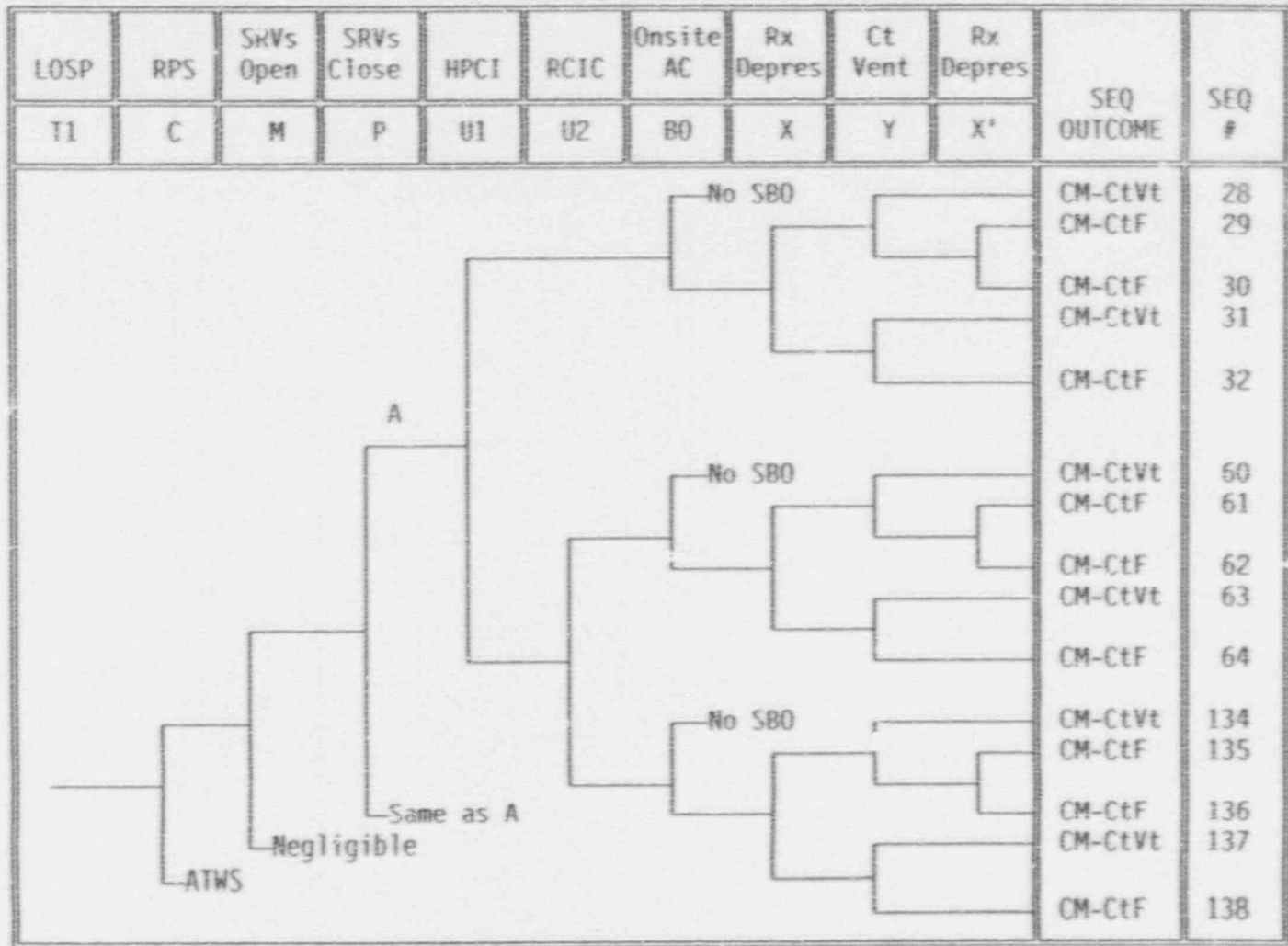


FIGURE 3.2 Station Blackout Event Tree



136 Reactor depressurization succeeds, containment venting fails, and the reactor fails to remain depressurized after containment failure (i.e., the reactor gradually becomes repressurized).

137 Reactor depressurization fails and the containment is vented.

138 Reactor depressurization fails and containment venting fails.

Reactor depressurization can be achieved by automatic or manual operation of the ADS or by manual operation of other SRVs. Operation of the SRVs either by the ADS system or by manual actions by the operators requires the availability of dc power. Reactor depressurization success implies the primary system is at a low pressure at the time of containment breach (failure or venting). Failure implies the primary system is at a high pressure.

Containment venting is only possible using local control since ac power is not available. Success implies the containment is vented and overpressurization is prevented. If containment venting fails, overpressurization will eventually occur.

If the station batteries are failed at the time of the loss of offsite power, the core degradation process will occur under high pressure conditions in the reactor vessel (i.e., Sequences 137 and 138 will occur) since the loss of dc power would also disable the operation of the ADS and SRVs for depressurizing the primary system. In addition, ac power recovery would be severely hampered by the loss of dc power (e.g., in reclosing breakers). These sequences are essentially equivalent to Sequences PBTBO and PBTBUX, discussed in Section 2.2.

If a SRV fails to reclose, after opening to relieve the initial primary pressure increase, or ADS is operable then Sequences 134, 135, and 136 apply since the primary system could be depressurized. Sequences 134 and 135 correlate to Sequence PBEM2 of Section 2.2. Sequence 136 resembles the Section 2.2 PBTBO sequence since the reactor fails to remain depressurized. The dominant cutsets (i.e., the component failure combinations that have a probability greater than  $1E-8$ ) for SSBO sequences are provided in Table 3.1. Cutsets 1, 2, 4, and 5 are of the PBTBO/PBTBUX type, while the remaining cutsets (3, 6, 7, 8, and 9) are of the PBEM2 type.

### 3.1.3 Long-term Station Blackout (LSBO)

Long-term station blackout sequences are Sequences 28-32 and 60-64. The progression of events common to these LSBO sequences is: a loss of offsite power occurs, the control rods scram the reactor, and the SRVs open to relieve the initial primary system pressure increase. The next event in the sequence addresses the potential for a SRV to stick in the open position. If a SRV

TABLE 3.1. Short-term Station Blackout Dominant Cutsets

CUTSET		CUTSET POINT ESTIMATE FREQUENCY
IE-TL0SP * DCP-BAT-LP-B2 * B-DCP-LP-BATS		3.7E-6
IE-TRTRIP * L0SP * DCP-BAT-LP-B2 * B-DCP-LP-BATS		3.4E-7
IE-TL0SP * S0RV * DCP-BAT-LP-B2 * B-DCP-LP-BATS		1.9E-7
IE-TMSIVC * L0SP * DCP-BAT-LP-B2 * B-DCP-LP-BATS		1.1E-7
IE-TLFW * L0SP * DCP-BAT-LP-B2 * B-DCP-LP-BATS		9.9E-8
IE-TRTRIP * L0SP * S0RV * DCP-BAT-LP-B2 * B-DCP-LP-BATS		1.7E-8
IE-TL0SP * DCP-BAT-LP-B2 * ACP-DGN-LP-EDG3 * RCI-TDP-FS-20S38 * RA-1D * RA-14D		1.6E-8
IE-TL0SP * DCP-BAT-LP-B2 * ACP-DGN-WA-EDG3 * RCI-TDP-FS-20S38 * RA-1D * RA-14D		1.6E-8
IE-TL0SP * ACP-DGN-LP-20G2 * B-ACP-LP-EDG3 * HCI-TDP-FS-20S37 * RCI-TDP-FS-20S38 * RA-1D		1.5E-8

TERM	DESCRIPTION	MEAN VALUE
IE-TL0SP	Loss of offsite power initiating event	7.0E-2/yr
DCP-BAT-LP-B2 <sup>a</sup>	Battery B2 failure (fails DG2 start and HPCT)	1.33E-3
B-DCP-LP-BATS <sup>a</sup>	Common mode beta factor for failure of 2nd battery (DG3)	4.0E-2
IE-TRTRIP	Turbine trip initiating event	2.4/yr
L0SP	Loss of offsite power after reactor trip	2.66E-3
S0RV	One SRV sticks open	5.0E-2
IE-TMSIVC	MSIV closure type initiating event	8.0E-1/yr
IE-TLFW	Loss of feedwater initiating event	7.0E-1/yr
ACP-DGN-LP-EDG3	DG3 failure to start or run	1.13E-2
RCI-TDP-FS-20S38	RCIC fails to start	4.84E-2
RA-1D	Failure to recover offsite power within 30 minutes	4.0E-1
RA-14D	Failure to recover a battery fault within 30 minutes	8.0E-1
ACP-DGN-WA-EDG3	DG3 maintenance unavailability	1.00E-2
ACP-DGN-LP-EDG2 <sup>b</sup>	DG2 failure to start or run	1.33E-2
B-ACP-LP-EDG3 <sup>b</sup>	Common mode beta factor for failure of 2nd diesel (DG3)	2.00E-2
RCI-TDP-FS-20S38	RCIC system (turbine-driven pump) fails to start	4.84E-2
HCI-TDP-FS-20S37	HPCT system (turbine-driven pump) fails to start	4.84E-2

<sup>a</sup>Together these make up the common mode failure of two dc buses, which also fail two diesels. The failure of diesels 2 and 3 results in the failure of emergency service water cooling, which in turn fails the remaining diesels (1 and 4). Subsequent common mode factors for other dc buses is applied at a beta factor of 1.0 per methodology guidelines. Failure to restore dc power in 30 minutes is 1.0 per non-recovery action RA-15D.

<sup>b</sup>Together these makeup the common mode failure of diesels 2 and 3, which is sufficient to fail all diesels, since the emergency service water cooling to all diesels is dependent on ac power from diesel 2 or 3.

3.17

fails to reclose after the pressure reaches its closure setpoint, essentially a LOCA is initiated. However, the sequences involving a stuck-open SRV are not explicitly modelled since the events that follow are the same as those without a stuck-open SRV. The only impact a stuck-open SRV has on the LSBO sequences is to cause the primary system to become depressurized.

Following the success or failure of the SRVs to reclose, either HPCI or RCIC initially provides coolant injection to the RCS. Sequences 28-32 involve HPCI initial success, while Sequences 60-64 involve RCIC initial success. During this time, the onsite emergency ac power source (i.e., diesel generators) fails because of diesel generator system and/or support system failures. Although there are four diesel generators, failure of diesel generators 2 and 3 (DG2 and DG3), is sufficient to cause the failure of the remaining diesels, since all of the diesels rely on emergency service water (ESW) for jacket cooling and the ESW system requires ac power from DG2 or DG3 to function. The HPCI and RCIC systems are still functional since they are able to provide coolant injection without ac power, using their turbine-driven pumps and dc-powered controls. However, after approximately six hours without being recharged the station batteries will be depleted, causing a loss of all vital instrumentation and failing the HPCI and RCIC systems. To a lesser degree, HPCI and RCIC could be failed by a variety of causes other than station battery depletion (e.g., high pool temperature, isolation on high temperature sensed by the steam line monitor, etc.). If ac power is not recovered within another three hours so that a source of coolant injection can be activated, the primary system inventory will boil off and core damage will begin.

The remaining events in the event tree do not address the concern for core damage, but rather address the potential for atmospheric release. The factors are the same as those discussed in Section 3.1.2 for SSBO sequences. The two sets of five LSBO sequences are as follows:

- 28 & 60      Reactor depressurization succeeds and the containment is vented.
- 29 & 61      Reactor depressurization succeeds, containment venting fails, and the reactor remains depressurized after containment failure.
- 30 & 62      Reactor depressurization succeeds, containment venting fails, and the reactor fails to remain depressurized after containment failure (i.e., the reactor gradually becomes repressurized).
- 31 & 63      Reactor depressurization fails and the containment is vented.
- 32 & 64      Reactor depressurization fails and containment venting fails.

If a SRV fails to reclose, after opening to relieve the initial primary pressure increase, then the primary system would be depressurized and

Sequences 28, 29, 60, and 61 would apply. These sequences are similar to the Section 2.2 PBTBS sequence. However, it should be noted that once the station batteries are lost, SRV control is lost (i.e., the SRVs cannot be held open without dc power) and the vessel can become repressurized. Under these conditions Sequences 30 and 62, which are similar to the Section 2.2 PBTB2 sequence, apply. If depressurization is failed, Sequences 31, 32, 63, and 64 apply. These sequences are also similar to the Section 2.2 PBTB2 sequence. The dominant cutsets (i.e., the component failure combinations that have a probability greater than  $1E-8$ ) for the LSBO sequences are provided as Table 3.2. All of the dominant cutsets are of the PBTBS type.

#### 3.1.4 Recriticality Potential Following Station Blackout

In this section, the dominant cutsets for each of the station blackout groups, provided in Tables 3.1 and 3.2, are modified to indicate the relative potential for a recriticality event to occur and the effectiveness of accident management strategies in eliminating and/or mitigating these events. For core damage to begin during a station blackout coolant injection must, during some period, be unavailable or inadequate. Recriticality is then possible if coolant injection is recovered at some later time after the control blades have melted. The most likely means of recovering most of the coolant injection systems is by restoring the offsite ac power supply to these systems. Once offsite ac power is restored, the operators will want to immediately provide core cooling by injecting water from these systems. If this injection occurs during the time between the start of blade melting and the start of fuel rod melting, the potential for recriticality may be a concern.

Since core damage will proceed from the central region of the core radially outward, the potential for recriticality in the outer regions may occur at a much later time than that for the central region and in fact may occur after fuel rod collapse and debris bed formation within the central region. Therefore, the time window for the potential for recriticality was conservatively assumed to be the time from the start of blade melting to the time of vessel failure. These parameters are provided in Table 2.1 and in Figure 2.9 for a number of the Peach Bottom accident scenarios.

The dominant short-term station blackout sequences (see Table 3.1) are similar to Sequences PBTB0, PBTBUX, and PBEM2 of Section 2.2 and the dominant long-term station blackout sequences are all similar to Sequence PBTBS of Section 2.2. The recriticality time windows for each of these sequences is provided in Table 3.3.

An estimate of the probability of a loss of offsite power event being recovered within the recriticality time window for each sequence is also given in Table 3.3. These probabilities are based on an evaluation of the duration



TABLE 3.2. Long-term Station Blackout Dominant Cutsets

CUTSET	CUTSET POINT ESTIMATE FREQUENCY
IE-TL0SP * ACP-DGN-LP-EDG2 * B-ACP-LP-EDG3 * RA-1J * RA-17J	3.3E-7
IE-TL0SP * ACP-DGN-LP-EDG2 * ACP-DGN-LP-EDG3 * RA-1J * RA-16J	2.1E-7
IE-TL0SP * ACP-DGN-LP-EDG2 * ACP-DGN-MA-EDG3 * RA-1J * RA-16J	2.1E-7
IE-TL0SP * ACP-DGN-LP-EDG3 * ACP-DGN-MA-EDG2 * RA-1J * RA-16J	2.1E-7
IE-TL0SP * ACP-DGN-LP-EDG2 * ESW-PSF-LF-103 * RA-1J * RA-16J	1.1E-7
IE-TL0SP * ACP-DGN-LP-EDG3 * ESW-PSF-LF-102 * RA-1J * RA-16J	1.1E-7
IE-TL0SP * ESW-PSF-LF-102 * ESW-PSF-LF-103 * RA-1J	9.1E-8
IE-TL0SP * ACP-DGN-MA-EDG2 * ESW-PSF-LF-103 * RA-1J * RA-16J	8.7E-8
IE-TL0SP * ACP-DGN-MA-EDG3 * ESW-PSF-LF-102 * RA-1J * RA-16J	8.7E-8
IE-TL0SP * ESW-PSF-LF-8 * ESW-XHE-FB-ECWPP * RA-1J	8.4E-8
IE-TL0SP * ACP-DGN-LP-EDG2 * B-ACP-LP-EDG3 * HCI-TDP-FS-20S37 * RA-1J * RA-17J	1.6E-8
IE-TL0SP * S0RV * ACP-DGN-LP-EDG2 * B-ACP-LP-EDG3 * RA-1J * RA-17J	1.6E-8
IE-TL0SP * S0RV * ACP-DGN-LP-EDG2 * ACP-DGN-LP-EDG3 * RA-1J * RA-16J	1.1E-8
IE-TL0SP * ACP-DGN-LP-EDG2 * ACP-DGN-LP-EDG3 * HCI-TDP-FS-20S37 * RA-1J * RA-16J	1.0E-8
IE-TL0SP * ACP-DGN-LP-EDG2 * ACP-DGN-MA-EDG3 * HCI-TDP-FS-20S37 * RA-1J * RA-16J	1.0E-8
IE-TL0SP * ACP-DGN-LP-EDG3 * ACP-DGN-MA-EDG2 * HCI-TDP-FS-20S37 * RA-1J * RA-16J	1.0E-8
IE-TL0SP * S0RV * ACP-DGN-LP-EDG2 * ACP-DGN-MA-EDG3 * RA-1J * RA-16J	1.0E-8
IE-TL0SP * S0RV * ACP-DGN-LP-EDG3 * ACP-DGN-MA-EDG2 * RA-1J * RA-16J	1.0E-8

TERM	DESCRIPTION	MEAN VALUE
IE-TL0SP	Loss of offsite power initiating event	7.0E-2/yr
ACP-DGN-LP-EDG2 <sup>2</sup>	DG2 failure to start or run	1.13E-2
B-ACP-LP-EDG3 <sup>2</sup>	Common mode beta factor for failure of 2nd diesel (DG3)	2.00E-2
RA-1J	Failure to recover offsite power within 6-8 hours	4.0E-2
RA-17J	Failure to recover diesel common mode fault in 6 hours	5.0E-1
ACP-DGN-LP-EDG3	DG3 failure to start or run	1.13E-2
RA-16J	Failure to recover a diesel hardware fault in 6 hours	6.0E-1
ACP-DGN-MA-EDG3	DG3 unavailable due to maintenance	1.09E-2
ACP-DGN-MA-EDG2	DG2 unavailable due to maintenance	1.09E-2
ESW-PSF-LF-103	Failure of jacket cooling to DG3	5.7E-3
ESW-PSF-LF-102	Failure of jacket cooling to DG2	5.7E-3
RA-18J	Failure to restore a diesel from maintenance in 6 hours	5.0E-1
ESW-PSF-LF-8	ESW MOV-0498 discharge valve closed due to maintenance	3.0E-5
ESW-XHE-FB-ECWPP	Operator failure to start ESW pump (in ESW) in 5 minutes	1.0
HCI-TDP-FS-20S37	HPCI system (turbine-driven pump) fails to start	4.04E-2
S0RV	One SRV stuck-open	5.0E-2

<sup>2</sup>Together these make up the common mode failure of diesels 2 and 3, which is sufficient to fail all diesels since the emergency service water cooling to all diesels is dependent on ac power from diesel 2 or 3.



TABLE 3.3. Recriticality Time Windows for Station Blackout Sequences

Sequence	Start of Blade Melt (min)	Start of Fuel Rod Melt (min)	Time of Vessel Failure (min)	Recriticality Window Span (min)	Absolute Probability of AC Power Recovery Within Recriticality Time Window
PBTB0	113	120	267	154	0.12
PBTBUX	109	134	200	91	0.08
PBEM2	127	132	288	161	0.11
PBTBS	649	716	767	118	0.01

of the loss of offsite power events from historical data (Ref. 3.3) and the percentage of those events which were terminated within each of the time windows. It is worth noting that  $\approx 60\%$  of all loss of offsite power events have been recovered within the first half-hour,  $\approx 70\%$  within the first hour,  $\approx 80\%$  within two hours, and  $\approx 90\%$  within four hours. No loss of offsite power events have lasted past 12 hours.

#### Short-term Station Blackout Recriticality Potential

To determine the probability of a recriticality event, the short-term station blackout sequences were modified to indicate the potential for recovering ac power in the recriticality time window. The modified dominant cutsets are provided in Table 3.4. For Cutsets 1, 2, 4, and 5, which are similar to PBTBO/PBTBUX of Section 2.2, event ACPOW12 is added to represent the fact that 12% of the loss of offsite ac power events (based on PBTBO) is estimated to be restored within the recriticality time window. For Cutsets 3, 6, 7, 8, and 9, which are similar to PBEM2 of Section 2.2, event ACPOW11 is added to represent the fact that 11% of the loss of offsite ac power events is estimated to be restored within the recriticality time window. For the last three cutsets (7, 8, and 9), the events representing the failure to recover ac and dc power (RA-1D and RA-14D) were deleted since the value used for event ACPOW11 is assumed to account for these events.

The core damage probability for the dominant short-term station blackout cutsets is approximately  $4.5E-6$  per reactor year. The probability of a recriticality event, based on the modified dominant short-term station blackout cutsets, is approximately  $5.6E-7$  per reactor year. Assuming that the operators would not immediately borate and initiate RHR suppression pool cooling at the time of reflood, using present guidance, the probability of suppression pool saturation and containment over-pressurization in about half an hour is also  $5.6E-7$  per reactor year.

To address the effectiveness of the accident management strategies of borating and establishing RHR suppression pool cooling at the time of reflood, discussed in Sections 2.0 and 4.0, to terminate the recriticality event and thus preventing suppression pool saturation and containment failure, the dominant cutsets were modified further. This modification accounts for the possibility that boron injection fails or RHR suppression pool cooling fails. Failure of either function is conservatively assumed to result in eventual containment failure, since the primary means of boration (i.e., from SLC) is only marginally adequate if the excess steam to the suppression pool is greater than about 10% power, which may occur if RHR suppression pool cooling fails. The value for boration failure is estimated to be  $5.0E-2$ . The SLC injection failure value is based on the NUREG/CR-4550 ATWS analysis value, since it is dominated by operator failure to initiate boration within a very short time frame ( $\approx 4$  minutes). The value for RHR suppression pool cooling failure is also estimated to be  $5.0E-2$ , assuming ac power has been restored

TABLE 3.4. Recriticality Potential for SSBO Dominant Cutsets

CUTSET	CUTSET POINT ESTIMATE FREQUENCY
IE-TLOSP * DCP-BAT-LP-B2 * B-DCP-LP-BATS * ACP0W12	4.5E-7
IE-TRTRIP * LOSP * DCP-BAT-LP-B2 * B-DCP-LP-BATS * ACP0W12	4.2E-8
IE-TLOSP * SORV * DCP-BAT-LP-B2 * B-DCP-LP-BATS * ACP0W11	2.1E-8
IE-TMSIVC * LOSP * DCP-BAT-LP-B2 * B-DCP-LP-BATS * ACP0W12	1.3E-8
IE-TLFW * LOSP * DCP-BAT-LP-B2 * B-DCP-LP-BATS * ACP0W12	1.2E-8
IE-TRTRIP * LOSP * SORV * DCP-BAT-LP-B2 * B-DCP-LP-BATS * ACP0W11	1.9E-9
IE-TLOSP * DCP-BAT-LP-B2 * ACP-DGN-LP-EDG3 * RCI-TDP-FS-20S38 * ACP0W11	5.5E-9
IE-TLOSP * DCP-BAT-LP-B2 * ACP-DGN-MA-EDG3 * RCI-TDP-FS-20S38 * ACP0W11	5.5E-9
IE-TLOSP * ACP-DGN-LP-EDG2 * B-ACP-LP-EDG3 * HCI-TDP-FS-20S37 * RCI-TDP-FS-20S38 * ACP0W11	4.2E-9

TERM	DESCRIPTION	MEAN VALUE
IE-TLOSP	Loss of offsite power initiating event	7.0E-2/yr
DCP-BAT-LP-B2 <sup>a</sup>	Battery B2 failure (fails DG2 start and HPCI)	1.33E-3
B-DCP-LP-BATS <sup>a</sup>	Common mode beta factor for failure of 2nd battery (DG3)	4.0E-2
ACP0W12	AC power restored within PB1B0 recriticality time window	1.2E-1
IE-TRTRIP	Turbine trip initiating event	2.4/yr
LOSP	Loss of offsite power after reactor trip	2.66E-3
SORV	One SRV sticks open	5.0E-2
ACP0W11	AC power restored within PBEM2 recriticality time window	1.1E-1
IE-TMSIVC	MSIV closure type initiating event	8.0E-1/yr
IE-TLFW	Loss of feedwater initiating event	7.0E-1/yr
ACP-DGN-LP-EDG3	DG3 failure to start or run	1.13E-2
RCI-TDP-FS-20S38	RCIC fails to start	4.84E-2
ACP-DGN-MA-EDG3	DG3 maintenance unavailability	1.09E-2
ACP-DGN-LP-EDG2 <sup>b</sup>	DG2 failure to start or run	1.13E-2
B-ACP-LP-EDG3 <sup>b</sup>	Common mode beta factor for failure of 2nd diesel (DG3)	2.00E-2
RCI-TDP-FS-20S38	RCIC system (turbine-driven pump) fails to start	4.84E-2
HCI-TDP-FS-20S37	HPCI system (turbine-driven pump) fails to start	4.84E-2

<sup>a</sup>Together these make up the common mode failure of two dc buses, which also fail two diesels. The failure of diesels 2 and 3 results in the failure of emergency service water cooling, which in turn fails the remaining diesels (1 and 4). Subsequent common mode factors for other dc buses is applied at a beta factor of 1.0 per methodology guidelines.

<sup>b</sup>Together these makeup the common mode failure of diesels 2 and 3, which is sufficient to fail all diesels, since the emergency service water cooling to all diesels is dependent on ac power from diesel 2 or 3.

and the dominant failure is the operator failure to establish RHR cooling capability immediately. The term BOR-RHR is used in the modified cutsets to represent the failure to terminate a recriticality event, assuming the accident management strategies are implemented.

The results of this modification are provided in Table 3.5. The probability of the short-term station blackout event resulting in a recriticality event and not being terminated before containment failure, even though accident management strategies are implemented, is  $5.6E-8$  per reactor year.

#### Long-term Station Blackout Recriticality Potential

To determine the probability of a recriticality event, the long-term station blackout sequences were modified to indicate the potential for recovering ac power in the recriticality time window. The modified dominant cutsets are provided in Table 3.6. For each of the dominant cutsets, which are similar to PBTBS of Section 2.2, event ACPOW1 is added to represent the fact that 1% of the loss of offsite ac power events is estimated to be restored within the recriticality time window. Event ACPOW1 replaces the events representing the failure to recover ac and dc power sources (RA-1J, RA-16J, RA-17J, and RA-18J) since the value used for event ACPOW1 is assumed to account for these events.

The core damage probability for the dominant long-term station blackout cutsets is approximately  $1.6E-6$  per reactor year. The probability of a recriticality event, based on the modified dominant long-term station blackout cutsets, is approximately  $6.9E-7$  per reactor year. Assuming that the operators would not immediately borate and initiate RHR suppression pool cooling at the time of reflood, using present guidance, the probability of suppression pool saturation and containment over-pressurization in about half an hour is also  $6.9E-7$  per reactor year.

Using the same logic as for the short-term station blackout analysis to address the effectiveness of the accident management strategies, discussed in Section 4.0, the dominant cutsets were modified further. In this modification boration failure is estimated to be  $5.0E-2$  and RHR suppression pool cooling failure is also estimated to be  $5.0E-2$ . The term BOR-RHR is used in the modified cutsets to represent the failure to terminate a recriticality event, assuming the accident management strategies are implemented.

The results of the modifications are provided in Table 3.7. The probability of the long-term station blackout event resulting in a recriticality event and not being terminated before suppression pool saturation and containment failure is  $6.9E-8$  per reactor year.

TABLE 3.5. Accident Management Strategies Implemented for SSBO Dominant Cutsets

CUTSET	CUTSET POINT ESTIMATE FREQUENCY
IE-TL0SP * DCP-BAT-LP-B2 * B-DGP-LP-BATS * ACP0W12 * BOR-RHR	4.5E-8
IE-TRTRIP * L0SP * DCP-BAT-LP-B2 * B-DGP-LP-BATS * ACP0W12 * BOR-RHR	4.2E-9
IE-TL0SP * S0RV * DCP-BAT-LP-B2 * B-DGP-LP-BATS * ACP0W11 * BOR-RHR	2.1E-9
IE-TMS1WC * L0SP * DCP-BAT-LP-B2 * B-DGP-LP-BATS * ACP0W12 * BOR-RHR	1.8E-9
IE-TL1W * L0SP * DCP-BAT-LP-B2 * B-DGP-LP-BATS * ACP0W12 * BOR-RHR	1.2E-9
IE-TRTRIP * L0SP * S0RV * DCP-BAT-LP-B2 * B-DGP-LP-BATS * ACP0W11 * BOR-RHR	1.9E-10
IE-TL0SP * DCP-BAT-LP-B2 * ACP-DGN-LP-EDG3 * RCI-TOP-FS-20538 * ACP0W11 * BOR-RHR	5.5E-10
IE-TL0SP * DCP-BAT-LP-B2 * ACP-DGN-MA-EDG3 * RCI-TOP-FS-20538 * ACP0W11 * BOR-RHR	5.5E-10
IE-TL0SP * ACP-DGN-LP-EDG2 * B-ACP-LP-EDG3 * RCI-TOP-FS-20537 * ACP0W11 * BOR-RHR	4.2E-10

TERM	DESCRIPTION	MEAN VALUE
IE-TL0SP	Loss of offsite power initiating event	7.0E-2/yr
DCP-BAT-LP-B2 <sup>a</sup>	Battery B2 failure (fails DG2 start and HPCI)	1.33E-3
B-DGP-LP-BATS <sup>a</sup>	Common mode beta factor for failure of 2nd battery (DG3)	4.0E-2
ACP0W12	AC power restored within PB100 recriticality time window	1.2E-1
BOR-RHR	Boatation injection failure or full RHR cooling failure	1.0E-1
IE-TRTRIP	Turbine trip initiating event	2.4/yr
L0SP	Loss of offsite power after reactor trip	2.66E-3
S0RV	One SRY sticks open	5.0E-2
ACP0W11	AC power restored within PBEM2 recriticality time window	1.1E-1
IE-TMS1WC	MSIV closure type initiating event	8.0E-1/yr
IE-TL1W	Loss of feedwater initiating event	7.0E-1/yr
ACP-DGN-LP-EDG3	DG3 failure to start or run	1.13E-2
RCI-TOP-FS-20538	RCIC fails to start	4.84E-2
ACP-DGN-MA-EDG3	EDG3 maintenance unavailability	1.00E-2
ACP-DGN-LP-EDG2 <sup>b</sup>	DG2 failure to start or run	1.13E-2
B-ACP-LP-EDG3 <sup>b</sup>	Common mode beta factor for failure of 2nd diesel (DG3)	3.88E-2
RCI-TOP-FS-20538	RCIC system (turbine-driven pump) fails to start	4.84E-2
HCI-TOP-FS-20537	HPCI system (turbine-driven pump) fails to start	4.84E-2

<sup>a</sup> Together these make up the common mode failure of two dc buses, which also fail two diesels. The failure of diesels 2 and 3 results in the failure of emergency service water cooling, which in turn fails the remaining diesels (1 and 4). Subsequent common mode factors for other dc buses is applied at a beta factor of 1.8 per methodology guidelines.

<sup>b</sup> Together these make up the common mode failure of diesels 2 and 3, which is sufficient to fail all diesels, since the emergency service water cooling to all diesels is dependent on ac power from diesel 2 or 3.



TABLE 3.6. Recriticality Potential for LSBO Dominant Cutsets

CUTSET	CUTSET POINT ESTIMATE FREQUENCY
IE-TL0SP * ACP-DGN-LP-EDG2 * B-ACP-LP-EDG3 * ACP0W1	1.7E-7
IE-TL3SP * ACP-DGN-LP-EDG2 * ACP-DGN-LP-EDG3 * ACP0W1	8.8E-8
IE-TL0SP * ACP-DGN-LP-EDG2 * ACP-DGN-MA-EDG3 * ACP0W1	8.8E-8
IE-TL0SP * ACP-DGN-LP-EDG3 * ACP-DGN-MA-EDG2 * ACP0W1	8.8E-8
IE-TL0SP * ACP-DGN-LP-EDG2 * ESW-PSF-LF-103 * ACP0W1	4.6E-8
IE-TL0SP * ACP-DGN-LP-EDG3 * ESW-PSF-LF-102 * ACP0W1	4.6E-8
IE-TL0SP * ESW-PSF-LF-102 * ESW-PSF-LF-103 * ACP0W1	2.3E-8
IE-TL0SP * ACP-DGN-MA-EDG2 * ESW-PSF-LF-103 * ACP0W1	4.4E-8
IE-TL0SP * ACP-DGN-MA-EDG3 * ESW-PSF-LF-102 * ACP0W1	4.4E-8
IE-TL0SP * ESW-PSF-LF-8 * ECW-XHE-F0-ECWPP * ACP0W1	2.1E-8
IE-TL0SP * ACP-DGN-LP-EDG2 * B-ACP-LP-EDG3 * HCI-TDP-FS-20537 * ACP0W1	8.0E-9
IE-TL0SP * S0RV * ACP-DGN-LP-EDG2 * B-ACP-LP-EDG3 * ACP0W1	8.0E-9
IE-TL0SP * S0RV * ACP-DGN-LP-EDG2 * ACP-DGN-LP-EDG3 * ACP0W1	4.6E-9
IE-TL0SP * ACP-DGN-LP-EDG2 * ACP-DGN-LP-EDG3 * HCI-TDP-FS-20537 * ACP0W1	4.2E-9
IE-TL0SP * ACP-DGN-LP-EDG2 * ACP-DGN-MA-EDG3 * HCI-TDP-FS-20537 * ACP0W1	4.2E-9
IE-TL0SP * ACP-DGN-LP-EDG3 * ACP-DGN-MA-EDG2 * HCI-TDP-FS-20537 * ACP0W1	4.2E-9
IE-TL0SP * S0RV * ACP-DGN-LP-EDG2 * ACP-DGN-MA-EDG3 * ACP0W1	4.2E-9
IE-TL0SP * S0RV * ACP-DGN-LP-EDG3 * ACP-DGN-MA-EDG2 * ACP0W1	4.2E-9

3.26

TERM	DESCRIPTION	MEAN VALUE
IE-TL0SP	Loss of offsite power initiating event	7.0E-2/yr
ACP-DGN-LP-EDG2 <sup>a</sup>	DG2 failure to start or run	1.13E-2
B-ACP-LP-EDG3 <sup>a</sup>	Common mode beta factor for failure of 2nd diesel (DG3)	2.09E-2
ACP0W1	AC power restored in PBTBS recriticality time window	1.0E-2
ACP-DGN-LP-EDG3	DG3 failure to start or run	1.13E-2
ACP-DGN-MA-EDG3	DG3 unavailable due to maintenance	1.09E-2
ACP-DGN-MA-EDG2	DG2 unavailable due to maintenance	1.09E-2
ESW-PSF-LF-103	Failure of jacket cooling to DG3	5.7E-3
ESW-PSF-LF-102	Failure of jacket cooling to DG2	5.7E-3
ESW-PSF-LF-8	ESW MOV-0498 discharge valve closed due to maintenance	3.0E-5
ECW-XHE-F0-ECWPP	Operator failure to start ECW pump (in ESW) in 5 minutes	1.0
HCI-TDP-FS-20537	HPCI system (turbine-driven pump) fails to start	4.84E-2
S0RV	One SRV stuck-open	5.0E-2

<sup>a</sup>Together these make up the common mode failure of diesels 2 and 3, which is sufficient to fail all diesels since the emergency service water cooling to all diesels is dependent on ac power from diesel 2 or 3.

TABLE 3.7. Accident Management Strategies Implemented for LS80 Dominant Cutsets

CUTSET	CUTSET POINT ESTIMATE FREQUENCY
IE-TL0SP * ACP-DGN-LP-EDG2 * B-ACP-LP-EDG5 * ACP0W1 * BOR-RHR	3.3E-9
IE-TL0SP * ACP-DGN-LP-EDG2 * ACP-DGN-LP-EDG3 * ACP0W1 * BOR-RHR	2.1E-9
IE-TL0SP * ACP-DGN-LP-EDG2 * ACP-DGN-MA-EDG3 * ACP0W1 * BOR-RHR	2.1E-9
IE-TL0SP * ACP-DGN-LP-EDG3 * ACP-DGN-MA-EDG2 * ACP0W1 * BOR-RHR	2.1E-9
IE-TL0SP * ACP-DGN-LP-EDG2 * ESM-PSF-LF-103 * ACP0W1 * BOR-RHR	1.1E-9
IE-TL0SP * ACP-DGN-LP-EDG3 * ESM-PSF-LF-102 * ACP0W1 * BOR-RHR	1.1E-9
IE-TL0SP * ESM-PSF-LF-102 * ESM-PSF-LF-103 * ACP0W1 * BOR-RHR	9.1E-10
IE-TL0SP * ACP-DGN-MA-EDG2 * ESM-PSF-LF-103 * ACP0W1 * BOR-RHR	8.7E-10
IE-TL0SP * ACP-DGN-MA-EDG3 * ESM-PSF-LF-102 * ACP0W1 * BOR-RHR	8.7E-10
IE-TL0SP * ESM-PSF-LF-8 * ESM-XHE-F0-ECWPP * ACP0W1 * BOR-RHR	6.4E-10
IE-TL0SP * ACP-DGN-LP-EDG2 * B-ACP-LP-EDG5 * HCI-TOP-FS-20S37 * ACP0W1 * BOR-RHR	1.6E-10
IE-TL0SP * SORV * ACP-DGN-LP-EDG2 * B-JP-LP-EDG5 * ACP0W1 * BOR-RHR	1.6E-10
IE-TL0SP * SORV * ACP-DGN-LP-EDG2 * ACP-DGN-LP-EDG3 * ACP0W1 * BOR-RHR	1.1E-10
IE-TL0SP * ACP-DGN-LP-EDG2 * ACP-DGN-LP-EDG3 * HCI-TOP-FS-20S37 * ACP0W1 * BOR-RHR	1.0E-10
IE-TL0SP * ACP-DGN-LP-EDG2 * ACP-DGN-MA-EDG3 * HCI-TOP-FS-20S37 * ACP0W1 * BOR-RHR	1.0E-10
IE-TL0SP * ACP-DGN-LP-EDG3 * ACP-DGN-MA-EDG2 * HCI-TOP-FS-20S37 * ACP0W1 * BOR-RHR	1.0E-10
IE-TL0SP * SORV * ACP-DGN-LP-EDG2 * ACP-DGN-MA-EDG3 * ACP0W1 * BOR-RHR	1.0E-10
IE-TL0SP * SORV * ACP-DGN-LP-EDG3 * ACP-DGN-MA-EDG2 * ACP0W1 * BOR-RHR	1.0E-10

TERM	DESCRIPTION	MEAN VALUE
IE-TL0SP	Loss of offsite power initiating event	7.0E-2/yr
ACP-DGN-LP-EDG2 <sup>a</sup>	DG2 failure to start or run	1.13E-2
B-ACP-LP-EDG5 <sup>a</sup>	Common mode beta factor for failure of 2nd diesel (DG3)	2.00E-2
ACP0W1	AC power restored in PBIBS recriticality time window	1.0E-2
BOR-RHR	Rotation injection failure or full RHR cooling failure	1.0E-1
ACP-DGN-LP-EDG3	DG3 failure to start or run	1.13E-2
ACP-DGN-MA-EDG3	DG3 unavailable due to maintenance	1.00E-2
ACP-DGN-MA-EDG2	DG2 unavailable due to maintenance	1.00E-2
ESM-PSF-LF-103	Failure of jacket cooling to DG3	5.7E-3
ESM-PSF-LF-102	Failure of jacket cooling to DG2	5.7E-3
ESM-PSF-LF-8	ESM MOV-0498 discharge valve closed due to maintenance	3.0E-5
ESM-XHE-F0-ECWPP	Operator failure to start ECM pump (in ESM) in 5 minutes	1.0
HCI-TOP-FS-20S37	HPCI system (turbine-driven pump) fails to start	4.04E-2
SORV	One SRV stuck-open	5.0E-2

<sup>a</sup>Together these makeup the common mode failure of diesels 2 and 3, which is sufficient to fail all diesels since the emergency service water cooling to all diesels is dependent on ac power from diesel 2 or 3.

## Station Blackout Recriticality Potential Results

The results of the sequence analysis are summarized in Table 3.8. Three categories are provided for comparison: 1) the probability of core damage, based on the NUREG/CR-4550 dominant station blackout cutsets, 2) the probability of a recriticality event occurring during core reflood for these cutsets, and 3) the probability of containment failure if the accident management strategies are implemented.

It is interesting to note that though the short-term station blackout sequences have a greater probability of core damage, the long-term station blackout sequences have a greater probability of experiencing a recriticality event. This is caused by the fact that the time for (and thus probability of) recovering ac power prior to core damage is greater for long-term station blackout sequences than for short-term station blackout sequences. This effectively lowers the probability of having a long-term station blackout result in core damage. However, if it is given that power is not restored prior to the commencement of core damage, the long-term station blackout sequences are also more likely to have power recovered within their recriticality time window.

The results indicate that the accident management strategies suggested in this report should provide a factor of 10 reduction in the potential for a recriticality event to cause containment failure (and subsequently further core damage), if implemented.

### 3.2 ANTICIPATED TRANSIENT WITHOUT SCRAM (ATWS)

The response of Peach Bottom Unit 2 to a postulated failure of the control rods to insert following an anticipated transient involves several events. The logic that depicts the sequence of events following an ATWS event at Peach Bottom Unit 2 is shown in the NUREG/CR-4550 ATWS event tree, provided as Figure 3.3.

ATWS makes up 12% of the plant core damage frequency and is one of the dominant sequences (along with station blackout) at Peach Bottom. The ATWS event tree headings are described below, followed by a discussion of the sequences and dominant cutsets.

#### 3.2.1 ATWS Event Tree Headings

The following event tree headings are discussed in the order that they appear in the ATWS event tree.

TABLE 3.8. Recriticality Analysis Results for Station Blackout Sequences

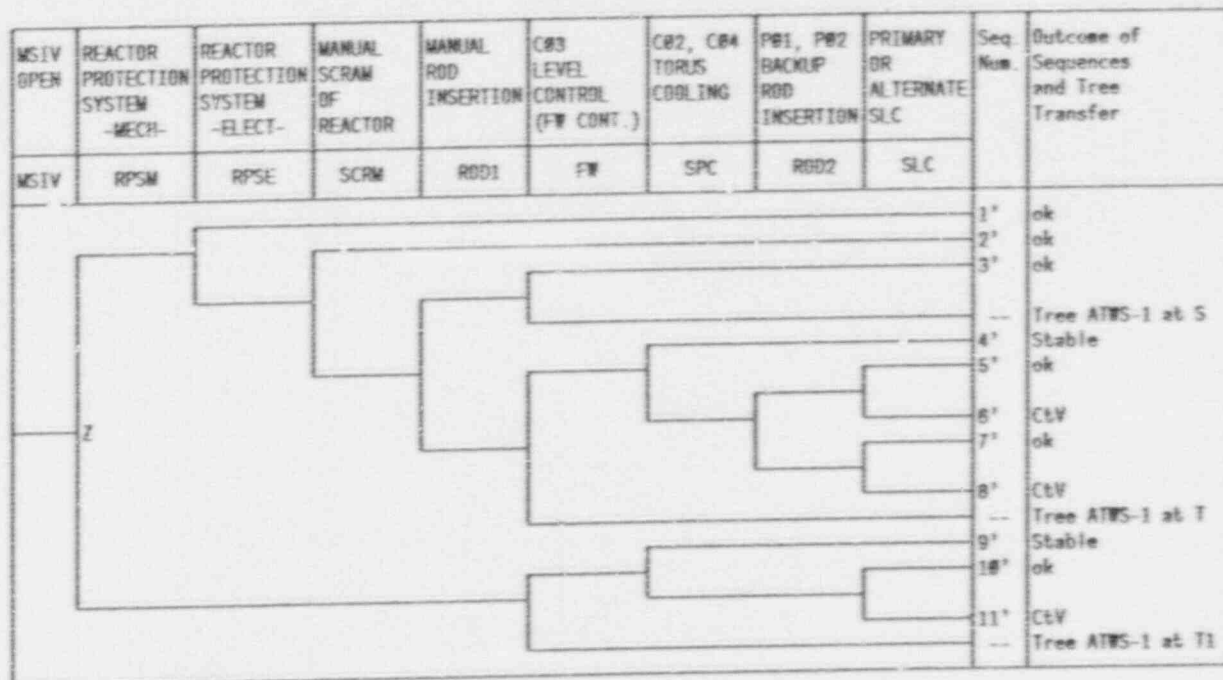
Sequence	Probability of Core Damage (per reactor year)	Probability of Containment Failure Without Strategies (per reactor year) <sup>1</sup>	Probability of Containment Failure Using Strategies (per reactor year)
SSBO	4.5E-6	5.6E-7	5.6E-8
LSBO	1.7E-6	6.9E-7	6.9E-8
TOTAL	6.2E-6	1.25E-6	1.25E-7

<sup>1</sup>This is also the probability per reactor year of a recriticality event.





3.31



\*CtV -- Containment Vulnerable

Figure 3.3. Peach Bottom Case B ATWS Event Tree (Tree ATWS-2).

#### Event T

A transient occurs which requires the reactor to be tripped. This is typically a transfer from another event tree (e.g., the LOSP event tree).

#### Event MSIV

The transient occurs with either the main steam isolation valves (MSIVs) closed (up-branch) or open (down-branch). There is the possibility during an ATWS that the MSIVs will remain open.

#### Event RPSM

RPS mechanical failure assumes that all of the control rods are left in the position that they occupied before the transient occurred. By definition, whatever causes RPS mechanical failure is assumed to be non-recoverable. Due to redundancy of means of scrambling the reactor for non-mechanical failures, failure of this event shows up in all dominant ATWS sequences.

#### Event RPSE

Failure of the RPS electrical system includes failure of the sensors, logic, RPS trip relays, and trip contacts. An electrical failure is assumed to prevent the RPS trip relay contact from opening. This failure can occur at the contacts themselves or between the contacts and the sensors. Unlike RPS mechanical faults, RPS electrical faults are recoverable. In the unlikely event that RPS electrical fails, the alternate rod insertion (ARI) system provides another means of ensuring that the control rods receive the signal to insert. The RPS electrical event tree heading includes the ARI function.

#### Event SCRM

If the RPS failure is an electrical failure, the plant operators can attempt to manually scram the control rods into the reactor. There are a number of different means of manually scrambling the reactor, however, if the RPS failure is mechanical, these efforts will not be successful.

#### Event ROD1

If, after attempting a manual scram, the control rods have not entered the reactor core, the operator will attempt a manual rod insertion. This is only possible if the scram signal can be reset. The operator will attempt to insert individual rods guided by a rod priority list kept at the control panel and is continued after the standby liquid control (SLC) system is initiated.

#### Event SLC

If the reactor cannot be shutdown using the control rods, the operators will initiate SLC before the torus temperature reaches 110°F.

#### Event RXHP

Immediately after initiating SLC, the operators try to maintain the reactor at a high pressure, so high pressure systems (e.g., HPCI) can be used, by defeating the ADS. Failure implies the ADS operates, thus lowering the reactor pressure and making high pressure systems unavailable.

#### Event SRVS

If a SRV is open or cycling during the ATWS, the operator will manually open the SRVs by holding a switch in the control room to a set position until the reactor vessel pressure drops to 950 psig. Success implies that the SRVs open and then close upon reaching 950 psig. Failure implies that two or more SRVs stick open causing an uncontrolled depressurization of the reactor.

#### Event LEV

Once the torus temperature reaches 110°F, the operator must lower reactor pressure vessel (RPV) level by terminating and preventing all injection into the RPV (except boron injection and CRD) until power is below 3% or all SRVs shut or the top of active fuel level is reached. As the top of active fuel level is approached, the operator must throttle HPCI to maintain this level. The up-branch implies the operator maintains the water level near, above, or oscillating near the top of the active fuel. Failure of this event (down-branch) implies the level is maintained too low (e.g., HPCI failure).

#### Event SPC

Once the torus reaches 110°F, the RHR and HPSW systems must be aligned to cool the torus. However, there are no major differences in the sequences with or without torus cooling.

#### Event DEP

When the torus temperature reaches 155°F, the operator will lower the reactor pressure using the SRVs. This would also be required if HPCI were lost, so that low pressure systems could be used to provide core cooling.

### Event INJ

HPCI is initially used to maintain level control. This event addresses the potential for HPCI to be terminated. If the torus temperature reaches  $\approx 220^{\circ}\text{F}$ , or the reactor pressure reaches 100 psig, or the containment pressure reaches 150 psia, HPCI will either fail or isolate. Success implies that HPCI continues to operate and the water level in the primary is restored with this system once sufficient boron is injected or the reactor is shutdown.

### Event LPIN

If HPCI fails or is isolated, the operator will attempt to maintain the water level at the top of the active fuel by using the condensate, LPCI, LPCS, or other systems. This is possible when the reactor pressure drops to  $\approx 300$  psig. Success implies operation of one pump such that water level is maintained to cool the core and eventually restored to normal levels after the reactor is shutdown. Failure may be caused by maintaining a level that is too low.

### Event ROD2

This event is addressed as yet another means of manually scrambling the reactor by locally venting the scram air header or the CRD withdraw line vent valve of each header. However, it was assumed that if all other attempts to scram the reactor have failed, this method would not be effective.

### Event FW

This event addresses the concern for continued operation of feedwater when the MSIVs remain open. The event FW down-branch implies that the MSIVs have subsequently closed following the initiating event and the logic is the same as if the MSIVs had never been open.

Due to the diversity of means of recovering from non-mechanical control rod insertion failures (e.g., alternate rod insertion system, manual scram, and manual rod insertion), mechanical failures are the only RPS failures that show up in the dominant ATWS cutsets. Therefore, a simplified ATWS event tree, depicting only the logic following mechanical RPS failures, is provided as Figure 3.4.

### 3.2.2 Dominant ATWS Sequences

As stated previously, the redundancy and diversity of means of recovering non-mechanical RPS failures results in these events making a negligible contribution to the plant risk of core damage. RPS mechanical

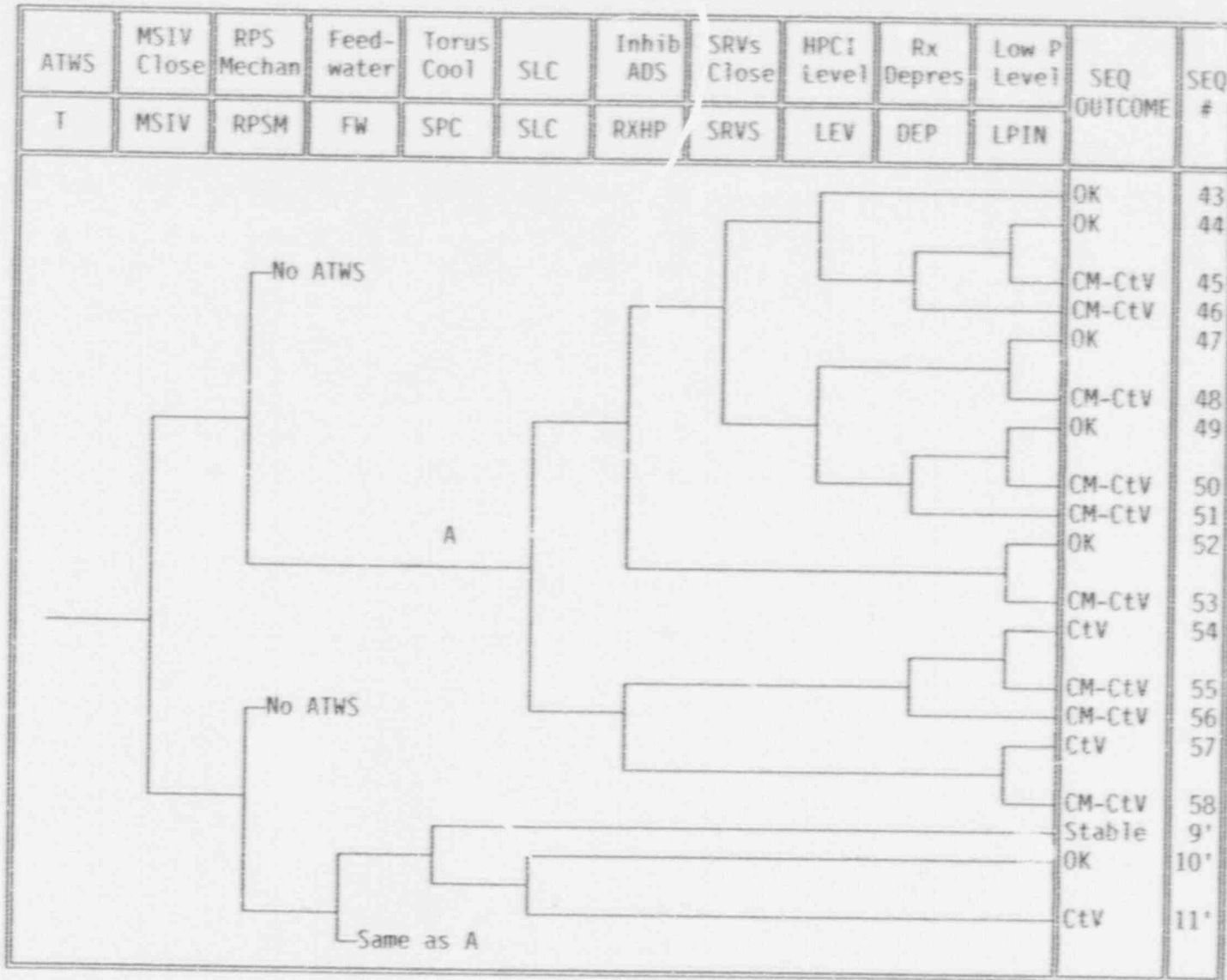


FIGURE 3.4 Simplified ATWS Event Tree



failures, making it impossible to insert the control rods into the core, are the only significant RPS failures.

Sequences 43 through 53 involve successful operation of the SLC system. In Sequence 43, the torus temperature quickly reaches 110°F, requiring the initiation of SLC and the inhibiting of the ADS. The SRVs do not stick open, and the water level is either kept at the top of the active fuel, too high, or oscillating. High water levels would result in high power levels and oscillating levels would cause major power oscillations. In either case, a larger amount of heat would be transferred to the suppression pool. Once the SLC has injected the boron into the bottom of the core, the ATWS would be terminated and the reactor would be in a safe stable state.

Sequences 44, 45, and 46 are similar to Sequence 43 except HPCI fails to function. If the operator depressurizes the reactor vessel and uses the low pressure systems to maintain the water level, once the SLC has injected sufficient boron into the core, the ATWS is terminated and the plant is in a safe state (Sequence 44). If the water level in the reactor vessel is not maintained above the top of the active fuel, core damage will commence (Sequence 45). If the reactor vessel is not depressurized after HPCI failure, the low pressure systems cannot be used to maintain the water level resulting in core damage and a containment vulnerable condition (Sequence 46). Sequence 46 makes the largest ATWS contribution to the plant risk of core damage.

Sequences 47 and 48 are identical to Sequences 44 and 45, respectively except two or more SRVs are stuck in the open position causing the reactor vessel to depressurize (eventually failing HPCI). Depressurization is not required in these sequences to use the low pressure systems, since the stuck-open SRVs provide this function.

Sequences 49 through 51 are similar to Sequences 44 through 46. In these sequences two or more SRVs are stuck open, depressurizing the reactor vessel, and HPCI fails to provide the initial coolant to the core. To avoid core damage, the operator must depressurize the reactor vessel quickly even though the SRVs are open. This is caused by the early failure of HPCI resulting in no initial core cooling.

In Sequences 52 and 53, SLC is successful but the operator fails to inhibit the ADS. Once the ADS functions, it will create a blowdown that requires the use of the low pressure systems, essentially failing HPCI. If the low pressure systems maintain the water level, the outcome is success (Sequence 52). If they fail, core damage and a vulnerable containment will result (Sequence 53).

Sequences 54 through 58 model the events following the failure of SLC. In Sequences 54, 55, and 56 the ADS is inhibited, while in Sequences 57 and 58 the ADS is not inhibited. In either case, HPCI, which maintained the water

level above the top of the active fuel, fails. For the first group of sequences, high suppression pool temperatures fail HPCI. For the second group, the fact that ADS is not inhibited causes the failure of HPCI. If the reactor vessel is depressurized and the low pressure systems are utilized to maintain water level (Sequences 54 and 57), a stable state can be reached. However, containment integrity may be threatened before the reactor can be shutdown which could in turn result in the failure of the low pressure systems and lead to core damage. Sequence 54 makes up the second largest and Sequence 57 makes up the fourth largest ATWS contribution to the probability of core damage.

If the operator fails to use the low pressure systems or if the systems fail to maintain an adequate level above the core, core damage will occur and the containment will be vulnerable (Sequence 55 and 58). If the reactor is not depressurized, the low pressure systems will not be able to function and core damage cannot be prevented (Sequence 56). This sequence makes up the third largest ATWS contribution to the plant risk of core damage.

Sequences 9', 10', and 11', addresses the sequences that result if MSIVs remain open after the initiating event occurs, thus allowing feedwater to continue to run. In Sequence 9' torus cooling is sufficient to cool the amount of heat being transferred to the suppression pool since the majority of the heat is bypassed to the condenser. In this sequence a stable state can be reached although shutdown does not occur.

In Sequences 10' and 11', torus cooling fails. If the SLC functions, the reactor can be shutdown before containment integrity is challenged (Sequence 10'). If the SLC fails, the containment will be vulnerable (Sequence 11').

Table 3.9 presents the dominant ATWS cutsets. It is worth noting that most of the sequences that make a significant contribution to the probability of core damage involve the failure to depressurize the reactor. This is partly due to the low failure rate for the operator not maintaining the water level above the top of the active fuel and partly due to the redundancy of low pressure systems available for core cooling, which makes sequences involving their failure a minor contributor.

### 3.2.3 Recriticality Potential Following ATWS

An ATWS event differs from the station blackout events discussed previously in that the reactor remains critical (since the control blades fail to insert) until either the control blades are inserted or the reaction is terminated by boration. If adequate boration occurs, the potential for recriticality is possible only if the boron concentration is diluted by extended injection. However, for ATWS scenarios in which boration (one of the

TABLE 3.9. ATWS Dominant Cutsets

CUTSET	CUTSET POINT ESTIMATE FREQUENCY
IE-TRTRIP * CMSIVA * RPS-M * HCI-TDP-FS-20S37 * DEP-XHE	1.1E-7
IE-TRTRIP * CMSIVA * RPS-M * SLC-XHE-FS * VENT-XHE-TC * CT-LEAK	1.1E-7
IE-TMSIVC * RPS-M * SLC-XHE-FS * VENT-XHE-TC * CT-LEAK	7.4E-8
IE-TRTRIP * CMSIVA * RPS-M * SLC-XHE-FS * DEP-XHE	7.4E-8
IE-TMSIVC * RPS-M * HCI-TDP-FS-20S37 * DEP-XHE	7.1E-8
IE-TLFW * RPS-M * SLC-XHE-FS * VENT-XHE-TC * CT-LEAK	6.5E-8
IE-TLFW * RPS-M * HCI-TDP-FS-20S37 * DEP-XHE	6.2E-8
IE-TMSIVC * RPS-M * SLC-XHE-FS * DEP-XHE	4.9E-8
IE-TLFW * RPS-M * SLC-XHE-FS * DEP-XHE	4.3E-8
IE-TRTRIP * CMSIVA * RPS-M * HCI-TDP-MA-20S37 * DEP-XHE	3.5E-8
IE-TRTRIP * CMSIVA * RPS-M * SLC-XHE-REL * VENT-XHE-TC * CT-LEAK	3.2E-8
IE-TRTRIP * CMSIVA * RPS-M * SLC-XHE-FS * VENT-XHE-TC * NO-CT-FAIL	2.5E-8
IE-TMSIVC * RPS-M * HCI-TDP-MA-20S37 * DEP-XHE	2.3E-8
IE-TRTRIP * CMSIVA * RPS-M * SLC-XHE-FS * ADS-XHE-INH2 * VENT-XHE-TC * CT-LEAK	2.3E-8
IE-TRTRIP * CMSIVA * RPS-M * SLC-XHE-REL * DEP-XHE	2.2E-8
IE-TLFW * RPS-M * HCI-TDP-MA-20S37 * DEP-XHE	2.1E-8
IE-TMSIVC * RPS-M * SLC-XHE-FS * VENT-XHE-TC * NO-CT-FAIL	1.6E-8
IE-TMSIVC * RPS-M * SLC-XHE-FS * ADS-XHE-INH2 * VENT-XHE-TC * CT-LEAK	1.5E-8
IE-TLFW * RPS-M * SLC-XHE-FS * VENT-XHE-TC * NO-CT-FAIL	1.4E-8
IE-TLFW * RPS-M * SLC-XHE-FS * ADS-XHE-INH2 * VENT-XHE-TC * CT-LEAK	1.3E-8
IE-TRTRIP * CMSIVA * RPS-M * SLC-XHE-FS * VENT-XHE-TC * CT-FAIL * COND-HPSW-XHE-TC	1.1E-8
IE-TIDRV * CMSIVA * RPS-M * HCI-TDP-FS-20S37 * DEP-XHE	1.0E-8

3.30

TERM	DESCRIPTION	MEAN VALUE
IE-TRTRIP	Turbine trip initiating event	2.4/yr
CMSIVA	Subsequent closure of MSIVs	5.0E-1
RPS-M	Mechanical failure of all control rods	1.0E-5
HCI-TDP-FS-20S37	HPCI system (turbine-driven pump) fails to start	4.84E-2
DEP-XHE	Operator failure to rapidly depressurize primary system	2.13E-1
SLC-XHE-FS	Operator failure to start SLC within 4 minutes	3.38E-2
VENT-XHE-TC	Failure to vent containment	9.0E-1
CT-LEAK	Containment leaks	4.5E-1
IE-TMSIVC	MSIV closure type initiating event	8.0E-1/yr
IE-TLFW	Loss of feedwater initiating event	7.0E-1/yr
HCI-TDP-MA-20S37	HPCI unavailable due to maintenance	1.6E-2
SLC-XHE-REL	SLC fails due to failure to realign properly after test	1.0E-2
NO-CT-FAIL	Containment does not fail	1.0E-1
ADS-XHE-INH2	Failure to inhibit ADS	1.4E-1
CT-FAIL	Containment fails	4.5E-1
COND-HPSW-XHE-TC	Operator fails to inject with condensate or HPSW	1.0E-1
IE-TIDRV	Inadvertent open relief valve transient initiating event	2.3E-1/yr

recommended accident management strategies) fails or is inadequate, the containment will eventually fail and core damage will occur unless the control blades are inserted. Recriticality is then only possible if the control blades are subsequently melted due to a loss of core cooling, as in the station blackout scenarios.

Based on the discussion above, it is believed that recriticality during or following an ATWS is not a major concern. Rather, the prompt termination of the ATWS event appears to be the main concern. It should be recognized, however, that the accident management strategies recommended in this report are the same strategies that are typically implemented for ATWS events.

### 3.3 REFERENCES

- 3.1 U. S. Nuclear Regulatory Commission, Office of Nuclear Regulatory Research, "Reactor Risk Reference Document," NUREG-1150, Volume 1, February 1987. (Draft for Comment)
- 3.2 A. M. Kolaczowski, et al, "Analysis of Core Damage Frequency From Internal Events: Peach Bottom, Unit 2," NUREG/CR-4550, Volume 4, SAND86-2084, October 1986.
- 3.3 R.L. Summitt, "Loss of Off-Site Power Initiating Event and Off-Site Power Restoration Evaluation," International Technology Corporation, June 1988. (Final Draft)

## 4.0 STRATEGY DESCRIPTIONS

Obviously, the best accident management strategy is to avoid the occurrence of a severe accident by having high quality operators with high quality procedures, equipment, maintenance and testing programs, surveillance programs, and training. However, should a severe accident occur, these same high quality operators and features would be challenged to mitigate and/or terminate the event. Providing, in advance, strategies to deal with such events would improve the response of the operators.

This section provides strategies that would be effective in mitigating and/or terminating a recriticality event during core reflood, following a severe accident, as described in Sections 2.0 and 3.0. Justification for the uses of each strategy is also provided. The strategies discussed in this section are generic in nature, though their implementation is to varying degrees plant-specific. For the purposes of this discussion the Peach Bottom plant is used as the reference BWR. For implementation at a specific BWR these strategies should be reviewed and modified to meet the specific needs and requirements of that plant.

Finally, it should be noted that the following strategies were developed based on the reactor instrumentation presently available. However, present instrumentation does not provide the operators with sufficient information to accurately assess the immediate potential for or the occurrence of control blade melting. The operators have to make decisions based on accident scenario progression and other derived information (e.g., time since core uncover). Other strategies might be gainfully employed if different or improved reactor instrumentation were available. Some instrumentation considerations are provided in Appendix G.

### 4.1 REFLOOD BORATION STRATEGY FOR CORE MELT EVENTS

#### 4.1.1 Strategy

The best alternative for conditions of known control blade melting, or in which control blade integrity cannot be determined, is to borate the core prior to or at the time of core reflood. The boron should be injected into the core as rapidly as possible to shutdown the reactor and thus limit the recriticality power level and suppression pool temperature. The means and procedures should be in place to use either the standby liquid control (SLC) system or alternate boration means, if the SLC pumps are unavailable, under these conditions.



#### 4.1.2 Justification

Based upon the information supplied in Section 2.0, it is believed that the likelihood of an energetic excursion is extremely small. If the heat load to the suppression pool is greater than the decay heat removal system can remove, the suppression pool temperature and containment pressure will increase. Based on analyses in Section 2.3, the operator is likely to have at least a half to two hours to inject boron to shutdown the reactor and arrest the increasing containment pressure, prior to containment failure.

If the SLC system is available, the injection of boron is a straightforward process. However, to avoid the potential for stratification of the injected boron solution, means should be established throughout the boration period to ensure that there is a sufficient continued upward movement of the lower plenum water into the lower core.

If the SLC pumps are not available, alternate means of boron addition will need to be initiated. Alternate means may include connecting the SLC boron supply tank to the high pressure coolant injection (HPCI) turbine-driven pump suction using temporary connections (e.g., fire hoses and appropriate fittings) or, if access to the boron supply tank is not possible, it may be prudent to borate the injection water supply tank (i.e., the condensate storage tank) to a concentration of 700 ppm <sup>10B</sup>.

Since the condensate storage tank is the normal suction source for the HPCI system, temporary connections would not be necessary to inject the borated water. However, maintenance of the condensate storage tank inventory and automatic transfer of HPCI suction to the suppression pool on high suppression pool level may affect the viability of this boration option. Should the HPCI system be unavailable for boration injection, the reactor core isolation cooling (RCIC) turbine-driven pump could be used in a similar manner as the HPCI turbine-driven pump. Since RCIC suction does not automatically transfer on high suppression pool level, it may be able to continue boration injection using the condensate storage tank.

Other options include depressurizing and using low pressure systems for boration. Since most of the low pressure system pumps are dependent on ac power, they may not be available during a station blackout. For these scenarios, ac power must be recovered before the low pressure systems can be a feasible option. To alleviate the dependency on ac power availability, a low pressure system pumping capability independent of the normal ac power sources may be worth consideration. This could be achieved in a number of ways, including: using a low pressure turbine-driven pump, using an independent diesel-driven pump (e.g., the firewater pumps), or using a dc-powered pony motor as a backup motor for a low pressure system pump.

With prior planning to assure procedures, equipment, and supplies are in place and the means for connecting injection systems to boron supplies or for adding boron to a water supply tank (other than the suppression pool) are available, this strategy would be practical.

## 4.2 HEAT REMOVAL STRATEGY FOR CORE MELT EVENTS

### 4.2.1 Strategy

To extend the time available for terminating a recriticality event, residual heat removal (RHR) suppression pool cooling capability should be established as soon as possible. This strategy involves the initiation of RHR pumps and associated heat exchangers in the suppression pool cooling mode at the time of core reflood. The high pressure service water (HPSW) system, which provides cooling water to each of the heat exchangers, must also function for the RHR suppression pool cooling capability to be established. Since these systems are dependent on ac power, this strategy is applicable to anticipated transients without scram (ATWS) scenarios. For station blackout scenarios, this strategy can be implemented only after ac power is recovered. In addition, if the full RHR capability is used for suppression pool cooling, then this system is not available for reactor vessel injection and other systems (e.g., low pressure core sprays) would need to be used to provide a controlled rate of vessel injection.

### 4.2.2 Justification

The function of the RHR system in the suppression pool cooling mode is to remove the heat dumped to the suppression pool during an accident. The RHR is capable of removing more than 7% of normal operating power in this mode. This capability may be able to handle all or part of the power load resulting from a recriticality event. Quickly establishing RHR suppression pool cooling would greatly extend the time available for shutting down the reactor (using the boration strategy above) and thus prevent suppression pool saturation and containment over-pressurization.

To function at full capacity, all four RHR pumps and associated heat exchangers must be aligned to suppression pool cooling and initiated. Under these conditions, RHR is not available for reactor vessel injection and other systems would be required to provide a controlled rate of vessel injection. If an injection signal is generated after initiating suppression pool cooling, the RHR system will automatically realign to the low pressure coolant injection (LPCI) mode. To return to suppression pool cooling it may be necessary to override a permissive using a switch in the control room. However, other injection sources should be verified operational and adequate

before overriding this permissive. In addition, for this strategy to be successful, the HPSW system must provide cooling water to the RHR heat exchangers.

This strategy would normally be used for ATWS events, but would also be useful for events where control blade melting is suspected, if ac power is available. It may only be necessary to assure that the operators are led back to the appropriate emergency procedure should damaged fuel be recovered with coolant.

## 5.0 CONCLUSIONS

For a PWR, reflooding is normally accomplished using borated water supplies; and recriticality is generally perceived not to be very credible. However, for a BWR, reflood is normally accomplished using unborated water; and recriticality is believed to be credible. Therefore, the focus of this report has been on the potential for recriticality events during core reflood in BWRs.

From Chapter 2.0 it is stated that for the assessment of BWR recriticality only the following issues are important:

- The relative time of control blade and fuel rod melting (separation of the control blades from the fuel rods is what makes recriticality possible).
- The core geometry changes occurring during melting and core reflood (the reactivity of the damaged core depends on the debris mass, fuel particle shapes, and porosity).
- The nature of the reactivity transient (the ability to manage the recriticality event depends on whether it is a core-damaging or explosive transient event or is a benign event, which gradually increases to higher power levels).

The conclusions pertaining to each of these topics are summarized below.

### 5.1 RELATIVE TIMING OF CONTROL BLADE AND FUEL ROD MELTING

If the water covering the BWR core lowers, and the temperatures in the core region increase sufficiently to melt the control blades, melted fuel (which occurs at still higher temperatures) could become critical upon reflood of the core with water.

Two experiments, DF-4 and CORA 16, confirm the early melt relocation of the control blades. Control blade melt relocation temperature is 200 to 300°F below the melting point of stainless steel (i.e., the control blades melt at 2250 to 2350°F). This compares to a fuel rod melt relocation temperature of approximately 4870°F. MARCH calculations indicate control blade melting is strongly correlated to the average core temperature, with melting starting when the average core temperature increases to approximately 1500°F and about half of the control blades melted when the average core temperature reaches 2750°F. This indicates that about half of the control blades can be expected to melt before there is significant fuel rod melting. This is important because early melting of the control blades makes recriticality, during BWR core reflood with unborated water, a credible occurrence.



## 5.2 CORE GEOMETRY CHANGES OCCURRING DURING MELTING AND CORE REFLOOD

During a severe accident in which core cooling has been lost, substantial changes to the as-designed fuel geometry would be expected. During an accident, the grid spacers and end fittings which define the rectangular spacing may melt or collapse, resulting in a loss of the regular geometry. Similarly, the fuel rod cladding could melt or break releasing fuel pellets in a random manner and the fuel pellets may shatter, forming smaller, irregularly shaped particles, or may melt, forming larger particles.

For an overheated core, there is significant potential for fuel rod shattering and debris bed formation when reflooded with water. The shattering of fuel rods has been observed in a number of experiments. Based on grab samples of TMI-2 core debris it is expected that debris beds, formed from shattered fuel rods, would probably be under-moderated and thus not a recriticality concern.

However, analysis indicates that without control blades relatively high reactivities are possible (and even likely for low boron concentrations) over a broad range of fuel particle sizes and fuel volume fractions for both unborated and fairly heavily borated reflood conditions. Based on the analysis, 700 ppm  $^{10}\text{B}$  is required to ensure subcriticality for all conditions.

## 5.3 NATURE OF THE REACTIVITY TRANSIENT

From reflood excursion analyses, it appears that a super prompt-critical excursion (in which some fuel vaporization, dispersal of molten fuel debris, rapid molten fuel-coolant interaction, and the production of a large pressure pulse capable of directly failing the vessel and/or containment occurs) is not likely under conditions of reflooding a hot, degraded core; even under conditions of maximum reflood rate. Doppler feedback, in itself, appears to be adequate to limit the energetics of reflood recriticality to a level below which the vessel would be threatened by a pressure pulse. It is more likely that the reactor would either achieve a quasi-steady power level or enter an oscillatory mode in which water periodically enters and is expelled from the core debris. In either case, the average power level achieved is determined by the balance between reactivity added and the feedback mechanisms. Criticality in debris beds will probably produce power levels no larger than 10% to 20% of normal power. At these levels, the coolant makeup systems could provide adequate coolant to remove the heat generated within the debris bed.

The more likely constraint on the timing for boron addition, to shutdown the reactor, is the challenge to the containment integrity from the excessive heat load dumped to the suppression pool. For this analysis containment failure is conservatively assumed to occur at 132 psia, which corresponds to a



suppression pool saturation temperature of 348°F. Analysis indicates that if excess steam (above RHR suppression pool cooling capability) is limited to about 3% full power, over two hours are available to establish core shutdown by boration and avoid containment failure. If the excess steam corresponds to 13% full power, only about a half hour may be available. Therefore, it is important to establish RHR suppression pool cooling as quickly as possible to extend the time available for shutting down the reactor.

The present SLC system is designed to provide boration in one-half to two hours. This rate appears to be marginally adequate to shutdown the reactor (without control blades) and avoid containment failure, assuming the boration is adequate and actuated at the same time as core reflood. Therefore, adding boron to the injected core water should be initiated as soon as possible following core damage to terminate the criticality of reflooded melted fuel. In addition, if the SLC system is used for boron addition, means should be established throughout the boration period to ensure that there is a sufficient continued upward movement of the lower plenum water into the lower core. This continued upward flow would prevent the potential for stratification of the injected boron solution.

APPENDIX A  $k_{\infty}$  CALCULATIONS

APPENDIX A  $k_{\infty}$  CALCULATIONS

TABLE A.1. Calculated  $k_{\infty}$  for Spherical Particles in Water (0 PPM  $^{10}\text{B}$ )

<u>Boron Concentration</u>	<u>Particle Radius (cm)</u>	<u>Fuel Volume Fraction</u>	<u>K-Infinity</u>
0	0.53	0.27	1.4032
0	0.53	0.28	1.4034
0	0.53	0.29	1.4029
0	0.53	0.30	1.4019
0	0.6239	0.28	1.4061
0	0.6239	0.29	1.4061
0	0.6239	0.30	1.4055
0	0.7	0.20	1.3718
0	0.7	0.28	1.4072
0	0.7	0.29	1.4076
0	0.7	0.30	1.4073
0	0.7	0.32	1.4051
0	0.7	0.40	1.3780
0	0.7	0.50	1.3151
0	1.0	0.20	1.3500
0	1.0	0.30	1.4077
0	1.0	0.31	1.4084
0	1.0	0.32	1.4085
0	1.0	0.34	1.4067
0	1.0	0.40	1.3898
0	1.0	0.50	1.3321
0	1.5	0.20	1.2956
0	1.5	0.30	1.3917
0	1.5	0.34	1.4010
0	1.5	0.35	1.4015
0	1.5	0.36	1.4014
0	1.5	0.40	1.3953
0	1.5	0.50	1.3492

TABLE A.2. Calculated  $k_{\infty}$  for Spherical Particles in Water (200 PPM  $^{10}\text{B}$ )

<u>Boron Concentration</u>	<u>Particle Radius (cm)</u>	<u>Fuel Volume Fraction</u>	<u>K-Infinity</u>
200	0.53	0.42	1.2157
200	0.53	0.43	1.2160
200	0.53	0.44	1.2155
200	0.6239	0.42	1.2187
200	0.6239	0.43	1.2192
200	0.6239	0.44	1.2192
200	0.7	0.40	1.2177
200	0.7	0.43	1.2211
200	0.7	0.44	1.2212
200	0.7	0.45	1.2209
200	0.7	0.50	1.2125
200	0.7	0.60	1.1672
200	1.0	0.40	1.2158
200	1.0	0.45	1.2249
200	1.0	0.46	1.2250
200	1.0	0.47	1.2247
200	1.0	0.50	1.2209
200	1.0	0.60	1.1811
200	1.5	0.40	1.1974
200	1.5	0.45	1.2177
200	1.5	0.48	1.2223
200	1.5	0.49	1.2228
200	1.5	0.50	1.2226
200	1.5	0.55	1.2144
200	1.5	0.60	1.1948
200	2.0	0.40	1.1669
200	2.0	0.50	1.2136
200	2.0	0.51	1.2147
200	2.0	0.52	1.2152
200	2.0	0.53	1.2152
200	2.0	0.54	1.2147
200	2.0	0.55	1.2134
200	2.0	0.60	1.2002

TABLE A.3. Calculated  $k_{\infty}$  for Spherical Particles in Water (500 PPM  $^{10}\text{B}$ )

<u>Boron Concentration</u>	<u>Particle Radius (cm)</u>	<u>Fuel Volume Fraction</u>	<u>K-Infinity</u>
500	0.53	0.53	1.0889
500	0.53	0.54	1.0890
500	0.53	0.55	1.0889
500	0.53	0.56	1.0881
500	0.53	0.57	1.0865
500	0.6239	0.53	1.0921
500	0.6239	0.54	1.0925
500	0.6239	0.55	1.0921
500	0.6239	0.56	1.0918
500	0.6239	0.57	1.0907
500	1.0	0.30	0.9095
500	1.0	0.50	1.0906
500	1.0	0.55	1.0997
500	1.0	0.56	1.1000
500	1.0	0.57	1.0999
500	1.0	0.58	1.0992
500	1.0	0.60	1.0966
500	1.0	0.70	1.0564
500	1.5	0.30	0.8543
500	1.5	0.50	1.0797
500	1.5	0.58	1.1014
500	1.5	0.59	1.1017
500	1.5	0.60	1.1015
500	1.5	0.70	1.0717
500	2.0	0.30	0.7944
500	2.0	0.50	1.0587
500	2.0	0.60	1.0976
500	2.0	0.61	1.0983
500	2.0	0.62	1.0984
500	2.0	0.63	1.0979
500	2.0	0.70	1.0792
500	2.0	0.80	1.0016



TABLE A.4. Calculated  $k_{\infty}$  for Spherical Particles in Water (1000 PPM  $^{10}\text{B}$ )

<u>Boron Concentration</u>	<u>Particle Radius (cm)</u>	<u>Fuel Volume Fraction</u>	<u>K-Infinity</u>
1000	0.53	0.60	0.9788
1000	0.53	0.62	0.9813
1000	0.53	0.63	0.9815
1000	0.53	0.64	0.9817
1000	0.53	0.65	0.9812
1000	0.6239	0.60	0.9811
1000	0.6239	0.62	0.9840
1000	0.6239	0.63	0.9846
1000	0.6239	0.64	0.9850
1000	0.6239	0.65	0.9846
1000	1.5	0.40	0.8022
1000	1.5	0.50	0.9166
1000	1.5	0.60	0.9828
1000	1.5	0.66	0.9979
1000	1.5	0.67	0.9986
1000	1.5	0.68	0.9988
1000	1.5	0.69	0.9984
1000	1.5	0.70	0.9974
1000	1.8	0.50	0.9013
1000	1.8	0.60	0.9768
1000	1.8	0.66	0.9969
1000	1.8	0.68	0.9992
1000	1.8	0.69	0.9995
1000	1.8	0.70	0.9992
1000	1.8	0.72	0.9968
1000	1.8	0.74	0.9918
1000	1.8	0.80	0.9601
1000	2.0	0.60	0.9715
1000	2.0	0.66	0.9950
1000	2.0	0.68	0.9984
1000	2.0	0.69	0.9995
1000	2.0	0.70	0.9993
1000	2.0	0.71	0.9990
1000	2.0	0.72	0.9981
1000	2.0	0.74	0.9940
1000	2.0	0.80	0.9630

APPENDIX B SPREADSHEET INPUT

APPENDIX B SPREADSHEET INPUT

Spreadsheet for UO2 Particles in (Borated) Water  
Prepared by R.A. Libby based on Model by A.L. Doherty  
QA by

Last revision 15 August 19 QAed on  
UO2 Rod in H2O: Radius, Pitch, Boron: 0.62 1.87 1000.00

Date: 8 15 89

THEORETICAL

Uranium Oxide Density (g/cc) Region 1	1.040E+01	(g/cc) 10.40
Moderator Density Region 2 (g/cc) Water	1.00	
Enrichment of Uranium	3.00%	
Wt% U	88.147%	
Wt% O	11.853%	
Region 1 Theoretical Density (g/cc)	10.400	
Pitch of Fuel Rods (cm)	1.87	
Radius of Fuel Rod (cm)	0.62	
Dancoff that NITAWL wants from McDAN's Avgc	0.1706	
Fuel Volume Fraction	0.34	
Moderator-to-Fuel Volume Ratio of Cell	1.92	
Boron Content of Cell (PPM)	1000.00	
H/U-235 of Cell	182.36	
Area of Cell (cm**2)	3.51375	
Radius of Cell (cm)	1.05757	
Rod Pitch (cm)	1.87450	

BULK DENSITIES

Real U density Region 1 (g/cc)	9.167
Real Moderator density Region 1 (g/cc)	1.233
Region 2 Moderator Bulk Density	1.000

Dimensions			
UO2 Rod in H2O: Radius, Pitch, Boron:	0.62	1.87	1000.00
Area of Region 1 (cc)		1.2018	
Region 1 OR (cm)		0.6185	
Mass of Oxygen in Region 1 (g)		1.4815	
Mass of Uranium in Region 1 (g)		11.0171	

Region 2 Moderator Thickness (cm)	0.4391
Area of Region 2 (cm**2)	2.3120
Region 2 OR (cm)	1.0576

Weight Percents	Region 1	Region 2
Uranium		
%U-235	3.00%	
%U-238	97.00%	

Weights in Moderators	Region 1	Region 2
%Boron	0.000%	0.100%
%Hydrogen	0.000%	11.179%
%Oxygen	100.000%	88.721%

U AMU 237.9605822

U Concentration in Region 1 (g/cc) 9.17

Mixtures	# Density	
	Number Densities	
	UO2	H2O+Boron
	Region 1	Region 2
U-238	2.2495E-02	
U-235	7.0462E-04	
Boron	0.0000E+00	5.9607E-05
Hydrogen	0.0000E+00	6.6792E-02
Mod-Oxygen	4.6399E-02	3.3394E-02
Sum # Dens.	0.06959865	0.10024591

APPENDIX C NITAWL INPUT



APPENDIX C NITAWL INPUT

0\$\$	21	2	3	22	30
	31	32	33	34	
1\$\$	0	8	0	0	0
	3	4	2	30	0
	-1	0			
T					
2\$\$	92238	-23801			
	92235	-23501			
	8016	-80161			
	5010				
	1001				
3**	23801	293	3	0.6239	0.6081
	3.9546E+01	2.2496E-02	1	15.9994	7.637
	1	235.044	11.700	1	1
	23501	293	3	0.6239	0.6081
	1.2625E+03	7.0465E-04	1	15.9994	243.815
	1	238.050788	10.6	1	1
4**	293	293	293	293	293
	293	293	293		
T					

APPENDIX D XSDRNPM INPUT

APPENDIX D XSDRNPM INPUT

		0			
0\$\$	40	41	22	42	23
	43	44	45	46	47
	48				
1\$\$	3	2	10	1	3
	2	6	4	1	1
	10	400	0	0	0
2\$\$	-2	-1	0	0	0
	0	0	0	0	0
3\$\$	1	0	0	0	0
	0	0	0	0	0
	0	0			
4\$\$	-2	27	0	-1	3
	4	30	-1	0	
5**	0.0001	0.0001	1	0	0
	1.420892	0	0	0	1
	0.0001	0.75			
T					
13\$\$	1	1	1	2	
	2	2			
14\$\$	23801	23501	80161	8016	
	1001	5010			
15**	0.02249600	0.00070465	0.04638369	0.03339389	
	0.06679242	0.00005961			
T					
33**	F1.0				
T					
35**	3I	0.00000000	5I	0.6239	
		0.7317			
36\$\$	4R		1 6R	2	
39\$\$		1	2		
40\$\$	F1				
51\$\$	1 2 3 4 5 6 7 8 9 10 11 12 13 14 15				
	16 17 18 19 20 21 22 23 24 25 26 27				
T					

APPENDIX E MCDAN INPUT

APPENDIX E MCDAN INPUT

input neutrs/batch (3000-5000)  
input number of batches (5)  
input geometry type (r=rods/s=sphere)  
input radius, mod. sig, vf or pitch

McDAN Version 7.13.89

r= 6.23900E-01 sig= 1.48800E+00 xmax = 6.72043E+00

vf= 6.50000E-01 pitch= 1.16102E+00

number of batches = 25 neutrs/batch= 5000

batch	c	avgc	std	avgx	rhits
1	6.52511E-01	6.52511E-01	0.00000E+00	4.08285E-01	5000
2	6.40096E-01	6.46303E-01	8.77862E-03	4.26922E-01	5000
3	6.50799E-01	6.47802E-01	6.72834E-03	4.12591E-01	5000
4	6.43651E-01	6.46764E-01	5.87257E-03	4.13940E-01	5000
5	6.39547E-01	6.45321E-01	6.02350E-03	4.20576E-01	5000
6	6.42681E-01	6.44914E-01	5.47885E-03	4.16257E-01	5000
7	6.36906E-01	6.43770E-01	5.84609E-03	4.22465E-01	5000
8	6.29762E-01	6.42019E-01	7.33639E-03	4.38025E-01	5000
9	6.50396E-01	6.42950E-01	7.40890E-03	4.09577E-01	5000
10	6.48033E-01	6.43458E-01	7.16777E-03	4.11765E-01	5000
11	6.45810E-01	6.43672E-01	6.83682E-03	4.15764E-01	5000
12	6.43674E-01	6.43672E-01	6.51865E-03	4.19832E-01	5000
13	6.41586E-01	6.43512E-01	6.26789E-03	4.20532E-01	5000
14	6.48603E-01	6.43876E-01	6.17382E-03	4.12897E-01	5000
15	6.35552E-01	6.43321E-01	6.32549E-03	4.29987E-01	5000
16	6.52394E-01	6.43888E-01	6.51842E-03	4.09648E-01	5000
17	6.36055E-01	6.43427E-01	6.59114E-03	4.30333E-01	5000
18	6.49785E-01	6.43780E-01	6.56761E-03	4.10522E-01	5000
19	6.40157E-01	6.43590E-01	6.43647E-03	4.21620E-01	5000
20	6.40276E-01	6.43424E-01	6.30847E-03	4.27065E-01	5000
21	6.48903E-01	6.43685E-01	6.26392E-03	4.16662E-01	5000
22	6.42254E-01	6.43620E-01	6.12056E-03	4.21132E-01	5000
23	6.41635E-01	6.43533E-01	5.99415E-03	4.18586E-01	5000
24	6.40977E-01	6.43427E-01	5.88557E-03	4.19757E-01	5000
25	6.35138E-01	6.43095E-01	5.99540E-03	4.33434E-01	5000



APPENDIX F DANCOFF CORRECTION FACTORS

APPENDIX F DANCOFF CORRECTION FACTORS

TABLE F.1. Dancoff Factors for Spherical Particles in Water

<u>Particle Radius (cm)</u>	<u>Volume Fraction</u>	<u>Particle Pitch (cm)</u>	<u>Dancoff Factor</u>
0.53	0.27	1.322	0.2190
0.53	0.28	1.306	0.2312
0.53	0.29	1.291	0.2426
0.53	0.30	1.276	0.2554
0.53	0.42	1.141	0.4045
0.53	0.43	1.132	0.4185
0.53	0.44	1.123	0.4303
0.53	0.53	1.056	0.5385
0.53	0.54	1.049	0.5501
0.53	0.55	1.043	0.5632
0.53	0.56	1.037	0.5744
0.53	0.57	1.030	0.5838
0.53	0.60	1.013	0.6201
0.53	0.62	1.002	0.6431
0.53	0.63	0.997	0.6530
0.53	0.64	0.991	0.6644
0.53	0.65	0.986	0.6750
0.6239	0.28	1.537	0.1950
0.6239	0.29	1.519	0.2054
0.6239	0.30	1.502	0.2177
0.6239	0.42	1.343	0.3614
0.6239	0.43	1.332	0.3743
0.6239	0.44	1.322	0.3877
0.6239	0.53	1.243	0.4980
0.6239	0.54	1.235	0.5110
0.6239	0.55	1.228	0.5217
0.6239	0.56	1.220	0.5354
0.6239	0.57	1.213	0.5472
0.6239	0.60	1.192	0.5826
0.6239	0.62	1.179	0.6081
0.6239	0.63	1.173	0.6191
0.6239	0.64	1.167	0.6319
0.6239	0.65	1.161	0.6431

TABLE F.1. Dancoff Factors for Spherical Particles in Water (Continued)

<u>Particle Radius (cm)</u>	<u>Volume Fraction</u>	<u>Particle Pitch (cm)</u>	<u>Dancoff Factor</u>
0.7	0.20	1.930	0.0948
0.7	0.28	1.725	0.1715
0.7	0.29	1.705	0.1822
0.7	0.30	1.686	0.1921
0.7	0.32	1.650	0.2138
0.7	0.40	1.531	0.3090
0.7	0.43	1.495	0.3449
0.7	0.44	1.484	0.3574
0.7	0.45	1.473	0.3697
0.7	0.50	1.422	0.4314
0.7	0.60	1.338	0.5577
1.0	0.20	2.756	0.0528
1.0	0.30	2.408	0.1258
1.0	0.31	2.382	0.1347
1.0	0.32	2.357	0.1445
1.0	0.34	2.310	0.1630
1.0	0.40	2.188	0.2265
1.0	0.45	2.104	0.2837
1.0	0.46	2.088	0.2958
1.0	0.47	2.073	0.3282
1.0	0.50	2.031	0.3455
1.0	0.55	1.967	0.4127
1.0	0.56	1.956	0.4264
1.0	0.57	1.944	0.4402
1.0	0.58	1.933	0.4541
1.0	0.60	1.911	0.4825
1.0	0.70	1.816	0.6315
1.5	0.20	4.135	0.0227
1.5	0.30	3.612	0.0700
1.5	0.34	3.464	0.0978
1.5	0.35	3.431	0.1060
1.5	0.36	3.399	0.1141
1.5	0.40	3.282	0.1498
1.5	0.45	3.155	0.2021
1.5	0.48	3.088	0.2373
1.5	0.49	3.067	0.2498
1.5	0.50	3.046	0.2612
1.5	0.55	2.951	0.3301
1.5	0.58	2.899	0.3775
1.5	0.59	2.883	0.3937

TABLE F.1. Dancoff Factors for Spherical Particles in Water (Continued)

<u>Particle Radius (cm)</u>	<u>Volume Fraction</u>	<u>Particle Pitch (cm)</u>	<u>Dancoff Factor</u>
1.5	0.60	2.867	0.4101
1.5	0.66	2.777	0.5152
1.5	0.67	2.762	0.5337
1.5	0.68	2.750	0.5543
1.5	0.69	2.736	0.5739
1.5	0.70	2.723	0.5937
1.8	0.50	3.656	0.2301
1.8	0.60	3.440	0.3837
1.8	0.66	3.333	0.4986
1.8	0.68	3.300	0.5412
1.8	0.69	3.284	0.5633
1.8	0.70	3.268	0.5860
1.8	0.72	3.237	0.6321
1.8	0.74	3.208	0.6806
1.8	0.80	3.126	0.8378
2.0	0.30	4.816	0.0423
2.0	0.40	4.376	0.1064
2.0	0.50	4.062	0.2115
2.0	0.51	4.035	0.2247
2.0	0.52	4.009	0.2383
2.0	0.53	3.984	0.2526
2.0	0.54	3.959	0.2689
2.0	0.55	3.935	0.2827
2.0	0.60	3.822	0.3695
2.0	0.61	3.801	0.3894
2.0	0.62	3.781	0.4081
2.0	0.63	3.761	0.4281
2.0	0.66	3.703	0.4907
2.0	0.68	3.666	0.5366
2.0	0.69	3.648	0.5650
2.0	0.70	3.631	0.5852
2.0	0.71	3.614	0.6121
2.0	0.72	3.597	0.6395
2.0	0.74	3.564	0.6928
2.0	0.80	3.473	0.8681

APPENDIX G

INSTRUMENTATION CONSIDERATIONS



## APPENDIX G

### INSTRUMENTATION CONSIDERATIONS

This appendix discusses the uses and limitations of existing reactor instrumentation during severe core damage accidents and provides considerations for improvements in severe accident management by using new types of instrumentation and/or by making unique and innovative applications of the presently available instrumentation.

The discussions in this appendix do not relate to the specific accident scenarios identified in the main body of this document. From the point of view of the operations staff the cause of the accident may be either clear or a source of confusion. What is known by the operations staff is that an unusual event has occurred. The staff must assess the event based on whatever instrumentation and indication is available and whatever is known about the event. This appendix discusses the potential benefits and limitations during severe accidents of the instrumentation that is presently available. In addition, additional instrumentation and innovative uses of present instrumentation are considered as a means to provide the operations staff with improved information on the conditions in the core.

#### G.1 EXISTING INSTRUMENTATION

This section discusses the benefits and limitations of the instrumentation that presently is available to the operations staff during a severe accident. The existing instrumentation that may be available for severe accident management includes:

- Liquid Level
- Vessel and Drywell Pressure
- Vessel Temperatures
- In-Core Instrumentation (LPRMs, IRMs, Source Range Monitors)
- Hydrogen Generation and Non-Condensable Gas Generation

##### G.1.1 Existing Liquid Level Devices

The existing liquid level sensors are differential pressure devices. There are triple redundant sets of sensing systems covering various ranges and are provided by different manufacturers. These sensing systems are all highly reliable and provide adequate liquid level sensing for all ranges of normal reactor operation. These instruments are known to indicate errors during portions of off-normal reactor operations and have specific Emergency

Operating Procedures (EOPs) for refilling reference legs and determining the accuracy of liquid level readouts. In some accident scenarios sufficient time to implement these procedures may not be available.

It should be noted that at the onset of a severe accident, only one set of the three liquid level sensing systems functionally covers the active fuel (the Gemac system). Further, below the bottom of the active fuel there is no liquid level sensing. Most accidents that result in fuel damage may require depressurization. EOPs for refilling reference legs should be implemented. In many other accident sequences, depressurization may be an integral part of the failure or the recovery actions and the liquid level sensing systems have the same status.

If the existing liquid level sensing systems are used, they will only give the operator a brief look at the start of the accident. It should be noted that the liquid level drop is a direct function of boil-away due to decay heat and that the operator has nominally one hour before core uncover to obtain an adequate supply of cooling water for the core before control blade damage/melting begins. At the same time, or up to an hour prior to the start of control blade melting, the liquid level sensing systems may cease to provide readings since the collapsed liquid level will have reached the bottom of the active fuel. Therefore, the existing liquid level systems are not wholly sufficient for definitive operator knowledge of a major core damage accident.

#### G.1.2 Existing Vessel and Drywell Pressure Sensing Systems

The pressures in the vessel and drywell can be well known during all accident scenarios. For the most part they are used for prevention and mitigation and are considered to be accurate and reliable.

#### G.1.3 Existing Temperature Sensing Systems

The temperature sensing systems available in BWRs today consist of thermocouples on the outside wall of the vessel, in the steam outlet pipes outside of main steam isolation valves, and on the vessel upper flange. The thermocouples can provide information very late in an accident scenario that can serve to warn of impending vessel failure or, in the case of recovery, can confirm that recovery is progressing. These temperature measurements, however, are inadequate for providing definitive information relating to the onset of fuel damage or recoverability of core cooling. Additional thermocouples located inside the vessel could provide interpretable data which could assist with accident mitigation.

#### G.1.4 Existing In-Core Instrumentation

The in-core instrumentation consists of the various radiation measurement devices. Of those, only the source range monitors (SRMs), which are ac power driven devices, and LPRMs, which are permanently mounted in the core, are considered potentially usable during severe accident scenarios.

#### G.1.5 Existing Hydrogen and Non-Condensable Gas Detection

The hydrogen and non-condensable gas detection systems provide inputs that confirm the progress of the accident.

### G.2 SEVERE ACCIDENT MANAGEMENT USING EXISTING INSTRUMENTATION

In most accidents, the initiating event would not normally cause fuel damage in and of itself, but rather, would require one or more additional adverse conditions that drive the accident to the fuel damage state. These additional events may be failures of equipment and/or erroneous operator actions. This type of accident leaves the plant in a weakened state and corrective response times are generally shortened and decisions must be made correctly and swiftly to prevent serious consequences. Mitigation of an accident can only be accomplished if appropriate systems exist to mitigate the accident. It also assumes that the operators have the necessary information and training to understand and handle the problem.

Considering existing instrumentation, the operators could make some judgments about fuel damage accidents and take certain actions to prevent or mitigate these accidents. Existing useful instrumentation consists of the Gemac liquid level devices, LPRMs, the hydrogen and non-condensable gas monitors, the drywell radiation monitors, and to some extent the SRMs. In addition, the vessel and containment pressures are controlling decisional tools that can lead the operator toward proper actions. The thermocouples on the vessel and at other locations within the drywell can provide information very late in an accident scenario that can serve to warn of impending vessel failure or, in the case of recovery, can confirm that recovery is progressing.

Given an accident that takes a few hours to vessel failure, the operators would be using the EOPs from the start of the initiating transient. They will know very early into the transient that they have a problem and that the EOPs, as presently configured, may not lead to the termination of the accident prior to severe consequences (e.g., core damage, containment pressurization, etc.). These EOPs do not progress beyond the point of slightly off-normal circumstances and assume that each subsequent action will eventually recover the vessel to shutdown cooling conditions. The operators will probably recognize they are in a serious problem sometime before actual core uncover occurs.

Control room procedures require the operators to use a tracking system which logs real time and tracks each action taken during the event, so the operators should be fully aware of the time from the start of the accident and the general conditions of the vessel and containment when the realization that they are in a core damage event becomes apparent. During any accident, operators may be able to track liquid level down to the bottom of the active fuel, if the existing liquid level systems are reading and if they believe the readings. In any event where the vessel pressure drops rapidly, there will be no useful or credible liquid level readings during the depressurization and the operators would tend to disregard subsequent liquid level readings unless there was sufficient time for the reference legs to refill or the reference legs were manually refilled.

Continuing with the accident scenario, the operators are tracking the liquid level down to the bottom of the active fuel. The rate at which the liquid level drops is a definitive indication of the time to control blade melting and fuel damage. Existing codes can be used to develop tables and graphs which could direct operators toward preventing or delaying damage, recovery without worsening conditions, or minimizing the effects of the accident.

With present EOPs and the operator's training, the operators would probably restore any available water source and inject it into the core to recover from the core damage event. Operator recovery may also be accomplished by controlled water level increases from selected sources. The procedures are understood by the emergency response teams but definitive actions are not formalized so the choice is up to the discretion of the senior person on-site at the time of the accident. Further, accident management related to containment pressure management must be dealt with in parallel to vessel injection actions during these accident. Present EOPs permit containment pressures of up to 60 psig at Peach Bottom, before venting is permitted. In the event of a core damage accident, the operators may want to reconsider early venting to mitigate later releases if vessel integrity is expected to be lost.

If any thermocouples indicate very high temperatures, these again are indicators of fuel damage and migration. They may be used to drive further actions by the operators but would not be used for control of the event.

The LPRMs are stationary in the core. As part of the normal shutdown procedures, the SRMs are driven into the core, providing there is ac power to do so. If normal liquid level readings are either not believed or not available, these systems can be used by the operators as an indication of liquid level within the lower two-thirds of the core. It is important to note that if the event is an anticipated transient without scram, the LPRMs will be reading on scale when water is present and will cease to read when water is lost. On the other hand, if the control blades are inserted, the LPRMs will



not be reading on scale but the SRMs (if inserted), will be on scale. The same is true of these devices, that as the water level drops in the core the individual sensors will cease to read on scale. The operators would have to reconfigure sensor outputs to obtain such readings, but reconfiguration is a matter of switching in the control room.

In conclusion, during severe accidents the instrumentation currently used provides only a historical record. The instrumentation does not provide an indication of the extent of control blade or fuel rod damage and does not give any indication for the potential for recriticality to occur during core reflooding. In addition, while general procedures can be derived from these indications (which could help operators manage an accident better) the operators are more likely to manage an accident without formal procedures, after performing actions specified in the EOPs.

### G.3 IMPROVEMENTS FOR SEVERE ACCIDENT MANAGEMENT

Once an accident progresses beyond the definition of an inadequate core cooling (ICC) accident there is no existing instrumentation that provides definitive information to the operators or the emergency response team except as noted above. There are additional desired methods of recovery after this point and it is important for the operators to know how much time they have to accomplish specific preventive, mitigative, or recovery actions. It is also important for the operators to know when to reflood, where to put that water, and how much should be used to mitigate or recover, while doing the least additional damage in an already difficult situation. In order to obtain complete and definitive information on liquid level over the entire vessel, additional instrumentation is needed to provide liquid level measurement from the top of the active fuel to the bottom of the vessel during all reactor accident conditions. The second, but less compelling need is for the operators to know when fuel damage starts and to be able to follow the fuel damage progression. Adding features to address these two areas would provide sufficient information for the operators and the emergency response teams to make appropriate and timely decisions and in applying available resources to the right solution in the most beneficial and timely manner.

The following sections describe potential improvements in liquid level sensing and fuel damage sensing to aid in severe accident management decisions. The improvements discussed are provided solely to indicate the type of improvements that could be implemented. It is recognized that there may be numerous other additional improvements that could accomplish the same sensing features. In addition, procedural enhancements and the use of expert systems that could help operator performance during severe accidents are discussed.



### G.3.1 Liquid Level Improvements

The easiest way to accomplish liquid level indications to the bottom of the vessel is to add a tap from the vessel drain line to an existing differential pressure measuring system. Since the drain line has water flow during normal operation, this system would be of no use or interest during normal operation and would be valved out of service. However, at the onset of an accident, this system could be valved in and the operators could therefore monitor liquid levels to the bottom of the vessel. This information may help the operator establish the time when all water in the plenum evaporates due to molten corium movement. If the operators have credible liquid level readings during the core damage event, this may help them understand core damage progression. However, in virtually all core damage events it would eventually be necessary to depressurize the vessel and depressurization could lead to a loss of water level indication when the reference leg loses water. This could lead the operators to mistakenly believe that the water level reading was correct, or ignore the readings because they do not believe the readings are credible. The system suggested above, to extend the present delta-P system to the bottom of the vessel would suffer the same lack of credibility. It may help the operator understand lower plenum phenomena. The development cost and cost-benefit studies will have to be performed before this improvement is made.

### G.3.2 Fuel Damage Indication Instrumentation

There is presently no instrumentation existing in BWR reactors that can provide information for the operator on the condition of the control blades and fuel during a severe accident. It is understood that the emergency response team and engineering can analyze existing hydrogen and non-condensable gas measurements and that they can also make some assumptions from radiation readings during the accident scenarios which are useful. However, this information does not directly indicate control blade and/or fuel damage and may not be available in a timely manner for managing the accident.

One approach would consist of a string of thermocouples installed in one or more LPRM strings. The thermocouple temperature range would be designed to detect the maximum peak cladding temperature. The development costs and cost-benefit studies for such a device should be prepared before it is implemented.

### G.3.3 Operator Performance Enhancements

Procedures that guide reactor operators beyond available EOPs could be quite beneficial. The logical extension of the EOPs into the realm of severe fuel damage can be accomplished with existing reactor systems by developing appropriate tables and graphs relating fuel damage to recorded liquid level drop at the start of the accident and dose rate increases as the water drops

down the core. Given the proper input information the existing fuel damage, codes can predict a range of damage conditions for possible accidents and tables and graphs can be developed from these data. The extended procedures could provide guidance on hydrogen evolution, metal-water reactions, times to expected vessel failure if nothing is done, proper actions to be taken if possible and time estimates for the operators to complete these actions, the potential for recriticality upon reflood under specific conditions, the actions necessary to protect the containment, and what systems to use and not use if recovery becomes possible at any point in the accident.

Utilizing the present liquid level information to develop accident management strategies to be used in the later accident stages is not an ideal approach to severe accident management. Full vessel liquid level would add significantly to the operator's knowledge of core damage progression and improve the chances of correctly coping with the events as they occur.

#### G.3.4 Expert Systems

For severe accident management, expert systems can be defined as a computer hardware and software system dedicated to providing definitive information to the operators and emergency response teams during a severe accident. This information would be used by the operators to direct them toward the proper and best resolution to the immediate problem. The system would monitor specific conditions and correlate these conditions to known accident scenarios and existing operating conditions, and provide potential resolution. Defined operating conditions would provide the operator with appropriate, approved, and recommended procedures during the entire course of an accident. The system would be advisory in nature requiring mostly yes/no input responses from qualified operators during the accident. Output would include recommendations to the operators relating to the best, approved approach to accident mitigation or termination.

Expert systems are to some extent currently used in some reactors. They can be designed to operate with the existing information from reactor instrumentation and provide a limited amount of help to the operators in the event of a core damage event. If additional reliable liquid level devices were installed, the value of expert systems to the operators would be greatly enhanced. In reactors where these systems are presently installed, their use in this mode should be considered. This system could be used to provide definitive information to the operators and emergency response teams during severe accident scenarios.

DISTRIBUTION

No. of  
Copies

OFFSITE

Edward C. Abbott  
ABZ, Incorporated  
Suite 150  
1175 Herndon Parkway  
Herndon, VA 22070

Chris Allison  
Idaho National Engineering Lab  
P.O. Box 1625  
Idaho Falls, Idaho 83415

Dr. George Apostolakis  
Mechanical, Aerospace and  
Nuclear Engineering Department  
School of Engineering and  
Applied Science  
University of California, Los  
Angeles  
Los Angeles, CA 90024

Jack Ballman  
Idaho National Engineering Lab  
P.O. Box 1625  
Idaho Falls, Idaho 83415

Dr. Marshall Berman  
Sandia National Laboratory  
Division 6517  
P.O. Box 5800  
Albuquerque, NM 87185

David Blanchard  
Tenera, L.P.  
1340 Saratoga-Sunnyvale Road  
Suite 206  
San Jose, CA 95129

Allen Camp  
Sandia National Laboratory  
Division 6424  
P.O. Box 5800  
Albuquerque, NM 87185

Dr. Hyla Cass  
The Learning Center  
16944 Ventura Blvd.  
Encino, CA 91316

Jeff Clymer  
Philadelphia Electric Company  
965 Cheslerbrook Blvd.  
Wayne, PA 19807-5651

Richard S. Denning  
Battelle Memorial Institute  
505 King Ave.  
Columbus, OH 43201

David Diamond  
Brookhaven National Laboratory  
Associated Universities,  
Incorporated  
Department of Nuclear Energy  
Upton Long Island, NY 11973

Susan Dingman  
Sandia National Laboratory  
Division 6412  
P.O. Box 5800  
Albuquerque, NM 87185

Dr. Ed Dougherty  
Science Applications  
International Corporation  
311 Park Place Blvd.  
Suite 666  
Clearwater, FL 34619

Dr. Robert E. Henry  
Faust & Associates, Inc.  
16W070 West 83rd Street  
Burr Ridge, IL 60521

Paul R. Hill  
Pennsylvania Power & Light  
Company  
2 North 9th Street  
Allentown, PA 18101

Steven Hodge  
Oak Ridge National Laboratory  
Mail Stop 8057  
Oak Ridge, TN 37831-8057

Cliff Hyman  
Oak Ridge National Laboratory  
Mail Stop 8057  
Oak Ridge, TN 37831-8057

Nirmal Jain  
North East Utilities  
P.O. Box 270  
Hartford, CT 06141-0270

Dr. David H. Johnson  
Pickard, Lowe & Garrick, Inc.  
2260 University Drive  
Newport Beach, CA 92660

Dr. William Kastenburg  
Mechanical, Aerospace and  
Nuclear Engineering Department  
School of Engineering and  
Applied Science  
University of California, Los  
Angeles  
Los Angeles, CA 90024

Dr. Moshen Katib-Rahbar  
P.O. Box 2034  
Rockville, MD 20847

Casimar Kukielka  
Pennsylvania Power & Light  
2 North 9th Street  
Allentown, PA 18101

Steve Lelewer  
Bechtel Corporation  
12440 East Imperial Highway  
Norwalk, CA 90650

Roger Locy  
James A. Fitzpatrick Nuclear Power  
Plant  
P.O. Box 41  
Lycoming, NY 13091

William J. Luckas  
Brookhaven National Laboratory  
Associated Universities  
Incorporated  
Department of Nuclear Energy  
Upton Long Island, NY 11973

Tim Messersmith  
Washington Public Power Supply  
System  
3000 George Washington Way  
Site 2, MB9720  
Richland, WA 99352

Dr. Richard Oehlberg  
Electric Power Research Institute  
3412 Hillview Avenue  
Palo Alto, CA 94303

Dr. David Okrent, Professor  
Mechanical, Aerospace and Nuclear  
Engineering Department  
School of Engineering and Applied  
Science  
48-121D Eng 4  
University of California, Los  
Angeles  
Los Angeles, CA 90024

Robert Pinelli  
GPU Nuclear Corporation  
One Upper Pond Road  
Parsippany, NJ 07054



Mike Podowski  
Department of Nuclear  
Engineering & Engineering  
Physics  
Rensselaer Polytechnic  
Institute  
NES Building  
Tibbits Avenue  
Troy, NY 12180-3590

Dr. Dana Powers  
Sandia National Laboratory  
Division 6422  
P.O. Box 5800  
Albuquerque, NM 87185

Wayne Russell  
Grand Gulf Nuclear Station  
P.O. Box 756  
Port Gibson, MI 39150

Jay Simms  
GPU Nuclear  
Oyster Creek Nuclear Generating  
Station  
P.O. Box 388  
Forked River, NJ 08731

Erik Soderman  
President  
Statens Karnkraftinspektion  
Sohlstedtgatan 11  
Box 27106  
S-102 52, Stockholm  
Sweden

5 Robert W. Tayloe, Jr.  
Battelle Memorial Institute  
505 King Ave.  
Columbus, OH 43201

Dr. Theo G. Theofanous,  
Professor  
Center for Risk Studies and  
Safety  
Department of Chemical &  
Nuclear Engineering  
University of California, Santa  
Barbara  
Santa Barbara, CA 93106

John Valente  
Brookhaven National Laboratory  
Associated Universities  
Incorporated  
Department of Nuclear Energy  
Upton Long Island, NY 11073

Dr. A. Telal Wassel  
Science Applications International  
Corporation  
21151 Western Avenue  
Torrance, CA 90501-1724

Kermit W. Whit  
Southern Company Services  
P.O. Box 1295, Bin B064  
Birmingham, AL 35201

Roger D. Wooten  
Battelle Memorial Institute  
505 King Ave  
Columbus, OH 43201

No. of  
Copies

ONSITE

27 Pacific Northwest Laboratory

L.R. Dodd  
D.G. Harrison (15)  
S.W. Heaberlin  
R.A. Libby  
W.B. Scott  
B.D. Shipp  
R.D. Tokarz  
Publishing Coordination  
Technical Report Files (5)

20 U.S. Nuclear Regulatory Commission

N. Lauben  
F. Odar (16)  
R.L. Palla  
B. Sheron  
L.M. Shotkin





THIS DOCUMENT WAS PRINTED USING RECYCLED PAPER.

UNITED STATES  
NUCLEAR REGULATORY COMMISSION  
WASHINGTON, D.C. 20555

OFFICIAL BUSINESS  
PENALTY FOR PRIVATE USE, \$300

SPECIAL FOURTH-CLASS RATE  
POSTAGE & FEES PAID  
USNRC  
PERMIT No. G-67

120555139531 1 1AN1RC1R11R3  
US NRC-OADM  
DIV FOIA & PUBLICATIONS SVCS  
TPS PDR-NUREG  
P-223  
WASHINGTON DC 20555